Cell to Cell Signalling during Vertebrate Limb Bud Development

Intercellulaire Communicatie tijdens de Ontwikkeling van Ledematen in Vertebraten

(Met een samenvatting in het Nederlands)

Proefschrift

ter verkrijging van de graad van doctor aan de Universiteit Utrecht op gezag van de Rector Magnificus, Prof. Dr. W.H. Gispen, ingevolge het besluit van het College voor Promoties in het openbaar te verdedigen op woensdag 24 maart 2004 des middags te 12.45

door

Lia Panman

geboren op 26 oktober 1974 te Veendam

Promotor: Prof. Dr. R. Zeller

The studies described in this thesis were performed in the Department of Developmental Biology, University Utrecht, Padualaan 8, 3584 CH Utrecht, The Netherlands

ISBN: 90-393-3626-1

Voor mijn ouders

Contents

CHAPTER 1

Introduction

Patterning the Limb Before and After SHH Signalling

Lia Panman[1] and Rolf Zeller[1,2]

[1]Dept. of Developmental Biology, Utrecht University, Padualaan 8
3584 CH Utrecht, The Netherlands
[2]Developmental Genetics, Department of Clinical-Biological Sciences
(DKBW), University of Basel Medical School, c/o Anatomy institute,
Pestalozzistrasse 20, CH-4056 Basel, Switzerland

Journal of Anatomy **202**: 3-12 (2003) (Modified)

Abstract

The vertebrate limb is one of the most relevant experimental models in which to analyse cell-cell signalling during patterning of embryonic fields and organogenesis. Recently, the combination of molecular and genetic studies with experimental manipulation of developing limb buds has significantly advanced our understanding of the complex molecular interactions coordinating limb bud outgrowth and patterning. Certain of these studies indicate the need to revise some of the "textbook views" of vertebrate limb development. In this review, we focus our discussion on how signalling by the polarizing region is established and how limb bud morphogenesis is controlled by both long-range and signal relay mechanisms. Furthermore, we discuss recent results showing that differential mesenchymal responsiveness to SHH signalling is established prior to its expression by the polarizing region.

1. A brief history of the limb bud mesenchymal organiser called polarising region or ZPA and the apical ectodermal ridge (AER)

A few decienia ago the seminal experiments by Saunders (1948) and Saunders and Gasseling (1968) led to the discovery of two major signalling centres controlling vertebrate limb pattern formation. The first one is a group of cells located in the posterior limb bud mesenchyme, the so-called polarising region or zone of polarising activity (ZPA, reviewed by Johnson and Tabin, 1997). The second signalling centre is a ridge of cells running along the distal margin of the limb bud ectoderm called apical ectodermal ridge (AER).

The AER maintains limb bud outgrowth in a proximal to distal direction by keeping the cells of the progress zone (layer of cells directly underlying the AER) in a proliferating, undifferentiated state (reviewed by Capdevila and Izpisua Belmonte, 2001). Removal of the AER results in truncation of the limb. The level of truncation along the proximal-distal axis of the limb depends on the time of AER removal. Ablation of the AER early during limb bud development truncates the limb at a proximal, while removal at a later stage during development only affects the digits (Summerbell et al., 1973). This observation can be explained by two controversial models. According to the progress zone model, a model that has been accepted for more than 30 years, cells measure the time they have spent in the progress zone by a so-called internal clock. This internal clock, which is controlled by the AER, is active as long the cells stay in the progress zone. Cells that leave the progress zone will adopt a fate according to the time they have spent in the progress zone. Cells that leave the progress zone early will adopt a proximal fate, while cells that have stayed a longer period in the progress zone will differentiate in more distal structures. Once the AER is removed, the clock will be arrested, resulting in a truncation of the limb (Summerbell et al., 1973). However recently, the progress zone model has been challenged by the early specification model (Dudley et al., 2002; Sun et al., 2002). According to this model, limb segments are already specified in broad domains from an early stage. These domains will expand during development and subsequently become determined to form skeletal elements. Removal of the AER will give rise to cell death in the mesenchyme, resulting in truncation of the limb

(Dudley et al., 2002). Because the domain of cell death is constant at all stages of limb bud development, at early stages proportionally more cells will undergo apoptosis than at later stage, resulting in ablation of proximal structures at earlier stages. The function of the AER is mediated by Fibroblast Growth Factors (FGF) signalling. FGFs are able to rescue limb bud patterning after AER removal (Niswander et al., 1993; Fallon et al., 1994). In the mouse limb bud four *Fgf* genes are expressed in the AER (*Fgf4, Fgf8, Fgf9* and *Fgf17;* Martin, 1998; Sun et al., 2000). To define the specific roles for these *Fgf*s during limb bud development, these genes have been knocked out. Individual loss of *Fgf4* (Moon et al., 2000; Sun et al., 2000), *Fgf9* (Colvin et al., 2001) and *Fgf17* (Xu et al., 2000) has no effect on limb bud development, whereas inactivation of *Fgf8* can result in hypoplasia of both proximally and distally localized skeletal elements (Lewandoski et al., 2000; Moon and Capecchi, 2000). However in the absence of both *Fgf4* and *Fgf8*, limb bud development fails totally, indicating that an AER lacking both *Fgf4* and *Fgf8* is not able to promote limb bud outgrowth. Interestingly, limb buds exposed to FGF4 and FGF8 signalling for a short period early during development, have skeletal defects at different levels along the proximal-distal axis, more severe than in *Fgf8* single mutant limbs (Sun et al., 2002). According to the progress zone model eliminating AER specific FGF signalling should result in truncations at a certain level along the proximal-distal axis. However in this case both proximal and distal skeletal elements are affected, favouring the early specification model (Dudley et al., 2002).

The polarising region is a classical organiser as defined by Spemann, (2001, reprinted), which instructs limb bud mesenchymal cells with respect to their proliferation potential and fate. This was established by transplantation of polarizing region cells from the posterior mesenchyme to ectopic anterior locations, which induces complete mirror image duplications of the distal-most limb skeletal elements (digits, Saunders and Gasseling, 1968). In addition, it was shown that several other embryonic organising centres such as the notochord and floorplate also possess polarising activity upon grafting to chicken limb buds. In trying to molecularly model polarizing region signalling, Wolpert, (1969) proposed that these cells produce a small diffusible molecule, termed morphogen. This morphogen would form a diffusion gradient across the limb bud and the polarity and fate of e.g. digit precursor cells would be determined by their response to specific thresholds (Fig. 1A; also known as “French flag” model, see Wolpert, 1969). Most appealing, Wolpert’s model provided a straightforward explanation for most, if not all, experimental manipulations of the polarising region in chicken limb buds and the theoretical basis to search for this mysterious morphogen signal. Tickle and colleagues (Tickle et al., 1982) achieved a first breakthrough by establishing that implantation of an inert bead soaked in retinoic acid into a chicken limb bud mimics transplants of polarising region cells perfectly. Retinoic acid is indeed present in the limb bud mesenchyme (Thaller and Eichele, 1987), but its specific production by polarising region cells could not been shown (see also below). The continued search for Wolpert’s morphogen led Tabin and

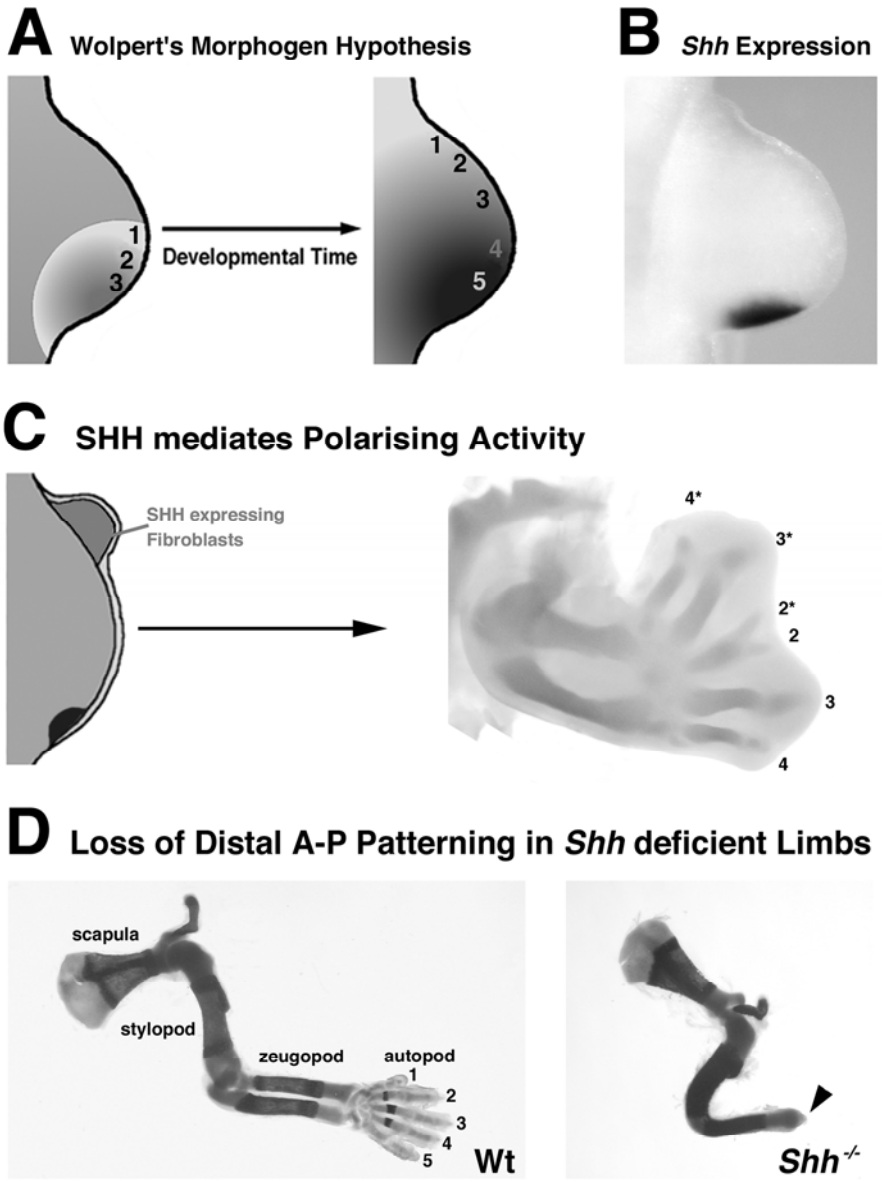

Figure 1. The Polarising Region and SHH signalling.
A. *Wolpert morphogen hypothesis (or French flag model): the posterior mesenchymal cells of the polarising region produce a small diffusible molecule, which forms a gradient and patterns the mesenchyme according to threshold values. The hypothetical thresholds that pattern digits are indicated by numbers 1-5 according to the five digits of mouse and human limbs (1: most anterior digit - thumb, 5: most posterior digit - little finger). The numbers do not represent the positions in which the digits will develop.* ***B.*** *Shh expression as revealed by whole mount in situ hybridisation in a mouse forelimb bud of embryonic day 10.5.* ***C.*** *Anterior grafts of fibroblasts expressing SHH into an early chicken wing bud induces mirror-image duplications of the digit pattern. 2-4 indicate normal digits (2: most anterior, 4; most posterior), 2*-4* indicate duplicated digits. Note reversal of antero-posterior polarity in induced anterior ectopic digits.* ***D.*** *Loss of distal limb structures and the digit arch in Shh$^{-/-}$ limb buds.* ***Wt****: Wild-type forelimb skeleton at embryonic day 15.* ***Stylopod****: humerus;* ***zeugopod****: ulna and radius;* ***autopod****: metacarpals and digits.* ***Shh$^{-/-}$****: Shh deficient mouse forelimb. Note: only one fused zeugopodal bone forms and the digit arch is completely absent, with the exception of a terminal phalange (arrow head). In contrast, one complete digit forms in hind limbs (Kraus et al. 2001, Chiang et al., 2001). All limb buds are oriented with anterior to the top and posterior to the bottom.*

colleagues (Riddle et al., 1993) to identify *Sonic hedgehog* (SHH), a homologue of the *Drosophila hedgehog* gene, as the signal expressed by the polarising region in vertebrate limb buds (Fig. 1B). Furthermore, SHH expression in fibroblasts is sufficient to endow them with polarising activity (as assessed by the induction of mirror image digit duplications; Fig. 1C). Inactivation of the *Shh* gene in the mouse results in a pleiotropic phenotype (for details see (Chiang et al., 1996) including complete disruption of distal limb development and digit arch formation (Fig. 1D; (Chiang et al., 2001; Kraus et al., 2001). Recently, it has been shown that the chick mutant *oligozeugodactyly* (*Ozd*), which lacks SHH function specifically in the limb bud has a limb phenotype similar to the *Shh* $^{-/-}$ mutant mouse (Ros et al., 2003). Detailed genetic analysis provides evidence for long range SHH signalling and threshold effects (see below), all in agreement with its proposed function as a morphogen. However, recent studies also showed that the SHH signal is relayed by activation of secondary signals in responding mesenchymal cells. Furthermore, many regulator genes defined as SHH targets by experimental manipulation of chicken limb buds are in fact activated prior to and/or independent of SHH signalling (see below). In agreement, te Welscher et al., (2002a) provided evidence that the limb bud mesenchyme is not nascent at the time when it receives the SHH signal, but prepatterned by an up-stream acting mechanism. These results show that SHH functions to maintain and modulate gene expression rather than acting as an inducer. Therefore, these recent insights are discussed in more detail in the following sections.

2. Our current view of how the polarizing region is established

During formation and patterning of the primary body axis, the positions of fore- and hindlimb fields are determined and polarised by still largely unknown molecular mechanisms. The potential to form limbs is initially spread throughout the flank (Hornbruch and Wolpert, 1991; Cohn et al., 1995; Vogel et al., 1996; Tanaka et al., 2000)). Prior to initiation of limb bud outgrowth, flank tissue possesses weak polarizing activity and the ability to activate *Shh* expression. During initiation of limb bud outgrowth, polarizing activity is restricted to the posterior mesenchyme and up-regulated concurrent with activation of SHH signalling. Molecular analysis of limbless-ness in snake embryos (Cohn and Tickle, 1999) and ectopic expression of *Hox* genes in mouse limb buds (Charité et al., 1994; Knezevic et al., 1997) indicates that the nested expression of *Hox* genes along the primary body axis may both position and polarise the limb field along its antero-posterior axis. In particular, anterior ectopic expression of the *Hoxb8* gene in forelimb buds results in establishment of an ectopic anterior SHH signalling centre and mirror image duplications of digits similar to polarizing region grafts (Charité et al., 1994). However, loss-of-function analysis of this and many other *Hox* genes alone or in combination has to date not revealed any essential functions for the so-called *Hox* code in positioning and/or polarisation of the limb field and polarizing region (see e.g. van den Akker et al., 2001). In contrast, retinoic acid seems essential during these early stages as inactivation of RALDH2, an enzyme necessary for retinoic acid synthesis, completely disrupts limb bud formation and activation of SHH signalling (Niederreither et al., 1999). Forelimb bud development of *Raldh2* deficient mouse embryos can be rescued by administration of retinoic acid during limb field stages and early

limb bud outgrowth (Niederreither et al., 2002). These studies establish that retinoic acid is critically required to induce SHH signalling during initiation of forelimb bud outgrowth. Niederreither et al. (2002) propose that retinoic acid and the bHLH transcription factor dHAND together activate *Shh* expression in the posterior mesenchyme (Fig. 2). This proposal is based on the fact that inactivation of the *dHAND* gene in mice and zebrafish disrupts SHH activation and severely impairs paired appendage (limb/ fin) bud development (Charite et al., 2000; Yelon et al., 2000). Ectopic expression of *dHAND* in limb buds in turn induces ectopic anterior *Shh* expression and digit polydactyly (Fernandez-Teran et al., 2000; McFadden et al., 2002). Interestingly, *dHAND* is initially expressed throughout the flank mesenchyme (reviewed by Cohn, 2000) as may be expected from the widespread competence to induce polarizing activity (Tanaka et al. 2000, see before). During initiation of limb bud formation, *dHAND* expression is rapidly restricted to the posterior limb bud mesenchyme, which may be crucial to restrict polarising activity to the posterior mesenchyme. Interestingly, expression of the *Gli3* transcriptional repressor (GLI3R, Wang et al., 2000) is activated in anterior mesenchyme concurrent with posterior restriction of *dHAND* (te Welscher et al., 2002a). These authors showed that posterior restriction of *dHAND* is disrupted in *Gli3* deficient mouse limb buds and further genetic analysis implicated the GLI3 repressor in correct the positioning of the *Shh* expression domain (Zuniga and Zeller, 1999). In *Gli3* deficient mouse limb buds, *dHAND* expression is maintained in the anterior mesenchyme and expression of “posterior” genes is anteriorly expanded much earlier than ectopic anterior SHH signalling can be detected. This early loss of posterior restriction in *Gli3* deficient limb buds (and not late ectopic anterior SHH signalling as previously assumed; (Masuya et al., 1995; Buescher et al., 1997) is the most likely cause of the digit polydactyly with associated loss of identity (Zuniga and Zeller, 1999). In *dHAND* deficient mouse limb buds, expression of *Gli3* and another “anterior” gene, *Alx4*, is conversely expanded posteriorly (te Welscher et al., 2002a). These studies establish that a mutual genetic antagonism between *Gli3* and *dHand* polarizes the nascent limb bud mesenchyme upstream of positioning and activating SHH signalling (Fig. 2).

This genetic interaction of *Gli3* with *dHand* uncovers essential components of the molecular mechanism, which positions the polarizing region at the posterior limb bud margin (Fig. 2). Previous work has also implicated FGF8 signalling from the AER in the activation of SHH signalling (Lewandoski et al., 2000). These results show that repression by anterior factors such as GLI3 in combination with retinoic acid and dHAND is crucial to polarise the limb bud and establish the polarizing region. In fact, the studies by te Welscher et al. (2002a) indicate that polarisation of the early limb buds mesenchyme is triggered by GLI3 mediated anterior repression of *dHAND* expression (step 1, Fig. 2). Therefore, it will be important to identify the gene products regulating *Gli3* expression in the anterior limb field mesenchyme.

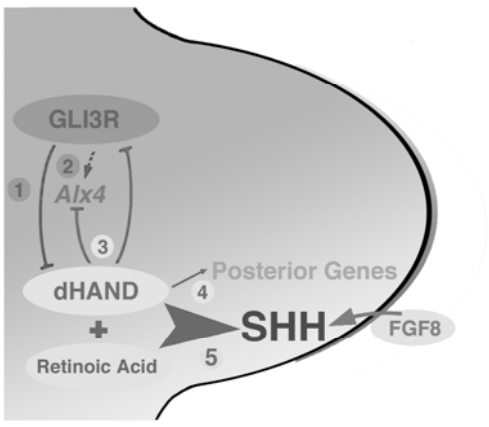

Figure 2. Mutual antagonistic interaction of Gli3R and dHAND prepatterns the mesenchyme and controls establishment of the polarising region.
1. *GLI3R restricts dHAND expression to the posterior mesenchyme during initiation of limb bud outgrowth.* ***2.*** *GLI3R acts upstream of other anterior genes such as ALX4 and is necessary for temporal up-regulation of Alx4 expression.* ***3.*** *dHAND in turn keeps Gli3 and Alx4 expression anteriorly restricted.* ***4.*** *The genetic interaction of Gli3 with dHAND controls activation and spatial expression of posterior genes such as 5'Hoxd, Gremlin, AER Fgfs (Fgf4, -9, -17).* ***5.*** *Last but not least, dHAND interacts with retinoic acid (and FGF8 expressed by the AER) to establish SHH signalling and thereby the polarising region in the posterior limb bud mesenchyme (scheme modified from te Welscher et al., 2002).*

Many "posterior" genes originally identified as transcriptional targets of SHH signalling are expressed much earlier than *Shh* and their distribution is regulated by GLI3 repressor activity (Zuniga and Zeller, 1999). In contrast to *Gli1* and *Patched* (*Ptc*), which are *bona vide* SHH targets, expression of mesenchymal SHH mediators such as e.g. *5'Hoxd* genes, *Bmp2*, *Gremlin* and *Fgfs* in the posterior AER (see below) is activated independent of and prior to SHH signalling (Zuniga et al., 1999; Sun et al., 2000; Chiang et al., 2001). In *Gli3* deficient mouse limb buds, the expression of these genes is anteriorly expanded independent of ectopic SHH signalling (Zuniga and Zeller, 1999, te Welscher et al., 2002a, te Welscher et al., 2002b). Therefore, it is likely that these genes are activated in response to retinoic acid and/or dHAND (see before) and excluded from anterior mesenchyme by GLI3 mediated repression. Taken together, these studies show that responsiveness to SHH signalling is established in the nascent mesenchyme by a prepatterning mechanism acting up-stream of SHH signalling (Fig. 2). Rapid downregulation of these genes in *Shh* deficient limb buds (Zuniga et al., 1999; Sun et al., 2000; Chiang et al., 2001) shows that SHH signalling is essential to maintain and elaborate expression during progression of limb bud morphogenesis as discussed below.

Furthermore, a cis-acting regulatory element has been identified that controls limb-specific expression of *Shh* (Lettice et al., 2002; Lettice et al., 2003). This regulatory element lies within an intron of the *Lmbr1* gene, located about 800 kb upstream from of the *Shh* coding region and is conserved between human, mouse, chick and fish. Mutations in this region cause the human limb disorder preaxial polydactyly (PPD) and the same region is disrupted in the polydactylous mouse mutants *Sasquatch* (*Ssq*) and *Hemimelic extra toe* (*Hx*). As upstream activators of *Shh* are not able to induce *Shh* expression in *Ozd* mutant limb (Ros et al., 2003) it might be that the *Ozd* mutation also disrupts a cis-acting regulatory element that drives *Shh* expression specifically in the limb bud. Although it cannot be ruled out that a trans-acting factor is affected in *Ozd* mutants. The human limb specific disorder Acheiropodia maps also within the *Lmbr1* locus (Ianakiev et al., 2001) and in contrast to PPD causes a phenotype similar to *Shh* $^{-/-}$ mutant and *Ozd* mutant limbs. It would be interesting to show whether *Ozd* maps to the orthologous region of *Acheiropodia.*

3. The long and short of SHH signalling

3a. Long range

Analysis of SHH signalling in chicken limb buds provided clear evidence that SHH can act as a long-range morphogenetic signal and elicits a

dose-dependent response as postulated by Wolpert's morphogen hypothesis (Yang et al., 1997). However, biochemical studies showed that the full-length SHH protein undergoes auto-proteolytic cleavage yielding a C-terminal peptide and the active N-terminal SHH peptide, which is covalently linked to cholesterol (Lee et al., 1994; Porter et al., 1995; Porter et al., 1996). Such cholesterol attachment results in retention of the active SHH peptide by plasma membranes, which poses an apparent paradox with respect to the proposed long-range signalling during limb bud development. To shed light on this rather puzzling biochemical finding, Lewis and co-workers (2001) generated a mouse mutant able to express a modified SHH peptide that can no longer be cholesterol modified. Analysis of mouse embryos expressing this modified SHH peptide during limb bud development showed that formation of anterior digits is disrupted, while posterior digits are normal. Therefore, the cholesterol modification is essential for full-range activity of SHH signalling. Furthermore, analysis of target gene expression and protein distribution shows that the signalling range of the mutant, non-cholesterated SHH peptide, but not polarising activity, is more restricted in comparison to the wild-type protein (Lewis et al., 2001).

Analysis of *Drosophila Hedgehog* (*Hh*) signalling showed that the *Dispatched* gene product is required to release cholesterol bound Hh protein from cells to enable long-range signalling (Burke et al., 1999). In the absence of *Dispatched*, Hh protein accumulates in cells, suggesting that the cleavage of the cholesterol modification by *Dispatched* is crucial for release and long-range signalling activity of *Hh* proteins (Burke et al., 1999). Recently, two murine *Dispatched* homologues have been identified (Caspary et al., 2002; Kawakami et al., 2002; Ma et al., 2002) of which only *mDispA* is functionally conserved. *MDispA* is nearly ubiquitously expressed, although there are some differences in expression levels throughout the embryo. There is a gradient of *mDispA* across the limb bud, from highest at the anterior to lowest at the posterior. Analyses of mDispA mutant embryos and biochemical experiments have demonstrated that mDispA function is required for HH signalling and cellular release of HH proteins in vertebrates (Caspary et al., 2002; Kawakami et al., 2002; Ma et al., 2002). Furthermore, Zeng et al. (2001) have shed light on a possible cellular mechanism that permits SHH to act long range. Experimental evidence reveals the existence of a multimeric, cholesterol-modified SHH peptide that is freely diffusible and seems to form a gradient across the limb bud. These authors propose that multiple; cholesterol-modified SHH peptides accumulate in lipid rafts to form a soluble and freely diffusible complex. Alternatively, cholesterated SHH peptides may traffic across the limb bud mesenchyme through cytonemes, which are long actin-based cellular processes extended by mesenchymal cells in response to FGF signalling (Ramírez-Weber and Kornberg, 1999). While it is clear that long-range SHH signalling is necessary during limb bud development, the underlying molecular and cellular mechanisms enabling such morphogenetic signalling remain in need of further investigation.

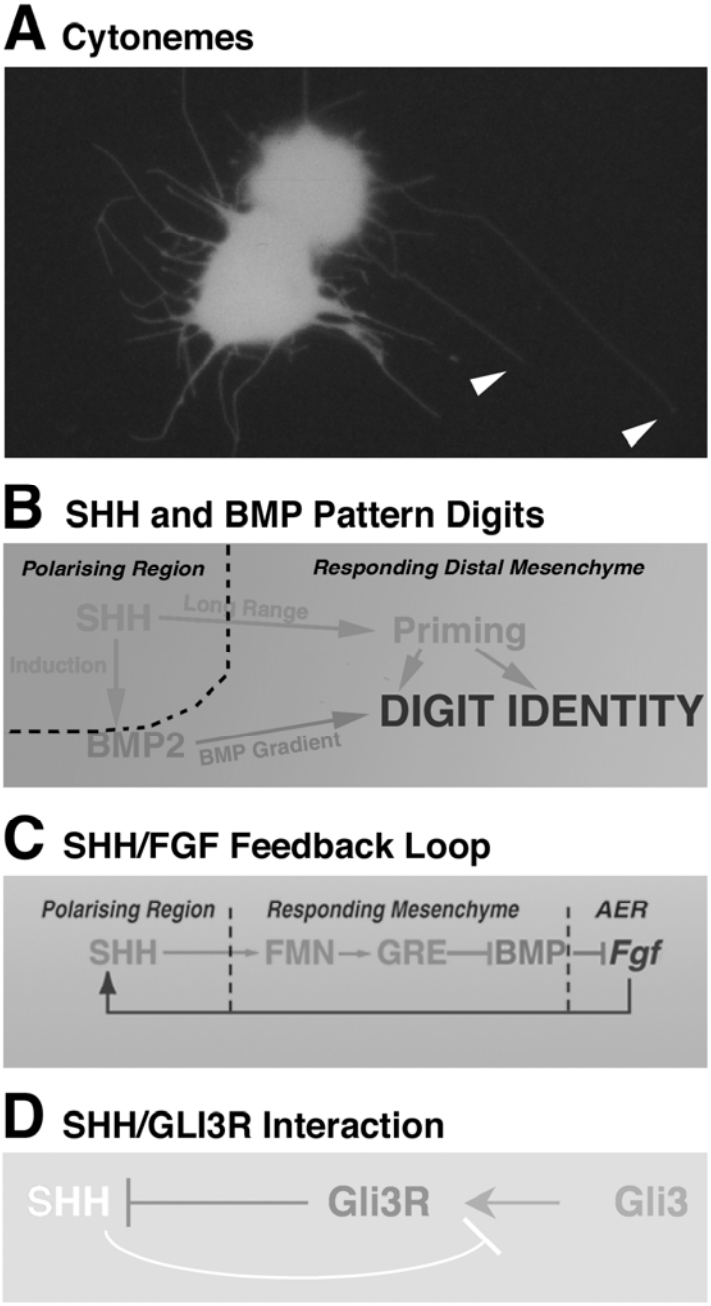

Figure 3. SHH signalling interactions in vertebrate limb buds.
A. *Posterior mouse limb bud mesenchymal cells form long actin-based cellular processes, called cytonemes. GFP-expressing limb bud mesenchymal cells were sandwiched with wild-type cells (non-fluorescent) and cultured for one hour in the presence of 10ng/ml FGF2 as described by Ramírez-Weber and Kornberg (1999). Arrowheads point to select cytonemes extending from two GPF positive cells on a layer of non-fluorescent wild-type cells.* ***B.*** *SHH and BMP interact to pattern digits. SHH signalling primes mesenchymal cells through long range signalling and induces BMP2 in some posterior mesenchymal cells. Graded BMP signalling provides primed mesenchymal cells with positional identity (modified from Drossopoulou et al., 2000).* ***C.*** *Establishment and maintenance of the SHH/FGF feedback loop. SHH up-regulates and maintains expression of the secreted BMP antagonist Gremlin in a Formin-dependent manner in posterior distal mesenchyme. Gremlin-mediated BMP antagonism enables expression of Fgfs such as Fgf4, Fgf9 and Fgf17 in the posterior AER. FGF signalling by the AER in turn maintains and propagates SHH signalling by the polarising region in the posterior-distal limb bud mesenchyme (modified from Zuniga et al., 1999).* ***D.*** *Antagonistic interaction of SHH with GLI3. SHH signalling by the posterior polarising region inhibits processing of the full-length GLI3 protein into an active repressor (GLI3R). Graded SHH signalling results in establishment of a GLI3R gradient with its highpoint in the anterior mesenchyme. GLI3R activity in turn participates in keeping Shh expression posteriorly restricted (modified from Wang et al., 2000).*

3b. Short range

Several mechanisms limit the range of SHH signalling during limb bud development to prevent ectopic activation of *Shh* target genes. The most direct of these mechanisms involves transcriptional up-regulation of the SHH receptor PTC in response to SHH signalling (Goodrich et al., 1996). In the

absence of SHH signalling, PTC inhibits the trans-membrane protein *Smoothened* (SMO) and thereby signal transduction and transcriptional activation of *Shh* target genes. One of these transcriptional targets is *Ptc* itself, which results in up-regulation of PTC activity in cells receiving the SHH signal. Genetic analysis in the mouse shows that SHH targets are ectopically activated in *Ptc1* deficient embryos (Goodrich et al., 1997). Reduction of PTC1 levels in mouse limb buds also results in ectopic anterior *Shh* expression and digit polydactyly (Milenkovic et al., 1999). In addition, PTC1 is also able to sequester the cholesterol-free SHH peptide, as reduction of PTC1 levels in mouse limbs expressing only the non-cholesterated SHH peptide also expands the SHH signalling range anteriorly (Lewis et al., 2001). In vertebrates, the SHH signalling range is further restrained by the Hedgehog-interacting protein, HIP (Chuang and McMahon, 1999). *Hip* expression is activated in limb bud mesenchymal cells in response to SHH signalling. The HIP protein generates an additional negative feedback loop by sequestering the ligand and thereby limiting the *Hedgehog* activity range (Chuang and McMahon, 1999).

3c. Signal relay

SHH activates the secondary signal BMP2 in a subset of responsive limb bud mesenchymal cells (Fig. 3B, Drossopoulou et al., 2000). BMP2 is a vertebrate homologue of *Dpp*, which is activated in *Drosophila* wing discs in response to Hh signalling (Basler and Struhl, 1994). However, BMP2 is not able to mimic all morphogenetic functions of SHH during vertebrate limb development. Ectopic expression of BMP2 in chicken limb buds only duplicates anterior most digits, in contrast to the complete digit duplications induced by ectopic SHH signalling (Duprez et al., 1996). Although BMP2 does not have the full morphogenetic potential of SHH, an important role for BMP2 in determining digit identities has been proposed. Experimental manipulation of chicken limb buds led Drossopoulou et al. (2000) to propose that mesenchymal cells are primed by long-range SHH signalling and that induction of *Bmp2* expression by SHH signalling results in graded BMP activity, which together with the priming effect of SHH specifies digit identity (Fig. 3B). Even during advanced limb development, when the digit primordia have long been determined, changes in interdigital BMP levels cause transformations of digit identities (Dahn and Fallon, 2000). This suggests that positional information is initially set by long-range SHH in combination with graded BMP signalling. However, identities of particular digits may only be specified much later under the influence of BMP signalling from the interdigital mesenchyme, just prior to the regression of this tissue by apoptosis. SHH acts also as a survival factor of the limb bud mesenchyme. Cell death is observed in the anterior mesenchyme of *Shh* deficient limb buds (Chiang et al., 2001; Ros et al., 2003). Remarkably, no cell death has been detected in the posterior mesenchyme that could account for the loss of posterior structures in *Shh* deficient limbs.

SHH not only signals to the limb bud mesenchyme, but maintains and propagates its own expression through establishment of a positive feedback loop between polarizing region and AER (Fig. 3C; SHH/FGF feedback loop, reviewed by Capdevila and Izpisua Belmonte, 2001). Rather than acting long-

range, the SHH signal is relayed to the AER through *Formin*-dependent activation of the BMP antagonist *Gremlin* in responding mesenchymal cells (Fig. 3C). *Gremlin*-mediated BMP antagonism enables expression of several *Fgfs* (*Fgf4, -9, -17*) in the posterior AER (Zuniga et al., 1999). FGF signalling by the posterior AER in turn maintains and propagates SHH signalling distally through the SHH/FGF feedback loop (Niswander et al., 1993; Laufer et al., 1994; Sun et al., 2000), thereby coordinating outgrowth with patterning. In the mouse *limb deformity* (*ld*) mutant, which has a mutation in the *Formin* gene, *Gremlin* expression is absent in the limb mesenchyme, which prevents establishment of the SHH/FGF feedback loop (Haramis et al., 1995; Zuniga et al., 1999). The limbs of *ld* mutant mice exhibit fusions of ulna and radius and digit syndactyly (reviewed by Zeller et al., 1999), indicating that antero-posterior patterning and to some extent outgrowth are affected. Recently, analysis of *Gremlin* mutant mice has demonstrated that *Gremlin* is allelic to *ld*, suggesting that *Formin* and *Gremlin* are regulated by a shared cis-regulatory element (Khokha et al., 2003; Michos et al., submitted; Zuniga et al., submitted). *Shh* deficient mouse embryos display a much more dramatic limb phenotype than *ld* mutants as only one zeugopod bone forms and the digit arch is absent (Chiang et al., 2001; Kraus et al., 2001). The phenotypic differences between *ld* and *Shh* mutant limbs indicate that SHH patterns the mesenchyme (Fig. 3B) largely independently of the SHH/FGF feedback loop (Fig. 3C).

4. GLI proteins and SHH signal transduction

In the *Drosophila* imaginal discs, nuclear response to Hh signalling is mediated by the *Cubitus interruptus* (*Ci*) transcription factor. In the absence of Hh signalling, the Ci protein is processed to generate a repressor of *Hh* target genes (Aza-Blanc et al., 1997). Hh signalling inhibits PKA-mediated Ci cleavage and the full-length Ci protein in turn acts as a transcriptional activator in the presence of Hh signalling (Methot and Basler, 1999). Several vertebrate *Ci* homologues, called GLI proteins, have been identified. In particular *Gli1* is a direct target of SHH signalling (Lee et al., 1997) and has been suggested to mediate response to SHH signalling (Ruiz i Altaba, 1998). However, the lack of a phenotype in *Gli1* deficient mice indicates that GLI1 alone is not sufficient to mediate nuclear response to SHH signal reception (Park et al., 2000). The neural tube phenotype of *Gli2* deficient mouse embryos suggests that GLI2 mediates aspects of SHH signalling during ventral neural tube patterning (Ding et al., 1998; Matise et al., 1998). However, neither *Gli2* deficient nor *Gli1*; *Gli2* double homozygous mouse embryos display striking limb phenotypes (Park et al., 2000), suggesting that another GLI protein regulates the expression of SHH target genes during limb bud morphogenesis. As discussed below, the GLI3 protein is a good candidate for regulating expression of genes in response to SHH signalling.

Full-length GLI3 may act as a positive mediator of SHH signalling in the limb bud (Dai et al., 1999; Sasaki et al., 1999). However in the absence of SHH signalling, the GLI3 protein is constitutively processed to a repressor similar to Ci in *Drosophila* (Wang et al., 2000). SHH signalling inhibits GLI3 processing and experimental evidence indicates that SHH signalling in the limb bud generates an antero-posterior GLI3 protein repressor gradient with highest GLI3 repressor levels in the anterior mesenchyme (Fig. 3D; Wang et

al., 2000). GLI3 mediates its repressor activity by binding to the co-repressor Ski, which recruits the histone deacetylase complex (Dai et al., 2002). The balance between SHH-mediated activation and GLI3-mediated repression of target genes might provide limb bud mesenchymal cells with the necessary positional cues to enable antero-posterior patterning (reviewed by Tickle, 2003). Indeed, analysis of *Shh* $^{-/-}$; *Gli3* $^{-/-}$ double mutant mouse embryos has revealed that antagonistic interactions between SHH and GLI3 control pattern formation. Despite the fact that the direct SHH transcriptional targets such as *Gli1* are not activated in double mutant embryos (Litingtung and Chiang, 2000), expression of many "posterior" genes (e.g. *5'Hoxd*, *Hoxa13*, *Gremlin*) and distal limb patterning are successively restored and anteriorly expanded by removing one or both *Gli3* alleles in the context of a *Shh* deficient limb bud. The progressive restoration of distal limb development may be due to GLI3-dose-dependent restoration of cell survival in *Shh* $^{-/-}$ mutant limb (te Welscher et al., 2002b). These results show that SHH normally functions to overcome GLI3 mediated repression and down-regulation of posterior genes to enable distal progression of limb morphogenesis. As limbs of *Shh* $^{-/-}$; *Gli3* $^{-/-}$ double mutant embryos are polydactylous and indistinguishable from *Gli3* single mutant limbs, these results confirm that GLI3 acts initially upstream of SHH. Subsequent balancing of graded SHH (and BMP, Fig. 3B; Drossopoulou et al., 2000) signalling with GLI3 repressor activity (Fig. 3D) enables co-ordinated progression of limb bud outgrowth and patterning to determine numbers and identity of digits.

In summary, SHH signalling prevents GLI3R formation in the posterior-distal mesenchyme (Fig. 3D) and thereby enables maintenance and propagation of the expression of posterior-distal genes (5'*Hoxd*, *Hoxa13*, *Gremlin* etc). Their expression is induced and positively regulated by factors acting upstream of SHH such as dHAND, most likely in combination with cellular response to retinoic acid (Fig. 2). Further research will have to shed light on the molecular cascades by which SHH inhibits processing of GLI3 to its active repressor form (GLI3R) and on the interactions by which GLI3R keeps SHH posteriorly restricted.

5. Role of *5'Hox* genes during limb development

In mammals, 39 *Hox* genes have been identified, which are arranged in four genomic clusters. *Hox* genes, which encode homeobox containing transcription factors, are involved in the anterior-posterior patterning of the vertebrate body axis. During development, *Hox* genes are spatially and temporally activated in a collinear manner. In other words, their activation corresponds to the order of the genes along the chromosome. As a consequence of collinearity, different combinations of Hox proteins are generated at different anterior-posterior positions along the embryonic axis. Tight spatio-temporal regulation of *Hox* genes is essential for patterning of the trunk (Krumlauf, 1994). In addition to their function along the primary embryonic axis, *Hox* genes are also required for limb bud development. Genetic analysis has demonstrated that the paralogous groups 9 to 13 of the *HoxA* and *HoxD* cluster are involved in patterning of the forelimb skeleton. While the paralogous groups 10-13 of the *HoxA* and *HoxD* cluster and *HoxC10* and *HoxC11* are required for hindlimb development. *Hox* genes are activated in a collinear fashion in the limb, similar to the embryonic axis. More

3' located genes of the *HoxA* and *HoxD* clusters are activated prior to more 5' located genes (Dolle et al., 1989; Nelson et al., 1996; Zakany and Duboule, 1999). This spatiotemporal activation of the *Hox* genes coincides with their functional domains in the limb such that 3' *Hox* genes are required for the patterning of proximal limb structures and 5' *Hox* genes for the distal structures (Fig. 4). Functional analysis has shown that *Hox9* and *Hox10* paralogs function to pattern the stylopod (Fromental-Ramain et al., 1996; Wellik and Capecchi, 2003), while *Hox11* paralogs are required for formation of the zeugopod (Davis et al., 1995) and *HoxD11* to *HoxD13* and *HoxA13* function in digit patterning (Fig. 4; Zakany et al., 1997; Kmita et al., 2002). In contrast to the collinear expression of the *5'HoxD* genes along the proximal-distal axis of the limb, these genes are expressed in a reverse collinear order in the digital domain (Nelson et al., 1996). The expression domains of the *5' HoxD* genes strongly overlap in the digital domain and transgenes inserted in the *HoxD* cluster are similarly expressed, suggesting that a single enhancer would control the expression of these genes in the autopod (van der Hoeven et al., 1996). Recently a distant global control region containing a digit enhancer has been defined, which drives the expression of *HoxD13* to *HoxD10* in the autopod (Fig. 5; Spitz et al., 2003). This enhancer has little promoter specificity and genes unrelated to *HoxD* genes can also be controlled by this digit enhancer. For example, *Evx2* and the *Lunapark* gene, which are located between the digit enhancer and *HoxD* complex, are expressed similar to *HoxD* genes in the autopod. With respect to the *HoxD* cluster, the enhancer most strongly interacts with *HoxD13* and progressively weaker with more 3' genes. The weakening effect of the enhancer on more 3' genes is not due to distance effects, but is due to titration of the enhancer activity is titrated by upstream promoters (Fig. 5). For example, deletion of the *HoxD13* locus results in a *HoxD12* expression profile that resembles wild-type *HoxD13* expression in the autopod and insertions of transgenes upstream of the *5'HoxD* cluster result in down-regulation of the *HoxD* genes (Fig. 5; Kmita et al., 2002; Monge et al., 2003). The mechanism by which the digit enhancer acts accounts for both quantitative and reversed collinearity of *5'HoxD* gene expression observed in the autopod (Dolle et al., 1991; Nelson et al.,1996).

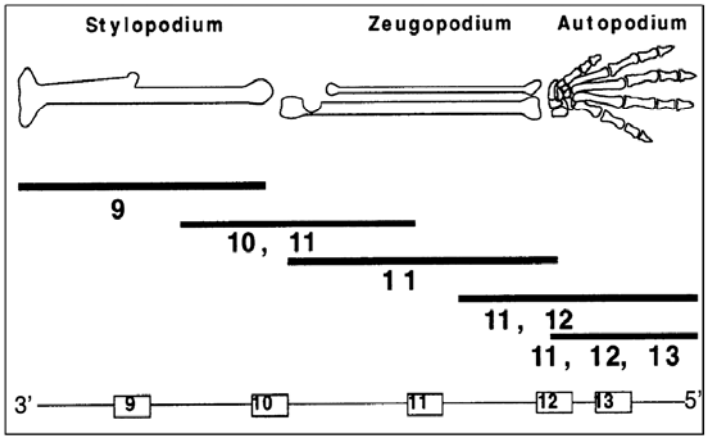

Figure 4. *Functional domains of 5' HoxA and HoxD genes in the forelimb, based on the effects of gene inactivations in mice. A schematic representation of the limb skeleton is shown above. Thick lines below indicate the extent of the anatomical regions of the limb affected by mutations in HoxA and HoxD genes belonging to the paralogous groups 9-13. Line at the bottom with boxes numbered*

9-13 represents the member of the HoxA and HoxD clusters that regulate limb bud patterning. Note that Hox12 only exists in the HoxD complex. Hox genes located in the 3' part of the cluster are required for patterning of proximal limb structures, while more 5' Hox genes are required for patterning of distal limb structures (from Zakany and Duboule, 1999).

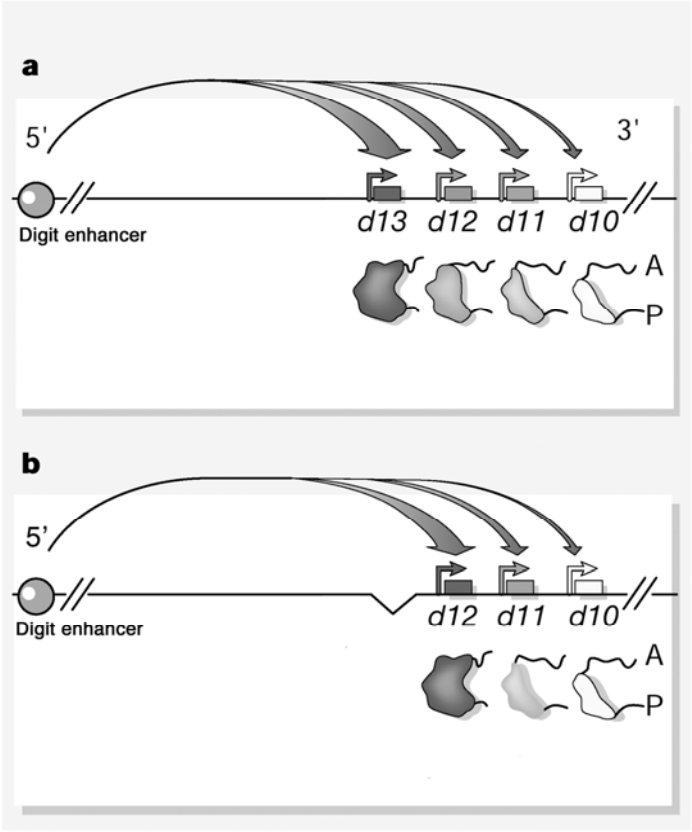

Figure 5. *A remote digit enhancer controls both quantitative and reversed collinearity of 5'HoxD gene expression in the autopod. (**A**) Digit enhancer located 5' of the HoxD cluster drives expression of HoxD13 to HoxD10 in the autopod. The activity of digit enhancer is titrated by different promoters and as a consequence the enhancer acts most strongly on HoxD13 and progressively less on more 3' Hox genes. The thickness of the black arrow indicates the strength of the interaction. (**B**) Activity of digit enhancer is titrated by promoters. Deletion of HoxD13 results in the digit enhancer interacting more efficiently with HoxD12. As a consequence HoxD12 is expressed in a HoxD13-like pattern and takes over the function of HoxD13 (from Zeller and Deschamps, 2002).*

In fishes, which lack structures homologues to the distal autopod of tetrapods, expression of *5'HoxD* genes do not expand anteriorly (Sordino and Duboule, 1996). Interestingly, it has been shown that the fish global control region, which contains regions with high homology to the mammalian global control region, lacks the digit enhancer activity (Spitz et al., 2003). Recruitment of the digit enhancer upstream of the *HoxD* cluster during evolution might have helped genesis of digits.

6. Scope of my PhD thesis

The vertebrate limb provides a model to study pattern formation of tissues during organogenesis. Previous work and data presented in my thesis contributes to the understanding how several signalling cascades are coordinated and interact to pattern the limb bud. In addition, these signalling cascades need to be tightly regulated. For example, SHH signalling controls patterning of the distal limb skeletal elements through induction of secondary signalling molecules, like BMPs and FGFs. Genes expressed in anterior limb mesenchyme like *Gli3* and *Alx4* are required to keep the *Shh* expression domain posterior restricted. In chapter 2, I analyse the phenotype of embryos that are deficient for both *Gli3* and *Alx4.* Analysis of *Gli3/Alx4* double mutant homozygous limbs has uncovered novel roles for *Gli3* and *Alx4* in patterning limb skeletal elements. In chapter 3 the differential responsiveness of wild-

type and mutant limb bud cells to SHH signalling is described. In addition, identification of *Jagged-1* and *Hey1* as downstream targets of SHH signalling during limb development is described. In chapter 4 I describe the limb phenotype of *Gremlin* mutant mice. Analysis of the mutant limb phenotype in combination with gain of function experiments has revealed that Gremlin mediates SHH signalling to the AER. In the final chapter, I discuss whether SHH acts as a morphogenic signal instructing limb bud patterning. In addition, I discuss the role of NOTCH signalling during limb bud development.

Chapter 2

Genetic interaction between *Gli3* and *Alx4* during limb and craniofacial development

Lia Panman[1], Thijs Drenth[1], Pascal te Welscher[1,3], Aimee Zuniga[1,2], Rolf Zeller[1,2]

[1]Department of Developmental Biology, Utrecht University, Padualaan 8, 3584 CH Utrecht, The Netherlands
[2]Developmental Genetics, Department of Clinical-Biological Sciences (DKBW), University of Basel Medical School, c/o Anatomy Institute, Pestalozzistrasse 20, CH-4056 Basel, Switzerland
[3]Present address: Laboratory of Biochemistry and Molecular Biology, Stazione Zoologica “Anton Dohrn”, Villa Comunale, 80121 Napoli, Italy

(Manuscript in preparation)

Summary

Anterior-posterior patterning of distal limb skeletal elements is controlled by the polarizing region (ZPA). The function of the ZPA during limb development is mediated by the signalling molecule *Sonic Hedgehog* (SHH). Mutual genetic antagonism between *Gli3* and *dHand* prepatterns the limb bud prior to SHH signalling resulting in establishment of the ZPA in posterior limb bud mesenchyme. Subsequently, the *Shh* expression domain is kept posteriorly restricted by *Gli3* and *Alx4,* which are both expressed in anterior limb bud mesenchyme. Disruption of either *Gli3* or *Alx4* results in establishment of an ectopic *Shh* domain and preaxial polydactyly. However the type of polydactyly observed in *Gli3* deficient limb differs from that of *Alx4* mutant limbs, suggesting that these genes might act in parallel pathways during limb development. Indeed, analysis of *Gli3* $^{-/-}$; *Alx4* $^{-/-}$ double homozygous mutant limbs reveals that *Gli3* and *Alx4* interact synergistically during patterning of all three groups of skeletal elements. The stylopod is severely malformed and the anterior skeletal element of the zeugopod is consistently lost in double mutant limbs. Furthermore digit numbers and identities are affected. However, no alterations in molecular markers of early limb patterning are observed in *Gli3* $^{-/-}$; *Alx4* $^{-/-}$ double mutant embryos, indicating that the two genes interact only during later developmental stages. In addition, *Gli3* $^{-/-}$; *Alx4* $^{-/-}$ double mutant embryos exhibit severe craniofacial defects.

Introduction

Tetrapod limb skeletal elements show a high variation in sizes, shapes and numbers between different species, although three skeletal segments are evident in all tetrapod limbs: proximally the stylopod, medially the zeugopod and distally the autopod. Limb skeletal elements are formed by endochondral ossifications, whereby mesenchymal cells condense and subsequently differentiate into chondrocytes to form a cartilaginous skeleton. These cartilage templates are ultimately replaced by bone during ossification (reviewed by Kronenberg, 2003). The patterning of limb skeletal elements is controlled by two signalling centres that integrate growth and anterior-posterior patterning of the limb (reviewed by Johnson and Tabin, 1997). The zone of polarizing activity (ZPA) functions as limb bud mesenchymal organizer by secreting the signalling molecule *Sonic hedgehog* (SHH; Riddle et al., 1993). SHH signals to the apical ectodermal ridge (AER), which in turn promotes limb bud outgrowth. Fibroblast growth factor (FGF) signalling by the AER regulates *Shh* expression (Niswander et al., 1993; Laufer et al., 1994) and results in establishment of a feedback loop between these signalling centres. SHH signalling regulates patterning of distal limb skeletal elements and ectopic SHH signalling causes digit duplications, while the lack of SHH signalling abolishes development of distal limb structures (Riddle et al., 1993; Chiang et al., 2001; Kraus et al., 2001).

Several independent mutations in mouse embryos disrupt the posterior restriction of *Shh,* which results in establishment of an anterior ectopic polarizing region and polydactylous limbs (Masuya et al., 1995; Buscher et al., 1997; Qu et al., 1997). Well characterized are the semidominant mouse mutant strains *Extra-toes* (*Xt*) and *Strong's luxoid* (*lst*), which both show preaxial polydactylous limbs. The zinc-finger encoding transcription factor *Gli3* is disrupted in the *Xt* mouse strain (Schimmang et al., 1992; Hui and Joyner, 1993), while the *aristaless*-related homeobox gene *Alx4* is mutated in the *Lst* mouse strain (Qu et al., 1998; Takahashi et al., 1998). However, the type of polydactyly differs between these two mouse mutants. For example, the polydactylous limb phenotype of *Gli3* deficient limbs is independent of SHH signalling, while polydactyly caused by disruption of *Alx4* is dependent on SHH signalling (te Welscher et al., 2002b). In addition, *Gli3* genetically interacts with *dHand* to prepattern the limb bud prior to SHH activation, while *Alx4* does not interact with *dHand* during these early stages (te Welscher et al., 2002a). The difference between *Gli3* and *Alx4* mutant limbs is also reflected by the differences in gene expression. For example, the *Hoxd13* domain is expanded anteriorly in *Gli3* deficient limbs from early stages onwards, while only a small anterior spot of *5'HoxD* expression appears late in *Alx4* deficient limb buds (Qu et al., 1997; Zuniga et al., 1999; te Welscher et al., 2002b). This indicates that *Gli3* and *Alx4* act in different pathways during limb bud development. As *Alx4* expression is reduced in *Gli3* deficient limbs, *Gli3* acts genetically most likely upstream of *Alx4* (te Welscher et al., 2002a). However the residual, more proximally restricted *Alx4* expression in *Gli3* $^{-/-}$ mutant limbs is in agreement with the proposal that *Gli3* and *Alx4* function in different pathways. To uncover possible redundant roles and synergistic interactions of *Gli3* and *Alx4* during limb bud patterning, we have generated *Gli3* $^{-/-}$; *Alx4* $^{-/-}$ double mutant embryos. Analysis of their mutant limbs reveals that *Gli3* and *Alx4* interact to pattern all three types of limb skeletal elements. Furthermore *Gli3* $^{-/-}$; *Alx4* $^{-/-}$ double mutant embryos display severe craniofacial defects.

Results

Gli3 and *Alx4* interact during patterning of limb skeletal elements

To reveal possible redundant roles for *Gli3* and *Alx4* during limb bud development, we have crossed *Gli3* $^{+/-}$; *Alx4* $^{+/-}$ double heterozygous mice to generate *Gli3* $^{-/-}$; *Alx4* $^{-/-}$ double homozygous embryos. At E16.5, no *Gli3* $^{-/-}$; *Alx4* $^{-/-}$ double homozygous embryos were recovered from litters due to embryonic lethality. However at E14.5, all genotypes were recovered at expected ratios. In total we have analyzed the skeletons of four *Gli3* $^{-/-}$; *Alx4* $^{-/-}$ double homozygous embryos. All limbs analyzed are of the same genetic background. Skeletal stains of E14.5 *Gli3* $^{-/-}$; *Alx4* $^{-/-}$ mutant forelimbs and hindlimbs reveals defects in stylopod, zeugopod and autopod skeletal elements with complete penetrance that are distinct from defects observed with any other genetic combination (Figs. 1-3). *Gli3* $^{-/-}$; *Alx4* $^{-/-}$ double mutant

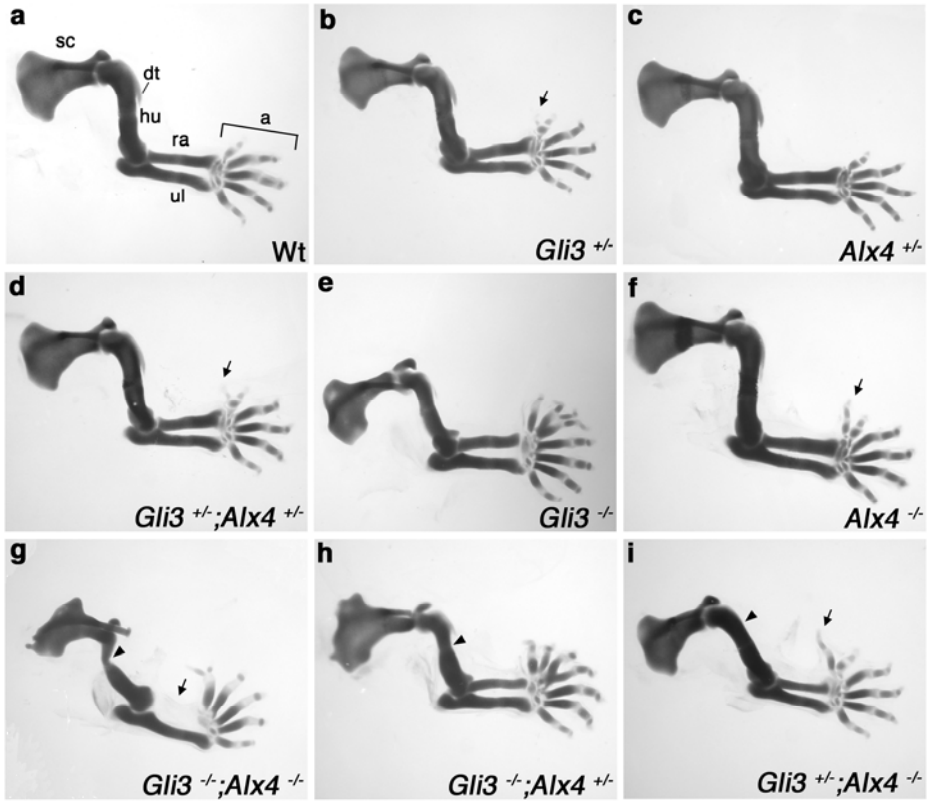

Fig. 1. *Skeletal stains of single and compound Gli3/Alx4 mutant limbs. All skeletal stains shown are of forelimbs of E14.5 embryos. Skeletal analysis shows that genetic interaction between Gli3 and Alx4 is required for patterning of the scapula, stylopod, radius and autopod. (**a**) Wild-type forelimbs. (**b**) Gli3 $^{+/-}$heterozygous forelimbs. Arrow points to small ectopic cartilage condensation. (**c**) Alx4 $^{+/-}$ heterozygous forelimbs, which is phenotypically wild-type. (**d**) Gli3 $^{+/-}$; Alx4 $^{+/-}$ double heterozygous mutant forelimbs, which is similar to Gli3 $^{+/-}$ heterozygous mutant forelimbs. Arrow points to small ectopic cartilage condensation. (**e**) Gli3 $^{-/-}$ homozygous forelimbs. Note the polydactylous forelimb phenotype and the loss of digit identity. (**f**) Alx4 $^{-/-}$ homozygous forelimbs. Arrow points to a duplicated preaxial digit 2. (**g**) Gli3 $^{-/-}$; Alx4 $^{-/-}$ double homozygous forelimbs. Arrow points to the region lacking the radius. Arrowhead points to the humerus, which is severely affected and lacks the deltoid tuberosity. Note the loss of digit identities. (**h**) The humerus of Gli3 $^{-/-}$; Alx4 $^{+/-}$ mutant forelimbs is mildly affected (arrowhead). The autopodal phenotype is similar to Gli3 $^{-/-}$ mutant forelimbs. (**i**) The humerus of Gli3 $^{+/-}$; Alx4 $^{-/-}$ mutant forelimbs lacks the deltoid tuberosity (arrowhead). Arrow points to a duplicated preaxial digit 2. Note that the autopodal phenotype is identical to Alx4 $^{-/-}$ mutant limbs. All panels are oriented with anterior to the top and distal to the right. a: autopod; dt: deltoid tuberosity; hu: humerus; ra: radius; sc: scapula; ul: ulna.*

forelimbs develop a slightly malformed shoulder girdle. However, the humerus of *Gli3* $^{-/-}$; *Alx4* $^{-/-}$ double mutant forelimbs is severely affected and lacks the deltoid tuberosity (dt; arrowhead, Fig.1g). In contrast *Gli3* $^{-/-}$ (Fig. 1e) and *Alx4* $^{-/-}$ (Fig. 1f) single mutant limbs develop a normal humerus. However, additional removal of one copy of either *Alx4* or *Gli3* in single homozygous mutant limbs results in a slightly enhanced phenotype (arrowheads Fig. 1h and i), suggesting a *Gli3* and *Alx4* dose-dependent requirement for patterning of the humerus. Most strikingly, *Gli3* $^{-/-}$; *Alx4* $^{-/-}$ double mutant forelimbs lack the radius (arrow, Fig. 1g), which is normal in all other genetic combinations analyzed. Furthermore, the phenotype of the *Gli3* $^{-/-}$; *Alx4* $^{-/-}$ double homozygous autopod is distinct from the autopodal phenotype observed in any other genetic combination (Fig. 1 and 3). The autopods of *Gli3* $^{-/-}$ mutant

limbs are polydactylous and form six to eight digits without distinct identities (Fig. 1e and Fig. 3b). Autopods of *Gli3* $^{-/-}$; *Alx4* $^{+/-}$ mutant limbs display a similar phenotype (Fig. 1h and Fig. 3e). In contrast, six digits with distinct identities develop in *Alx4* $^{-/-}$ mutant polydactylous limbs (Fig. 1f and Fig. 3c). Again, the *Alx4* $^{-/-}$ mutant autopod phenotype is not changed by additional removal of one copy of *Gli3* (Fig. 1i and Fig. 3f). However, removal of both *Gli3* and *Alx4* results in a complete loss of digit identity in forelimbs (Fig. 1g and Fig. 3d) as seen in *Gli3* $^{-/-}$ single mutant limbs (Fig. 1e). In addition, digit numbers of *Gli3* $^{-/-}$; *Alx4* $^{-/-}$ double homozygous forelimbs varies between five and six. We never observed more than six digits in double mutant limbs, which is in contrast to the up to eight digits that form in *Gli3* $^{-/-}$ single mutant limbs (compare Fig. 1g with Fig. 1e). The distinct forelimb autopod phenotype of *Gli3* $^{-/-}$; *Alx4* $^{-/-}$ double homozygous embryos suggest that *Gli3* and *Alx4* interact to pattern the autopod of the forelimb (Fig. 1 and 3). No significant differences are observed between *Gli3* $^{+/-}$; *Alx4* $^{+/-}$ double heterozygous (Fig. 1 and Fig. 2d) and *Gli3* $^{+/-}$ single heterozygous mutant limbs (Fig. 1b and Fig.2b).

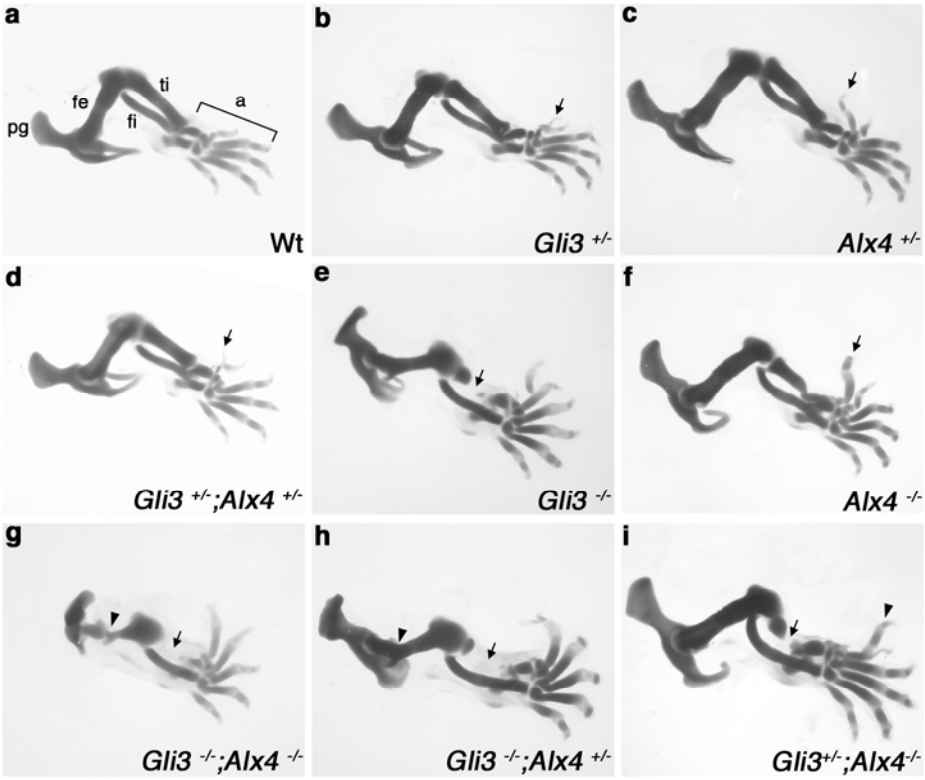

Fig. 2. *Skeletal phenotypes of single and compound Gli3/Alx4 mutant hindlimbs of E14.5. Skeletal analysis reveals that Gli3 and Alx4 genetically interact during patterning of the pelvic girdle, femur, tibia and autopod. (**a**) Wild-type hindlimbs. (**b**) Gli3* $^{+/-}$ *heterozygous hindlimbs.*

*Arrow points to a split digit 1. (**c**) Alx4 $^{+/-}$ heterozygous hindlimbs. Arrow points to a duplicated preaxial digit 2. (**d**) Gli3 $^{+/-}$; Alx4 $^{+/-}$ double heterozygous hindlimbs, which is similar to Gli3 $^{+/-}$ heterozygous hindlimbs. Arrow points to a split digit 1. (**e**) Gli3 $^{-/-}$ homozygous hindlimbs. Arrow points to the rudimentary tibia. Note the polydactylous limb phenotype and the loss of digit identities. (**f**) Alx4 $^{-/-}$ homozygous hindlimbs. Arrow points to a duplicated preaxial digit 2. (**g**) Gli3 $^{-/-}$; Alx4 $^{-/-}$ double homozygous mutant hindlimbs. Arrow points to the region lacking the tibia. Arrowhead indicates the malformed femur. In addition the pelvic girdle is affected. 4 to 5 digits form without distinct identities. (**h**) The femur of a Gli3 $^{-/-}$; Alx4 $^{+/-}$ mutant hindlimb is mildly affected (arrowhead), while the tibia is truncated (arrow). 5 digits form, which do not show distinct identities. (**i**) Gli3 $^{+/-}$; Alx4 $^{-/-}$ mutant hindlimbs. Arrow points to the tibia, which is truncated. Arrowhead points to a duplicated preaxial digit 2. Panels are oriented with anterior to the top and distal to the right. a: autopod; fe: femur; fi: fibula; pg: pelvic girdle; ti: tibia.*

Similar to the forelimbs, *Gli3* and *Alx4* have redundant functions during hindlimb development (Fig. 2). The pelvic girdle and femur of *Gli3* $^{-/-}$; *Alx4* $^{-/-}$ mutant hindlimbs are severely malformed (arrowhead, Fig. 2g). The femur of *Gli3* $^{-/-}$; *Alx4* $^{+/-}$ compound mutant limbs (arrowhead Fig. 2h) is slightly affected, while *Gli3* $^{-/-}$ single homozygous limbs (Fig. 2e) develop a normal femur, suggesting a dose dependent requirement of *Gli3* and *Alx4* during femur development. In contrast to the forelimb, the zeugopod of *Gli3* $^{-/-}$ single and *Gli3* $^{-/-}$; *Alx4* $^{+/-}$ and *Gli3* $^{+/-}$; *Alx4* $^{-/-}$ compound mutant hindlimbs are affected (arrow in Fig. 2e, h, i). In these mutant limbs only a rudimentary tibia is formed. The tibia is totally missing in *Gli3* $^{-/-}$; *Alx4* $^{-/-}$ double mutant hindlimbs (Fig. 2g), suggesting a dose dependent requirement for *Gli3* and *Alx4* during tibia formation. Finally, patterning of the hindlimb autopod is also affected in *Gli3* $^{-/-}$; *Alx4* $^{-/-}$ mutant limbs as only four to five digits without distinct identities form (Fig. 2g). In contrast to the forelimb, the *Gli3* $^{-/-}$; *Alx4* $^{-/-}$ double homozygous hindlimb autopod phenotype resembles that of *Gli3* $^{-/-}$ single and *Gli3* $^{-/-}$; *Alx4* $^{+/-}$ compound mutant hindlimbs, which also develop five digits lacking distinct identities (compare Fig. 2g with 2e and 2h). In contrast digits of *Alx4* $^{-/-}$ single (Fig. 2f) and *Gli3* $^{+/-}$; *Alx4* $^{-/-}$ (Fig. 2i) compound mutant hindlimbs retain distinct identities. Analysis of skeletons cleared with KOH for only a short period reveals that removal of the interdigital mesenchyme by apoptosis (Macias et al., 1999) is delayed in *Gli3* deficient limbs (Fig. 3). At E14.5 mesenchymal cells of the interdigital regions have undergone apoptosis in wild-type, *Alx4* $^{-/-}$ single and *Gli3* $^{+/-}$; *Alx4* $^{-/-}$ compound mutant limbs, thereby eliminating the interdigital mesenchyme (arrows in Fig. 3a, c and f). In contrast, webbing is apparent in mutant limbs lacking both copies of *Gli3* gene (arrowheads Fig. 3b, d, and e).

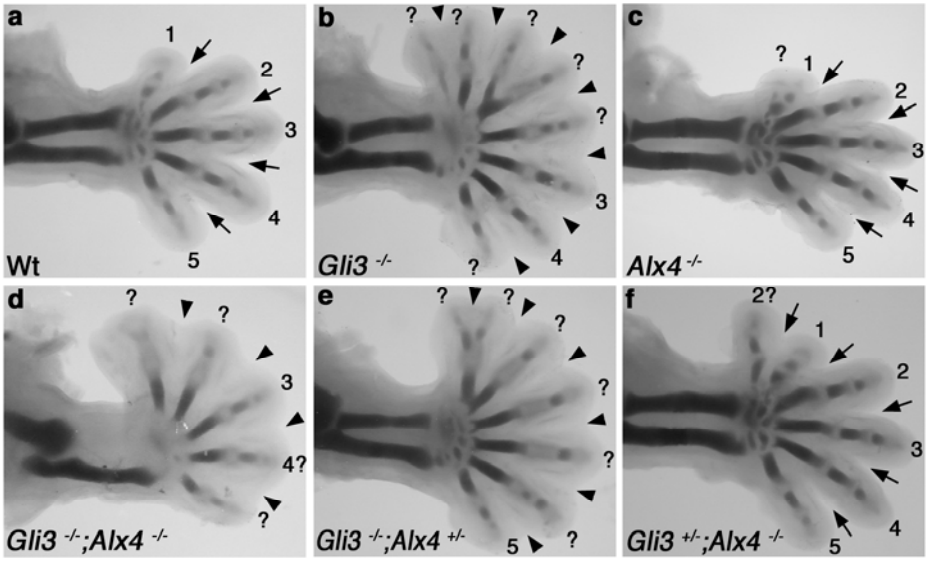

Fig. 3. *Skeletal stains of E14.5 embryos that have been cleared by KOH for only a short period to visualize the remaining interdigital mesenchyme. In wild-type (**a**), Alx4 $^{-/-}$ single (**c**) and Gli3 $^{+/-}$; Alx4 $^{-/-}$ (**f**) mutant forelimbs the interdigital mesenchyme is regressing (arrows). (**b, d, e**) Resorption of the interdigital mesenchyme is delayed in Gli3 deficient forelimbs (arrowheads). Digits are numbered according to their identities. Question marks indicate digits with unclear identities (**b, d, e**). (**b, d, e**) Digit identities are lost in Gli3 deficient forelimbs. (**c, f**) Digits of Alx4 $^{-/-}$ single and Gli3 $^{+/-}$; Alx4 $^{-/-}$ mutant forelimbs have distinct identities. All limbs shown are forelimbs. Panels are oriented with anterior to the top and distal to the right.*

With respect to losing the radius, it is well possible that the cartilage element giving rise to the radius initially forms in *Gli3* $^{-/-}$; *Alx4* $^{-/-}$ mutant limbs, but that it is not maintained. However, analysis of cartilage elements of E12.5 forelimbs by Alcian green staining reveals that in absence of both *Gli3* and *Alx4,* the cartilage model giving rise to the radius is also absent at this stage (arrow, Fig. 4d). Interestingly, also in *Gli3* $^{-/-}$; *Alx4* $^{+/-}$ compound mutant limb buds, the radius cartilage model is only weakly apparent (arrow, Fig. 4e), which indicates that the formation of the radius cartilage model is delayed in *Gli3* $^{-/-}$; *Alx4* $^{+/-}$ mutant limbs.

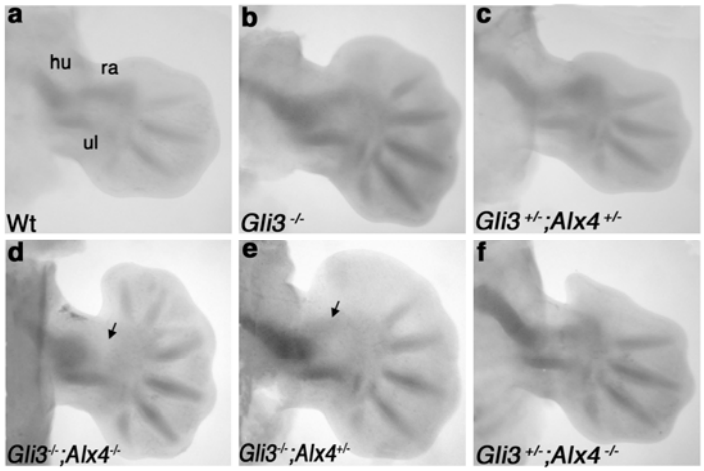

Fig. 4. *Cartilage elements of single and Gli3/Alx4 compound mutant forelimbs of E12.5 embryos. The cartilage was visualized by Alcian green staining. (**a, b, c, f**) The cartilage element giving rise to the*

*radius is detectable in (**a**) wild-type, (**b**) Gli3$^{-/-}$, (**c**) Gli3 $^{+/-}$; Alx4 $^{+/-}$ and (**f**) Gli3 $^{+/-}$; Alx4 $^{-/-}$ mutant embryos. (**d**, **e**) In contrast the radius cartilage element is lacking in Gli3 $^{-/-}$; Alx4 $^{-/-}$ double homozygous limbs (arrow in **d**) and only weakly apparent in Gli3 $^{-/-}$; Alx4 $^{+/-}$ mutant limbs (arrow in **e**). Limbs are oriented with anterior to the top and distal to the right. hu: humerus; ra: radius; ul: ulna.*

Skeletal abnormalities in *Gli3* $^{-/-}$; *Alx4* $^{-/-}$ double homozygous mutant limb are not caused by alterations of early limb bud patterning

SHH signalling is essential for anterior-posterior patterning of the zeugopod and autopod (Chiang et al 2001; Kraus et al., 2001). A single zeugopodal element forms in *Shh* deficient limb buds similar to *Gli3* $^{-/-}$; *Alx4* $^{-/-}$ double mutant limbs. Therefore, we analyzed *Shh* expression in *Gli3* $^{-/-}$; *Alx4* $^{-/-}$ mutant limb buds. However, *Shh* remains expressed in *Gli3/Alx4* single and compound mutant limb buds of E10.75 (Fig. 5a-d and data not shown), indicating that the defects in patterning of distal skeletal elements in *Gli3* $^{-/-}$; *Alx4* $^{-/-}$ mutant limb are not due to altered SHH signalling at this stage.

5'Hoxa and *5'Hoxd* genes regulate patterning of limb skeletal elements (Zakany et al., 1997). Therefore we analyzed the expression of *Hoxa11, Hoxd11* and *Hoxd13* in wild-type and *Gli3/Alx4* single and compound mutant limbs (Fig. 5e-p). The paralogous *Hoxa11* and *Hoxd11* genes interact to specify the ulna and radius (Davis et al., 1995). The absence of radius in *Gli3* $^{-/-}$; *Alx4* $^{-/-}$ double mutant limb buds suggest that *Hoxa11* or *Hoxd11* expression might be altered. However, normal levels of *Hoxa11* (Fig. 5h) and *Hoxd11* (Fig. 5l) transcripts are detected in *Gli3* $^{-/-}$; *Alx4* $^{-/-}$ double mutant limbs in comparison to wild-type limbs (Fig. 5e and i). At 11.5 *Hoxd13* expression is restricted to the distal limb mesenchyme in wild-type embryos (Fig. 5m), consistent with the role of *Hoxd13* in autopod patterning (Dolle et al., 1993). Misexpression of *Hoxd13* inhibits the formation of the zeugopod (Goff and Tabin, 1997). In *Gli3* $^{-/-}$; *Alx4* $^{-/-}$ double mutant limbs of E11.5 *Hoxd13* expression domain is confined to the autopodal region and no ectopic proximal expression is observed (Fig. 5p), indicating that the absence of the radius is not caused by altered *Hoxd13* expression. The expression domains of *Hoxa11, Hoxd11* and *Hoxd13* (Fig. 5h, l, p) in *Gli3* $^{-/-}$; *Alx4* $^{-/-}$ double mutant limbs are identical to *Gli3* $^{-/-}$ single mutant limb buds (Fig. 5f, j, n) and different from *Alx4* $^{-/-}$ single mutant limb buds (Fig. 5g, k, and o), indicating that *Gli3* acts upstream of *Alx4* in regulating *Hox* gene expression.

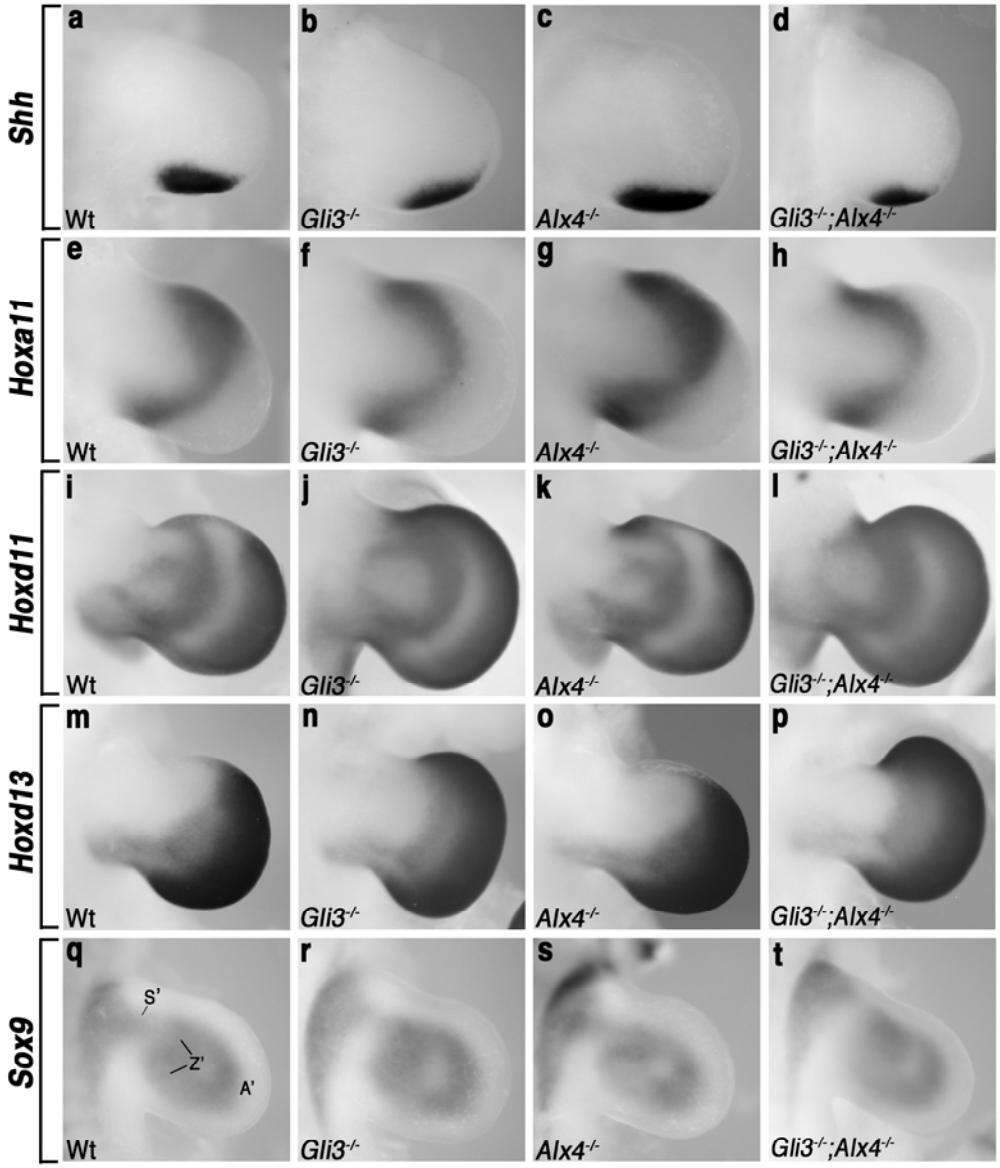

Fig. 5. *Molecular analysis of genes involved in limb bud patterning in (**a, e, i, m, q**) wild-type (wt), (**b, f, j, n, r**) Gli3 $^{-/-}$, (**c, g, k, o, s**) Alx4 $^{-/-}$ single homozygous and (**d, h, l, p, t**) Gli3 $^{-/-}$; Alx4 $^{-/-}$ double homozygous mutant limb buds. (**a-d**) Shh expression in wild-type and mutant limb buds (E10.75). There are no significant differences in Shh expression between wt and mutant limb buds. (**e-h**) Expression of Hoxa11 in wild-type and mutant limb buds (E11). Note that the Hoxa11 expression domain in Gli3 $^{-/-}$; Alx4 $^{-/-}$ mutant limb is identical to the one in Gli3 $^{-/-}$ mutant limb buds. (**i-l**) Hoxd11 expression in wt and mutant limb buds (E11.5). Again the Hoxd11 expression domain in Gli3 $^{-/-}$; Alx4 $^{-/-}$ double and Gli3 $^{-/-}$ single mutant limb buds are similar. (**m-p**) Hoxd13 expression is detected in distal limb mesenchyme of wt and mutant limb buds (E11.5). The Hoxd13 expression in Gli3 $^{-/-}$; Alx4 $^{-/-}$ double mutant limbs resembles the one of Gli3 $^{-/-}$ single mutant limb buds. (**q-t**) Sox9 expression in wt and mutant limb buds (E11). Sox9 is a marker of precartilagenous condensations. Comparison of wt and mutant embryos shows that no significant differences are apparent. S': prospective stylopod; Z': prospective zeugopod; A': prospective autopod. All limb buds are oriented with anterior to the top and distal to the right.*

Sox9 is expressed in cells of mesenchymal condensations that prefigure the limb skeletal elements (Wright et al., 1995). Analysis of *Sox9* expression reveals that the formation of mesenchymal condensations takes place in *Gli3* $^{-/-}$; *Alx4* $^{-/-}$ double mutant limbs of E11 (Fig. 5t), in a pattern similar to wild-type, *Gli3* $^{-/-}$ and *Alx4* $^{-/-}$ single mutant limb buds (Fig, 5q-s). These results indicate that the initial steps in cartilage formation are not affected in *Gli3* $^{-/-}$; *Alx4* $^{-/-}$ double mutant limbs.

As no striking changes are observed in expression of genes involved in limb bud patterning, this analysis cannot explain the *Gli3* $^{-/-}$; *Alx4* $^{-/-}$ double mutant limb skeletal phenotype. This suggests that the alterations specific for the *Gli3* $^{-/-}$; *Alx4* $^{-/-}$ limb phenotype are not a consequence of alterations in early limb bud patterning, but might rather result from defects in cartilage formation and/or differentiation.

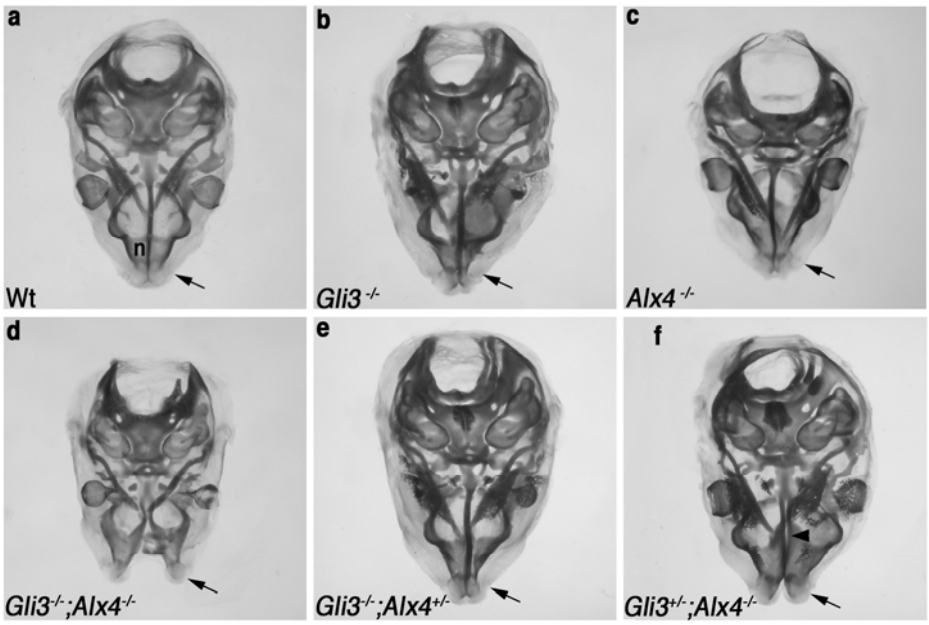

Fig. 6. *Analysis of the craniofacial skeleton reveals defects Gli3; Alx4 compound mutant embryos. Pictures show a dorsal view of the skulls of E14.5 embryos. Arrows point to the nasal bones in (**a**) wild-type, (**b**) Gli3* $^{-/-}$ *single, (**c**) Alx4* $^{-/-}$ *single, (**d**) Gli3* $^{-/-}$*; Alx4* $^{-/-}$ *double , (**e**) Gli3* $^{-/-}$*; Alx4* $^{+/-}$ *and (**f**) Gli3* $^{+/-}$*; Alx4* $^{-/-}$ *mutant embryos. (**d**) The nose region of Gli3* $^{-/-}$*; Alx4* $^{-/-}$ *double mutant embryos is clefted (arrow). (**f**) Gli3* $^{+/-}$*; Alx4* $^{-/-}$ *compound mutant embryos also show a cleft nasal tip (arrow) and a clefted nasal septum (arrowhead). n: nasal bone.*

Gli3 and *Alx4* interact synergistically during craniofacial development

In addition to the limb patterning defects, we detected craniofacial abnormalities in embryos deficient for both *Gli3* and *Alx4* (Fig. 6). Analysis of skeletal stains of E14.5 *Gli3/Alx4* single and double mutant skulls reveals synergistic genetic interactions between *Gli3* and *Alx4* during craniofacial development. The craniofacial phenotype observed in *Gli3* $^{-/-}$; *Alx4* $^{-/-}$ double mutant embryos includes severe clefting of the nose region (arrow, Fig. 6d), which is completely penetrant. The two lateral halves of the nasal cartilage are spaced wide apart. *Gli3* $^{+/-}$; *Alx4* $^{-/-}$ mutant skulls also display a split nasal tip and a cleft nasal septum (arrow, Fig. 6f), while no facial clefting is observed in all other genotypes.

Discussion

Skeletal analysis of *Gli3/Alx4* single and compound mutant limbs has uncovered additional roles for *Gli3* and *Alx4* in patterning of limb skeletal elements. The studies reveal a dose dependent requirement of *Gli3* and *Alx4* for normal stylopod patterning. Malformation of the stylopod has not been observed in *Gli3* and *Alx4* single homozygous mutant limbs, likely because of functional compensation. In addition, the zeugopod of *Gli3* $^{-/-}$; *Alx4* $^{-/-}$ double mutant limbs lacks the cartilage elements giving rise to the radius in forelimbs and the tibia in hindlimbs. The specific loss of the anterior zeugopodal cartilage element in *Gli3* $^{-/-}$; *Alx4* $^{-/-}$ double mutant limbs points to complementary functions of *Gli3* and *Alx4* in formation of the radius. However, truncation of the tibia in *Alx4* $^{-/-}$ and *Gli3* $^{-/-}$ single homozygous limbs has been reported before (Johnson, 1967; Qu et al., 1998), suggesting that both *Gli3* and *Alx4* function specifically during formation of the tibia. As disruption of either *Gli3* or *Alx4* results in polydactylous limbs, we expected a possible enhancement of the polydactylous phenotype in *Gli3* $^{-/-}$; *Alx4* $^{-/-}$ double mutant limbs. However, only five to six digits form in forelimbs and -in some cases- only four digits in hindlimbs of *Gli3* $^{-/-}$; *Alx4* $^{-/-}$ double mutant mice. One possible explanation for the mild or lack of polydactyly in *Gli3* $^{-/-}$; *Alx4* $^{-/-}$ double mutant limbs is the possible redundant or antagonistic functions of *Gli3* and *Alx4* during chondrogenesis in the anterior limb. Furthermore, digit identities are lost in limbs lacking *Gli3*. In contrast, *Alx4* $^{-/-}$ single and *Alx4* $^{-/-}$*; Gli3* $^{+/-}$ compound mutant limbs have digits with distinct identities, suggesting a specific role for *Gli3* in specification of digit identities (see also te Welscher et al., 2002b). Furthermore, *Gli3* is expressed by the interdigital mesenchyme (Hui and Joyner, 1993), whose regression is delayed in *Gli3* deficient and compound mutant limb buds. These results indicate that GLI3 normally promotes apoptosis of the interdigital mesenchyme. In agreement, apoptosis is reduced in limb buds of *Gli3* deficient embryos (Aoto et al., 2002). Severe nasal clefting is observed in *Gli3* $^{-/-}$; *Alx4* $^{-/-}$ double mutant embryos. Both *Gli3* and *Alx4* are expressed in mesenchyme of the frontonasal processes (Hui et al., 1994; Qu et al., 1997), where they might complement one another as nasal clefting is not observed in the skulls of *Gli3* $^{-/-}$ and *Alx4* $^{-/-}$ single homozygous embryos. Mild nasal clefting occurs already in *Gli3* $^{+/-}$; *Alx4* $^{-/-}$ compound mutant skulls, suggesting a dose dependent requirement for *Gli3* in the context of an *Alx4* deficiency during craniofacial development. Previously, it has been reported that *Alx4* is functionally redundant with *Cart1* and *Alx3* during patterning of the frontonasal regions (Qu et al., 1999; Beverdam et al., 2001). Double homozygous *Alx3* $^{-/-}$; *Alx4* $^{-/-}$ and *Alx4* $^{-/-}$*; Cart1* $^{-/-}$ embryos also display severe nasal clefting. The cleft nose phenotype of *Alx3* $^{-/-}$; *Alx4* $^{-/-}$ double homozygous embryos has been attributed to increased cell death affecting the presumptive nasal processes (Beverdam et al., 2001). In addition, the authors observed abnormal lateral outgrowth of nasal processes from early stages onwards, which may also underlie the defects in *Gli3* $^{-/-}$; *Alx4* $^{-/-}$ double mutant embryos.

Specific loss of radius and tibia has also been observed in limbs of other mouse mutant strains. For example, the zeugopod of forelimbs lacking both *Fgf4* and *Fgf8* consists of a single ulna cartilage (Sun et al., 2002). The radius also fails to form in the hyperplastic forelimb buds of retinoic acid-

rescued *Raldh2* $^{-/-}$ mutant embryos (Niederreither et al., 2002). Furthermore, hindlimbs of mice lacking the transcription factors *Pitx1* and *Pitx2* lack the tibia (Marcil et al., 2003). Reduction in limb bud size may explain the loss of limb skeletal elements in *Fgf4; Fgf8* and *Pitx1*$^{-/-}$; *Pitx2* $^{-/-}$ double mutant limbs (Sun et al., 2002; Marcil et al., 2003). However, the sizes of *Gli3* $^{-/-}$; *Alx4* $^{-/-}$ double mutant limb buds is comparable to wild-type limb buds. Therefore, reduction of cell numbers cannot account for the absence of the radius in *Gli3* $^{-/-}$; *Alx4* $^{-/-}$ double mutant limbs. The mouse mutation *Ulnaless* (*Ul*) affects limb development resulting in a severe reduction of both zeugopod skeletal elements. The *Ul* mutant phenotype can be attributed to deregulated *5'Hoxd* gene expression (Spitz et al., 2003), as proximal ectopic *Hoxd13* together with reduced *Hoxd11* expression is observed (Herault et al., 1997; Peichel et al., 1997). However, no specific alterations of *5'Hoxd* expression domains are observed in *Gli3* $^{-/-}$; *Alx4* $^{-/-}$ double mutant limb bud in comparison to *Gli3* $^{-/-}$ and *Alx4* $^{-/-}$ single mutant limb buds. Therefore, the molecular alterations causing truncation of the stylopod and loss of the anterior zeugopodal element in *Gli3* $^{-/-}$; *Alx4* $^{-/-}$ double mutant limbs remain unknown.

In forelimbs lacking both *Fgf4* and *Fgf8,* the numbers of skeletal progenitor cells that form the zeugopodal elements are reduced, likely resulting in loss of the radius (Sun et al., 2002). However, analysis of the *Sox9* distribution in *Gli3* $^{-/-}$; *Alx4* $^{-/-}$ double mutant limb buds indicates that the skeletal progenitor cells are normal. The apparently normal *Sox9* expression in *Gli3* $^{-/-}$; *Alx4* $^{-/-}$ double mutant limb buds suggests that formation of the chondrogenic mesenchymal condensations may be normal in these mutant limbs. In conclusion, the absence of the radius cartilage element in *Gli3* $^{-/-}$; *Alx4* $^{-/-}$ mutant embryos is most like not caused by an early patterning defect, but rather caused by defects in the precursor cells, which differentiate into chondrocytes to form the radius cartilage model.

Materials and Methods

Mouse strains and embryos

To obtain *Gli3* $^{-/-}$; *Alx4* $^{-/-}$ double homozygous mutant embryos *Gli3* $^{+/-}$; *Alx4* $^{+/-}$ double heterozygous mice were intercrossed. Embryos and mice were genotyped as described by te Welscher et al. (2002b). No double homozygous mutant embryos were recovered after embryonic day E15. Day of vaginal plug detected was considered as embryonic day 0.5.

Whole-mount in situ hybridization

Embryos dissected in PBS were fixed in 4% paraformaldehyde (PFA) and processed as described by (Haramis et al., 1995). Whole-mount *in situ* hybridization using digoxygenin-labeled antisense riboprobes was preformed as described by Haramis et al. (1995). Embryos were age-matched by determining their somite number (variation ± 2 somites).

Cartilage and bone staining

Embryos of E12.5 were fixed 5% TCA and subsequently stained with Alcian green to visualize the cartilage. Embryos were cleared with methyl salicylate.

Embryos of E14.5 were stained for cartilage and bone using standard Alcian blue and Alizarin red staining.

Acknowledgements

The authors are grateful to V. Portegijs and H. Goedemans for technical assistance. We thank G. Martin for providing the *Sox9* probe and F. Meijlink for advice. This study was supported by the faculty of biology, University of Utrecht, grants from the Dutch KNAW (to A.Z.) and NWO (to R.Z.).

Chapter 3

Differential responsiveness of limb bud mesenchyme to SHH signalling is mediated by secondary signals

Lia Panman[1], Gwen Soete[1,4], Gerhard K. H. Przemeck[3], Aimee Zuniga[1,2], Rolf Zeller[1,2]

[1]Department of Developmental Biology, Utrecht University, Padualaan 8, 3584 CH Utrecht, The Netherlands
[2]Developmental Genetics, Department of Clinical-Biological Sciences (DKBW), University of Basel Medical School, c/o Anatomy Institute, Pestalozzistrasse 20, CH-4056 Basel, Switzerland
[3]GSF, institute of Experimental Genetics, Ingolstaedter Landstrasse 1, D-85764 Neuherberg, Germany
[4]Present address: NIOB/KNAW Hubrecht Laboratorium, Uppsalalaan 8, 3584 CT Utrecht, The Netherlands

(Manuscript in preparation)

Summary

Patterning of the anterior-posterior axis of the vertebrate limb is controlled by mesenchymal cells of the polarising region (ZPA), which functions as a limb organizer. The signalling molecule *Sonic hedgehog (Shh)* is expressed by cells of the polarising region and gain- and loss-of-function studies have demonstrated that SHH signalling mediates the function of the limb organizer. SHH patterns the limb through activation of secondary signalling molecules like BMP2 and the BMP antagonist *Gremlin*. Here we show that SHH also regulates expression of the NOTCH ligand *Jagged-1* in the distal limb bud mesenchyme. Furthermore, activation of *Hey1,* a target of NOTCH signalling, is also dependent on SHH signalling and modulated by Jagged-1. *Shh* expressing cells grafted into wild-type and *Shh* deficient limb buds elicit a fast but differential response to SHH in mesenchymal cells. Limb bud mesenchymal cells respond to SHH signalling by differential activation of secondary signals. In *limb deformity* (*ld*) homozygous mutant limb buds, transduction of the SHH signal to the AER is disrupted. Analysis of *Jagged-1* and *Hey1* expression in *ld/ld* mutant limb buds establishes that these genes are regulated by mesenchymal-epithelial interactions, similar to *5'HoxD* genes. Furthermore, we provide evidence that SHH mediated regulation of *Jagged-1* participates in the development of the limb bud vascular system. Our results suggest that SHH acts upstream of *Jagged-1* during regulation of the limb bud vascular system.

Introduction

During vertebrate limb bud development, patterning of the anterior-posterior axis of the distal limb is under control of *Sonic Hedgehog* (SHH) signalling. *Shh* is expressed by cells of the polarising region (ZPA), which functions as a limb organizer (Riddle et al., 1993). Anterior grafts of *Shh* expressing cells induce digit duplications (Riddle et al., 1993) in a dose and time dependent manner (Yang et al., 1997), mimicking the activity of the ZPA. Formation of the digital arch is disrupted in *Shh* deficient embryos (Chiang et al., 1996; Chiang et al., 2001; Kraus et al., 2001). In addition, only one zeugopodal skeletal element forms in forelimbs of *Shh* deficient embryos (Chiang et al., 2001; Kraus et al., 2001). Targets of SHH signalling like *5'HoxD* genes*, Bmp2, Gremlin* and *Fgf4* are initially expressed in *Shh* $^{-/-}$ limbs (Zuniga et al., 1999; Chiang et al., 2001), suggesting that the limb mesenchyme is not nascent at the time it receives the SHH signal. Indeed, recently it has been shown that mutual antagonism between *Gli3* and *dHand* prepatterns the limb prior to *Shh* activation (te Welscher et al., 2002a). *Gli3* restricts *dHand* to posterior limb mesenchyme resulting in *Shh*-independent early activation of *Gremlin, Bmp2,* and *5'HoxD* genes in posterior limb bud (see Te Welscher et al., 2002a). Subsequently, *dHand* activates *Shh* expression in posterior mesenchyme (Charite et al., 2000). Activation of SHH

signalling is required for the maintenance of *Shh* target genes, as they are rapidly down-regulated in *Shh* deficient limb buds (Zuniga et al., 1999; Chiang et al., 2001). During subsequent limb bud development, *Gli3* and *Shh* are expressed in complementary domains due to mutual genetic repression (Masuya et al., 1995; Buscher et al., 1997; Wang et al., 2000). Furthermore, SHH signalling inhibits proteolytic cleavage of full-length GLI3 protein to a transcriptional repressor (Wang et al., 2000). The mouse *Extra-toes* (*Xt*) mutation disrupts the *Gli3* gene (Schimmang et al., 1992; Hui and Joyner, 1993), resulting in a polydactylous limb phenotype. Previously it was assumed that the polydactylous limb phenotype was a consequence of ectopic SHH signalling (Masuya et al., 1995; Buscher et al., 1997). However, analysis of *Gli3* $^{-/-}$*; Shh* $^{-/-}$ double mutant limbs has revealed that the polydactylous limb phenotype of *Gli3* $^{-/-}$ mutant limbs arises independently of SHH signalling (Litingtung et al., 2002; te Welscher et al., 2002b). Furthermore, analysis of these double mutant limbs shows that SHH establishes limb patterning through inhibition of GLI3 mediated transcriptional repression (te Welscher et al., 2002b).

The Hedgehog (HH) protein undergoes autocatalytic cleavage and is concomitantly linked to cholesterol (Porter et al., 1996), which is required cholesterol modification to exert its function in tissue patterning (Lewis et al., 2001; Cooper et al., 2003; Gallet et al., 2003). Because cholesterol modified HH proteins are attached to the surface membrane, it was assumed that SHH might signal short rather than long-range during vertebrate limb bud development. However, analysis of transgenic mice that express a mutant SHH protein that cannot be cholesterated establishes that cholesterol modification is necessary for long-range signalling (Lewis et al., 2001). In agreement, the distribution of cholesterol-modified SHH proteins exceeds the *Shh* expression domain by a considerable distance, indicating that the cholesterol modified SHH protein is able to move through the limb bud mesenchyme (Lewis et al., 2001).

SHH regulates anterior-posterior patterning of the limb bud through activation of secondary signalling molecules. For instance, experimental evidence indicates that SHH specifies digit identities in combination with BMP2 signalling (Yang et al., 1997; Drossopoulou et al., 2000). These studies resulted in the proposal that SHH signalling primes limb bud mesenchymal cells and induces BMP2, which in turn specify digit identities by acting on SHH-primed cells (Drossopoulou et al., 2000). Furthermore, the SHH signal is relayed to the apical ectodermal ridge (AER) by the BMP antagonist *Gremlin* (Zuniga et al., 1999; Khokha et al., 2003; Michos et al., submitted). The mouse *limb deformity* (*ld*) mutations directly disrupt *Gremlin* expression in the limb bud mesenchyme (Michos et al., submitted; Zuniga et al., submitted) and display the same limb phenotype as *Gremlin* $^{-/-}$ mutant mice. Establishment of feedback loop signalling between the SHH expressing polarising region and the AER is disrupted in embryos lacking Gremlin, which affects both the outgrowth and patterning of the distal limb bud (Haramis et al., 1995; Zuniga et al., 1999; Michos et al., submitted). *Shh* expression is not up-regulated in *ld/ld* mutant limb buds and activation of *Fgfs* and *Bmps* in the AER is disrupted (Haramis et al., 1995; Zuniga et al., 1999; Michos et al., submitted). Most likely as a consequence of disrupting the SHH/AER feedback loop, the

distal-anterior expansion of *5'HoxD* expression domains is delayed in *ld/ld* mutant limb buds (Haramis et al., 1995).

NOTCH signalling plays an important role in establishment of cell fates and boundaries in both invertebrates and vertebrates (reviewed by Artavanis-Tsakonas et al., 1999). From studies most in the *Drosophila* it is known that NOTCH signalling participates in patterning the wing disc (Irvine and Vogt, 1997), while much less is known about the potential functions of NOTCH signalling during appendages development in vertebrates. Several genes that are part of the NOTCH signalling pathway are expressed in vertebrate limb buds (Laufer et al., 1997; Mitsiadis et al., 1997, Rodriguez-Esteban et al., 1997; Jiang et al., 1998; Vargesson et al., 1998; Leimeister et al., 1999). For example, the NOTCH ligand *Jagged-2* is expressed by the AER and loss-of-function studies established that *Jagged-2* is required for regulation of AER morphology and function (Jiang et al., 1998). In contrast, *Jagged-1*, and *Hey1* are both expressed in distal limb bud mesenchyme during early limb bud development (Mitsiadis et al., 1997; Leimeister et al., 1999), indicative of possible roles in distal limb bud patterning. *Jagged-1* encodes a ligand for NOTCH receptors (Lindsell et al., 1995), while *Hey1* is downstream target of NOTCH signalling (Maier and Gessler, 2000). In humans, haploinsufficiency for *Jagged-1* causes the Alagille syndrome (Li et al., 1997; Oda et al., 1997) affecting heart, kidneys, face, skeleton and other organs. Mice lacking *Jagged-1* die during mid-gestation due to vascular defects (Xue et al., 1999), but fail to display Alagille syndrome like phenotypes. *Hey1* belongs to a subfamily of mammalian *Hairy-* and *Enhancer of Split* related genes (Leimaster et al., 1999). In *Drosophila,* genes encoded by the *Enhancer of Split* locus are primary targets of NOTCH signalling (reviewed by Artavanis-Tsakonas et al., 1999). Indeed, the *Hey1* promoter is responsive to NOTCH signalling (Maier and Gessler, 2000) and *Hey1* expression in the presomitic mesoderm is disrupted in mice lacking the NOTCH ligand *Delta-like3* (Dunwoodie et al., 2002). Here we establish that *Jagged-1* and *Hey1* expression in the limb bud mesenchyme depends on SHH signalling. We define the temporal and spatial kinetics of these and other genes in response to SHH signalling wild-type and mutant limb buds. Our studies provide first insights into differential mesenchymal response to SHH signalling and the kinetics of activating secondary signals to relay SHH signalling. Furthermore, we provide evidence that SHH acts upstream of *Jagged-1* during regulation of vascularization of the limb bud mesenchyme.

Results

During limb bud development, *Shh* targets are activated in a polarized fashion in the wild-type limb bud. To study the dynamics and range of SHH signalling in the limb bud, we examined the responsiveness of target genes to SHH signalling in wild-type and mutant limbs buds. Comparative analysis of *Shh* and its targets *Gremlin, Bmp2* and *Hoxd13* (Zuniga et al., 1999; Chiang et al., 2001) in wild-type limb buds between E10.25 and E10.75 (Fig. 1A-L) reveals their very dynamic and differential expression. *Shh* expression is initiated around E9.5 by the cells of the ZPA (Masuya et al., 1997). During

subsequent limb bud development, *Shh* expression levels increases and its expression is propagated distally in the posterior mesenchyme (Fig. 1A-C). In contrast, the expression of *Gremlin, Bmp2* and *5'HoxD* genes are expanded anteriorly within the distal limb bud mesenchyme (Fig. 1D-L; Duboule, 1992; Zuniga et al., 1999; Lewis et al., 2001). Furthermore, the *Shh* expression domain (Fig 1A-C; Riddle et al., 1993) abuts the one of *Gremlin* (Fig. 1G-I; Zuniga et al., 1999) and overlaps partially with the ones of *Bmp2* (Fig. 1D-F) and *Hoxd13* (Fig. 1J-L; Duprez et al., 1996). *Bmp2* expression is first activated in the AER (Fig.1D) and only subsequently in the limb mesenchyme (Fig. 1E), suggesting *Bmp2* may be a rather late target of SHH signalling in the limb bud mesenchyme. In contrast, *Gremlin* and *Hoxd13* are activated prior to and independent of SHH signalling in the posterior limb bud mesenchyme (Zuniga et al., 1999; Chiang et al., 2001).

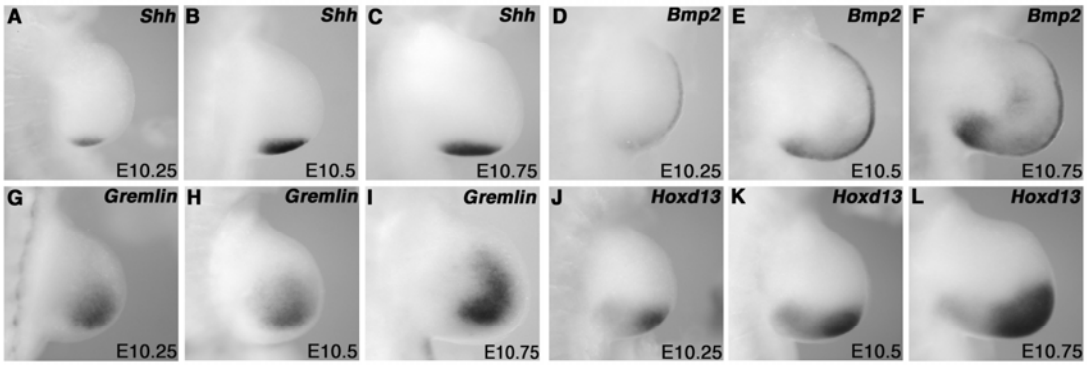

Fig. 1. *Distribution of Shh target genes in the forelimb bud during early stages of limb patterning. Expression pattern of Shh (A-C), Bmp2 (D-F), Gremlin (G-I) and Hoxd13 (J-L) in forelimb buds of wild-type (Wt) embryos between E10.25 and E10.75.*

Identification of *Jagged-1* and *Hey1* as novel mesenchymal targets of SHH signalling

Expression screening of NOTCH pathway ligands, receptors and targets in wild-type and *Shh* deficient mouse limb buds resulted in identification of *Jagged-1* and *Hey1* as SHH dependent target genes. In wild-type forelimb buds *Jagged-1* expression is activated around E10.25 (Fig. 2A). During subsequent limb bud development, *Jagged-1* expression is up-regulated and anteriorly expanded in the distal limb bud mesenchyme (Fig. 2A-C). *Hey1* expression is detected slightly prior *Jagged-1* (Fig. 2I) and regulated with kinetics similar to *Jagged-1* during later developmental stages (Fig. 2J, K). Neither *Jagged-1* (Fig. 2H) nor *Hey1* (Fig. 2P) are expressed in *Shh* deficient limb buds, which places both genes genetically downstream of SHH signalling in the limb bud mesenchyme. In *ld* mutant limb buds, *Shh* expression is not maintained due to lack of *Gremlin* (Zuniga et al., 1999; Michos et al., submitted). To establish whether expression of *Jagged-1* and *Hey1* is dependent on *Gremlin* mediated SHH/AER feedback signalling, we analyzed their expression in *Gremlin* deficient *ld* mutant limb buds. Both *Jagged-1* (Fig. 2E) and *Hey1* (Fig. 2M) are expressed at initially reduced level in *ld* mutant limbs and their subsequent up-regulation and anterior expansion (Fig. 2F, G, N, O) is delayed in *ld* mutant limb buds. The dynamic regulation of *Jagged-1* and *Hey1* expression in wild-type and *ld* mutant limb buds is reminiscent to *5'Hoxd* genes (Haramis et al., 1995), whose expression is also

modulated by SHH signalling (Riddle et al., 1993; Laufer et al., 1994; Chiang et al., 2001). Furthermore, both *Jagged-1* (Fig. 2D) and *Hey1* (Fig. 2L) expression is expanded anteriorly similar to *5'HoxD* genes in *Xt/Xt* mutant limb buds, which lack the *Gli3* gene (Schimmang et al., 1992; Hui and Joyner, 1993; Zuniga and Zeller, 1999). Transverse sections through the limb bud show that *Jagged-1* is expressed in the core mesenchyme like *5'HoxD* genes (Fig. 2S and data not shown), while *Gremlin* is restricted to the superficial dorsal and ventral limb bud mesenchyme (Fig. 2R; Merino et al., 1999). These results (Fig. 2S, R) show that targets of SHH signalling are activated in spatially restricted expression domains within the limb bud mesenchyme.

Fig. 2. *Analysis of Jagged-1 and Hey1 expression in wild-type and mutant limb buds with altered or no SHH signalling. (A-C) Jagged-1 expression in wild-type forelimb buds between E10.25 and E11. (D) Jagged-1 expression domain is anteriorly expanded in Xt/Xt forelimb buds (E11). (E-G) Delay of Jagged-1 expression in ld mutant forelimb buds. (H) Shh deficient forelimb buds (E10.5) lack Jagged-1 expression. (I-K) Hey1 expression in wild-type forelimb buds between E10.25 and E11. (L) Anterior expansion of Hey1 in Xt/Xt forelimb buds (E11). (M-O) Delay of Hey1 expression in ld mutant forelimb buds. (P) Hey1 expression is absent in*

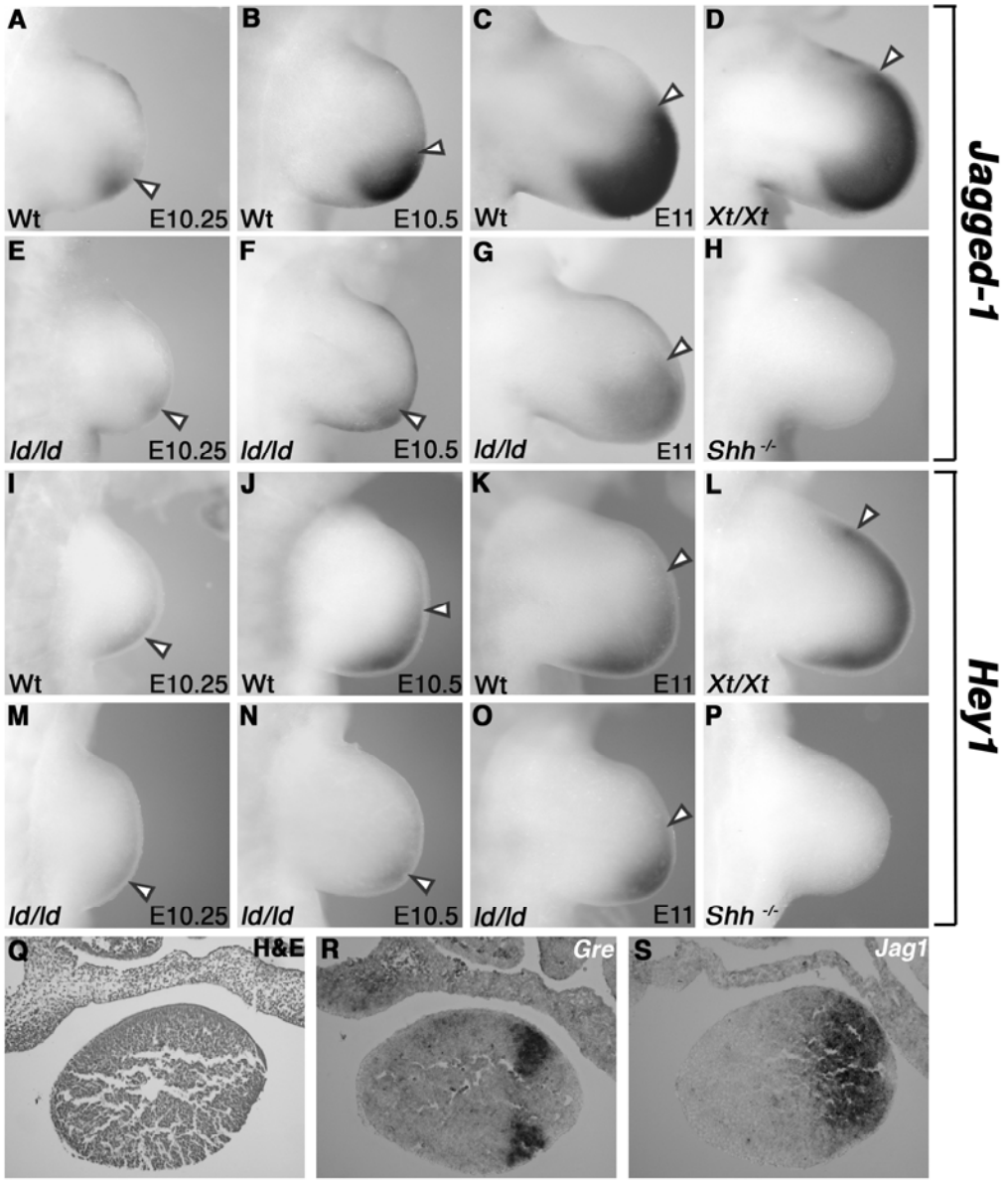

Shh $^{-/-}$ mutant forelimb bud (E10.5). Open arrowheads mark the anterior expression boundary.

(Q) Transverse section of limb stained with hematoxylin and eosin. (R) Gremlin is expressed in superficial dorsal and ventral limb bud mesenchymal cells. (S) Jagged-1 is expressed in the core mesenchyme of the limb bud. (A-P) Posterior is to the bottom and distal to the right. (Q-S) Posterior is to the right, ventral to the bottom.

Shh target genes respond differentially to ectopic anterior SHH signalling

To investigate the kinetics of differential responsiveness to SHH signalling, we performed a time course of gene induction following anterior placement of *Shh* expressing cells. We investigated ectopic gene activation after 3 to 22 hours of exposure to anterior *Shh* expressing cells in cultured mouse limb buds. None of the genes analyzed is induced after 3 hours in culture (data not shown). *Gli1,* which is a direct target of SHH signalling (Lee et al., 1997), is induced in cells around the graft after 6 hours of culture (Fig. 3A, B), thereby establishing the lower limit of direct mesenchymal response to SHH signalling in cultured mouse limb buds. Following 9 hours of culture *Gremlin* is induced in mesenchymal cells distal to the graft (Fig. 3C, D; Zuniga et al., 1999). Nine hours of exposure to ectopic SHH signalling also results in activation of *Jagged-1* (Fig. 3G, H) and *Hey1* (Fig. 3K, L). Also these genes are always induced distal to the graft and prolonged exposure to SHH signalling causes up-regulation of *Jagged-1* expression (Fig. 3I, J). *Bmp2* has been proposed as a transcriptional target mediating long-range SHH signalling (Laufer et al., 1994; Drossopoulou et al., 2000). Level of *Bmp2* transcripts is reduced in the limb bud mesenchyme and *Bmp2* is not activated in the AER of *Shh* deficient embryos (Fig. 4A; Chiang et al., 2001; Lewis et al., 2001). In chick limb buds, ectopic anterior SHH signalling induces ectopic *Bmp2* expression in both mesenchyme and AER (Laufer et al., 1994). However, no ectopic activation of *Bmp2* transcripts is detected in the mesenchyme of wild-type mouse limb buds after prolonged ectopic anterior SHH signalling (15 hours and 22 hours; Fig. 3E, F; data not shown), while *Bmp2* expression in the AER is expanded (Fig. 3E, F). These results show that *Shh* target genes, with the exception of *Bmp2*, are induced in the anterior limb bud mesenchyme of wild-type embryos within 6 to 9 hours after initiation of ectopic SHH signalling.

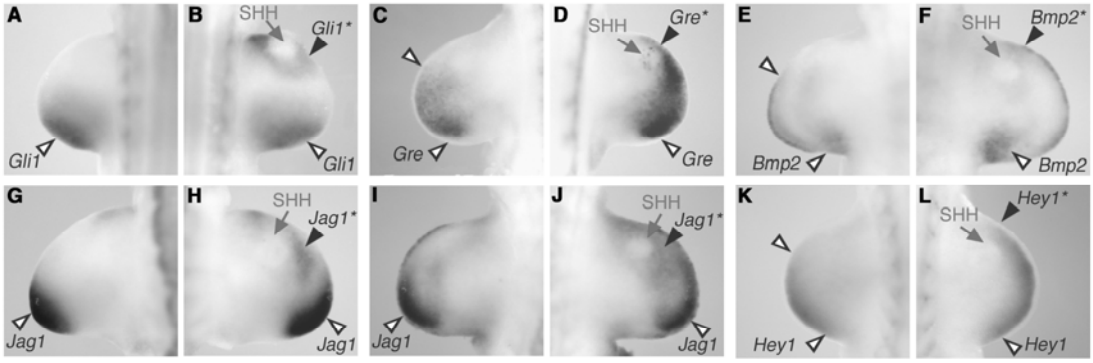

Fig. 3. *Differential responsiveness of genes to ectopic SHH signalling. Wild-type forelimb buds of E10.5 received an anterior graft of Shh expressing cells (arrow) and were cultured for 6, 9 or 15 hrs. Asterisks and filled arrowheads mark the ectopically induced expression domains. Open arrowheads the endogenous expression domains. (A) Endogenous Gli1 expression in cultured control limb bud. (B) SHH induces ectopic Gli1 transcripts after 6 hrs of culture. (C) Endogenous Gre expression in cultured control limb bud. (D) Ectopically induced Gre transcripts by Shh expressing cells after 9 hrs of culture. (E) Endogenous Bmp2 expression in cultured control limb bud. Note the posterior-proximal expression domain in the mesenchyme and AER expression. (F) Shh expressing cells induce anterior expansion of Bmp2 expression in the AER, after 15 hrs of culture. No expansion of Bmp2 expression in the mesenchyme was observed. (G) Endogenous Jagged-1 expression in control limb bud cultured for 9 hrs. (H) Ectopically induced Jagged-1 transcripts by Shh expressing cells after 9 hrs of culture. (I) Endogenous expression of Jag1 in control limb bud cultured for 15 hrs. (J) Ectopically induced Jagged-1 transcripts after 15 hrs of culture. (K) Endogenous Hey1 expression in cultured limb bud. (L) Ectopic Hey1 transcripts are induced after 9 hrs of culture by Shh expressing cells. Posterior is to the bottom.*

The mesenchyme of *Shh* deficient limb buds remains responsive to SHH signalling

Mesenchymal cells of *Shh* $^{-/-}$ mutant limb buds may lose their competence to respond to SHH signalling due to cell death (Chiang et al., 2001; te Welscher et al., 2002b) or posterior expansion of the transcriptional repressor GLI3 (Chiang et al., 2001). To establish whether *Shh* $^{-/-}$ mesenchymal limb bud cells remain responsive to SHH signalling, we grafted *Shh* expressing cells into the posterior limb bud mesenchyme of *Shh* $^{-/-}$ embryos (E10.5). While anterior grafts of *Shh* expressing cells fail to activate *Bmp2* expression in the mesenchyme (Fig. 3F), posterior grafts restore mesenchymal *Bmp2* expression in *Shh* $^{-/-}$ limb buds (Fig. 4A, B). Interestingly, mesenchymal *Bmp2* expression is always up-regulated proximally to the SHH graft, indicating that proximal limb bud cells responds differentially to SHH signalling (Fig. 4A, B). Also *Bmp2* expression in the AER is activated upon restoring SHH signalling (Fig. 4B). In *Shh* deficient limb buds, *Gre* expression is initiated but not maintained and propagated (Zuniga et al., 1999). Low levels of *Gre* transcripts remain in *Shh* $^{-/-}$ limb buds in culture (Fig. 4C). Posterior grafts of *Shh* expressing cells result in significant restoration of *Gre* expression in *Shh* mutant limb buds within 15 hours (Fig. 4D). Restoration of SHH signalling in *Shh* deficient limb buds also rescues *Jagged-1, Hey1* and *Hoxd13* expression (Fig. 4F, H and data not shown). The ability of *Shh* expressing cells to restore gene expression in the posterior mesenchyme of

Shh deficient limb buds shows that these cells have retained their responsiveness.

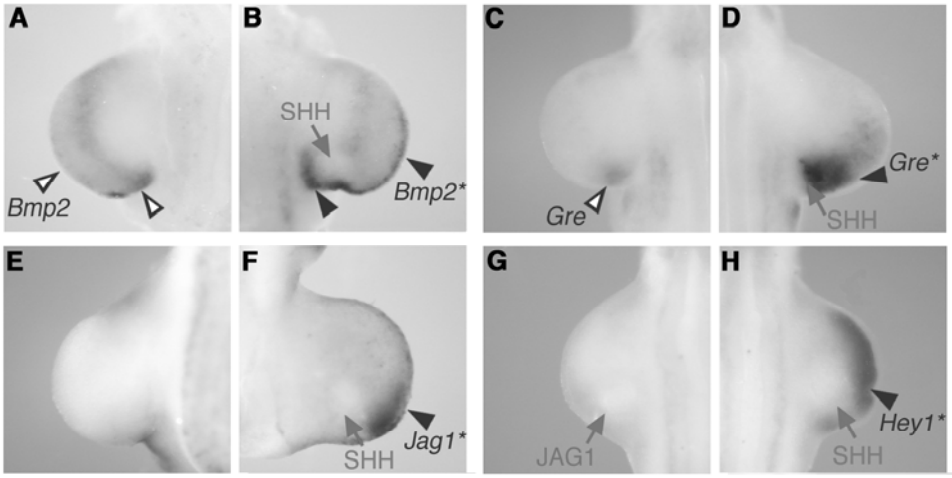

Fig. 4. *Shh expressing cells rescue target genes in Shh deficient limb buds. Shh deficient forelimb buds of E10.5 were grafted with Shh expressing cells and cultured for 15 hrs. Arrows indicate the position of Shh and Jagged1-Fc expressing cell aggregates. Asterisks and filled arrowheads mark induced transcripts. Open arrowheads mark the endogenous expression domains. (A) Bmp2 expression in control limb bud. Note the absence of Bmp2 transcripts in the AER and reduced mesenchymal expression. (B) Graft of Shh expressing cells rescue Bmp2 expression in the AER and up-regulates posterior-proximal Bmp2 expression. (C) Low levels of Gre transcripts are present in control limb bud. (D) Shh expressing cells up-regulate Gre expression. (E) Jag1 is not expressed in control limb bud. (F) Graft of Shh expressing cells rescue Jag1 expression in the limb bud. (G) Jag1 expressing cells are not able to induce Hey1 expression (H) Grafts of Shh expressing cells induce Hey1 expression. Posterior is to the bottom.*

Hey1 is a downstream target of *Jagged-1* in the limb bud mesenchyme

The SHH/AER the feedback loop is disrupted in *ld* mutant limb buds lacking *Gremlin* (Zuniga et al., 1999; Michos et al., submitted). Posterior grafts of *Shh* expressing cells into *ld* mutant limb buds progressively restores *Hey1* expression in culture (9 hours, (Fig. 5A, B); 15 hours, (Fig. 5C, D). *Jagged-1* expression is up-regulated in *ld* mutant limb buds with similar kinetics upon exposure to *Shh* expressing cells (data not shown). This prompted us to investigate the relationship between these genes further. As Jagged-1 is a NOTCH ligand and *Hey1* a target of NOTCH signalling, we hypothesized that *Jagged-1* may act upstream of *Hey1* during limb bud development. To ectopically activate Jagged-1 signalling in the limb bud mesenchyme, cells expressing a soluble form of *Jagged-1* were used (*Jagged1-fc*; Hicks et al., 2000). Previously, it has been shown that soluble Jagged1-fc protein interacts with NOTCH receptors (Shimizu et al., 1999; Hicks et al., 2000) to activate signal transduction (Varnum-Finney et al., 1998; Sestan et al., 1999). Rather unexpectedly, posterior grafts of *Jagged1-fc* expressing cells fail to restore *Hey1* expression in *Shh* deficient limb buds (Fig. 4G). This is in agreement with the fact that anterior grafts of *Jagged1-fc* expressing cells fail to induce *Hey1* expression in wild-type limb buds (data not shown). However, posterior grafts of *Jagged1-fc* expressing cells into *ld* mutant limb buds results in up-regulation of *Hey1* expression after 9 hours in culture (Fig. 5E, F). After 15 hours of culture, *Hey1* expression is even further up-regulated (Fig. 5G, H). Similar results were obtained using grafts of cells expressing the full-length

form of *Jagged-1* (data not shown). The ability of Jagged-1 to up-regulate *Hey1* expression in *ld* mutant limb buds, indicates that Jagged-1 functions to positively modulate *Hey1* expression in the limb bud mesenchyme rather than inducing its expression. Indeed, activation of *Hey1* precedes *Jagged-1* in wild-type limb buds (Fig. 2A, I). To confirm that Jagged-1 signalling regulates *Hey1* expression, we analyzed *Hey1* expression in embryos homozygous for the *Headturner* (*Htu*) mutation. A missense mutation in the *Jagged-1* gene causes the *Htu* phenotype (Kiernan et al., 2001), which is similar to the phenotype of *Jagged-1* null mutants (Xue et al., 1999). In agreement with gain-of-function experiments, *Hey1* expression is absent from *Htu* homozygous limb buds (Fig. 5I, J; E10.75). In contrast, *Gremlin* is normally expressed in the contralateral limb bud of the same embryo (Fig. 5K, L), indicating that *Gremlin* expression is independent of *Jagged-1* function.

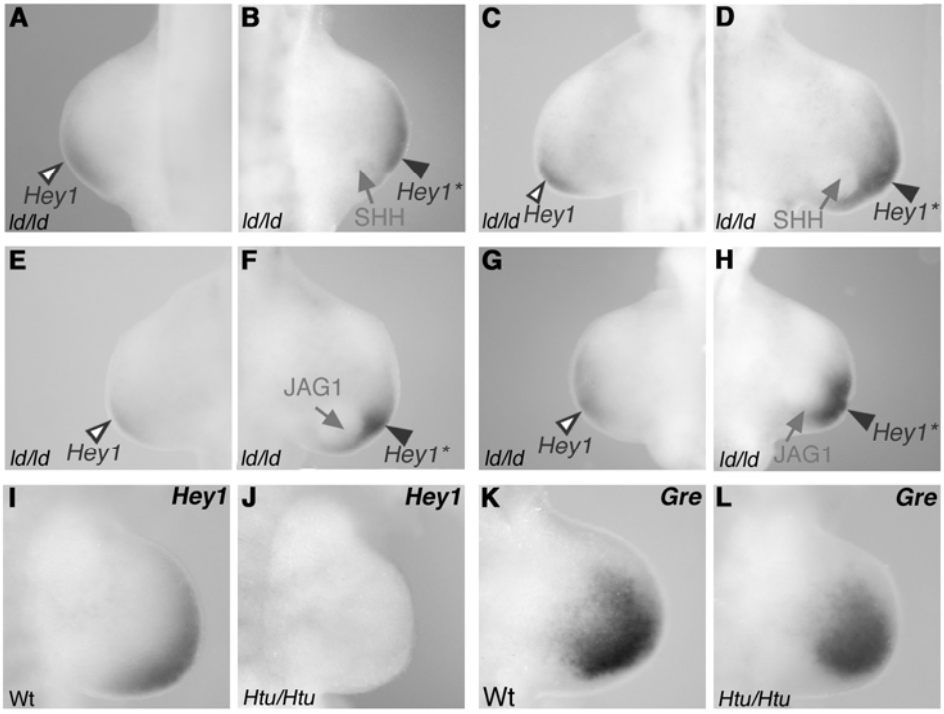

Fig. 5. *Jagged-1 modulates Hey1 expression in the limb bud mesenchyme. (A-H) ld mutant forelimb buds of E10.5 were cultured for 9 and 15 hrs and received a posterior graft of either Shh expressing cells or Jagged1-Fc expressing cells (arrows). Asterisks and filled arrowheads point to increased Hey1 expression in the grafted limb bud. Open arrowheads indicate the endogenous Hey1 expression domain in the control limb bud. (A) Endogenous*

Hey1 expression control limb bud cultured for 9 hrs. (B) Graft of Shh expressing cells up-regulate Hey1 expression after 9 hrs. (C) Endogenous Hey1 expression in control limb bud cultured for 15 hrs. (D) Up-regulation of Hey1 expression by graft of Shh expressing cells after 15 hrs of culture. (E) Endogenous Hey1 expression in ld mutant control limb bud cultured for 9 hrs. (F) Graft of Jagged1-Fc expressing cells up-regulate Hey1 expression after 9 hrs of culture. (G) Endogenous Hey1 expression in ld mutant control limb bud cultured for 15 hrs. (H) Up-regulation of Hey1 expression in limb buds that received graft of Jagged1-Fc expressing after 15 hrs of culture. (I-L) Hey1 and Gremlin expression in Wt and Htu mutant forelimb buds of E10.75. (I) Hey1 expression in a wild-type limb bud. (J) Hey1 expression is lost in Htu/Htu homozygous limb buds. Gremlin expression in (K) wild-type and (L) Htu/Htu homozygous limb buds, which are contralateral to the ones shown in I and J. Gremlin expression is normal in Htu mutant limb buds. Posterior is to the bottom.

Maintenance of the SHH/AER feedback loop in *ld* mutant limb bud rescues *Jagged-1* and *Hoxd13* expression

In *ld* mutant limb bud signalling between the mesenchyme and AER is disrupted, due to lack of *Gremlin* (Haramis et al., 1995; Zuniga et al., 1999). Posterior grafts of *Gremlin* or *Fgf4* expressing cells into *ld* mutant limb buds can restore the feedback loop between ZPA and AER within 9 hours (Fig. 6A-D). Posterior grafts of *Gremlin* and *Fgf4* expressing cells restore *Shh* (Fig. 6B, C) and in the case of *Gremlin* also *Fgf4* (Fig. 6D) expression after only 9 hours in culture. Furthermore, posterior grafts of *Gremlin* (Fig. 6E, F), *Fgf4* (Fig. 6G, H) and *Shh* (data not shown) expressing cells up-regulate *Jagged-1* expression in *ld* mutant limb buds after 15 hours. Similarly, grafts of *Gremlin* (Fig. 6I, J), *Fgf4* (Fig. 6K, L) and *Shh* (data not shown) expressing cells restore *Hoxd13* expression in posterior mesenchyme of *ld* mutant limb buds. These results show that Gremlin mediated establishment of feedback signalling between the *Shh* expressing polarizing region and the *Fgf* expressing AER regulates the dynamic expression of *Jagged-1* and *Hoxd13* in the limb bud mesenchyme.

Evidence for a role *Jagged-1* in patterning of the limb bud vascular system.

Notch signalling has been implicated in development of the vascular system. For instance *Jagged-1* deficient mice die because of defects affecting their vascular system (Xue et al., 1999; Kiernan et al., 2001). *EphrinB2* is specifically expressed by arteries (Wang et al., 1998; Adams et al., 1999) and SHH regulates *EphrinB2* expression in the dorsal aorta of zebrafish embryos by activation of NOTCH signalling (Lawson et al., 2002). Therefore, we analyzed the developing vascular system in *Shh* and *Jagged-1* deficient limb buds. In wild-type limb buds of E10.5, *EphrinB2* is expressed in the proximal and in the distal-posterior part of the limb bud mesenchyme (arrow Fig. 7A). By E11 *EphrinB2* is also expressed in the core mesenchyme of the limb bud (arrowhead Fig. 7C). However, in *Shh* deficient limb buds, *EphrinB2* expression is lacking from the distal-posterior mesenchyme (arrow Fig. 7B and D). In contrast, the proximal *EphrinB2* domain seems expanded distally in *Shh* $^{-/-}$ mutant limb buds in comparison their wild-type counterparts (arrowhead Fig. 7D). The endothelium of blood vessels was visualized using the PECAM1 antigen (Fig. 7E-H). No differences are observed between wild-type and *Shh* $^{-/-}$ mutant embryos during early limb bud development (Fig. 7E, F; E10.5). However, differences in the pattern of blood vessels became apparent during progression of limb bud development (Fig. 7G, H; E11). The

organisation of blood vessels in the core mesenchyme in *Shh* deficient limb buds differs from their wild-type counterparts (arrow Fig. 7G, H). Furthermore, *EphrinB2* is expressed in *Htu/+* limb buds similarly to wild-types (Fig 7I, J), while it is significantly down-regulated in both the limb bud mesenchyme of *Htu/Htu* homozygous embryos (Fig. 7K). Taken together, these results provide evidence for a role of SHH and Jagged-1 in patterning of the limb bud vascular system.

Fig. 6. *Jag1 and Hoxd13 expression depends on the maintenance of the SHH/AER feedback loop. Arrows indicate position of Fgf4 and Gremlin expressing cell aggregates. Asterisks and filled arrowheads mark induced transcripts. Open arrowheads mark the endogenous expression domains. (A-D) Restoration of feedback loop in ld homozygous limb buds by Gremlin and Fgf4. ld homozygous limb buds of E10.5 were cultured for 9 hrs. (A) Shh is expressed at reduced level in ld mutant limb buds. (B and C) Both Gre (B) and Fgf4 (C) expressing cells up-regulate Shh expression in ld mutant limb buds within 9 hrs (compare with control limb (A). (D) Grafts of Gre expressing cells restore Fgf4 expression in the AER within*

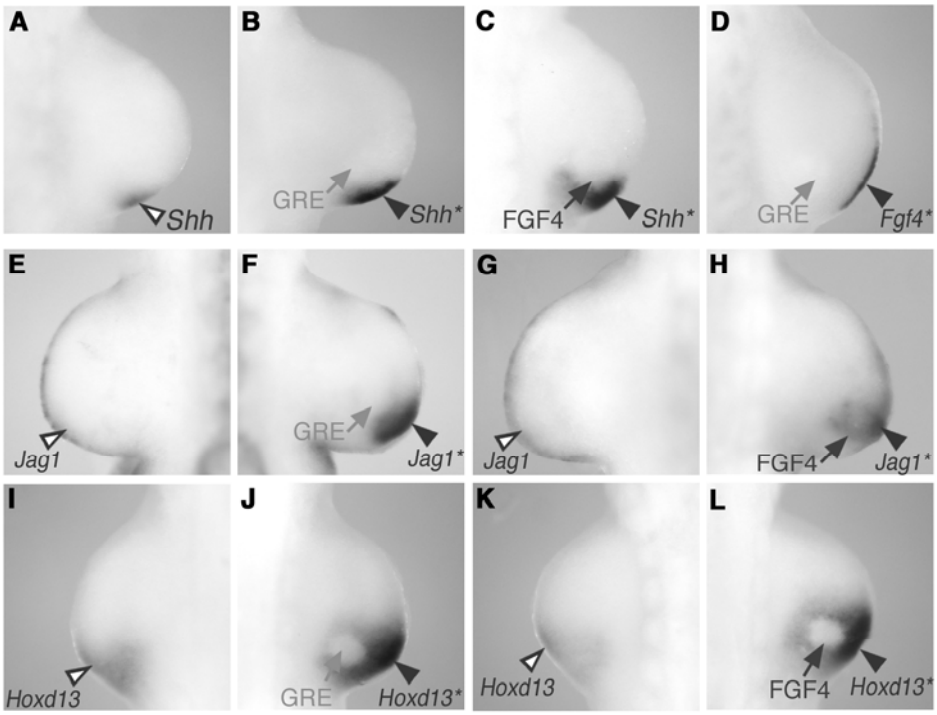

9 hrs. (E-L) Up-regulation of Jagged-1 and Hoxd13 expression in ld homozygous limb buds that have received a graft of Gre or Fgf4 expressing cell aggregates. ld homozygous limb buds were cultured for 15 hrs. (E) Endogenous Jagged-1 expression in cultured control limb bud. (F) Gre expressing cells up-regulate Jagged-1 expression. (G) Endogenous Jagged-1 expression in cultured control limb bud. (H) Up-regulation of Jagged-1 expression in cultured limb bud that received graft of Fgf4 expressing cells. (I) Endogenous Hoxd13 expression in cultured control limb bud. (J) Up-regulation of Hoxd13 expression in cultured limb bud that received graft of Gremlin expressing cells. (K) Endogenous Hoxd13 expression in cultured control limb bud. (L) Graft of Fgf4 expressing cells restore Hoxd13 expression in cultured limb bud. Posterior is to the bottom.

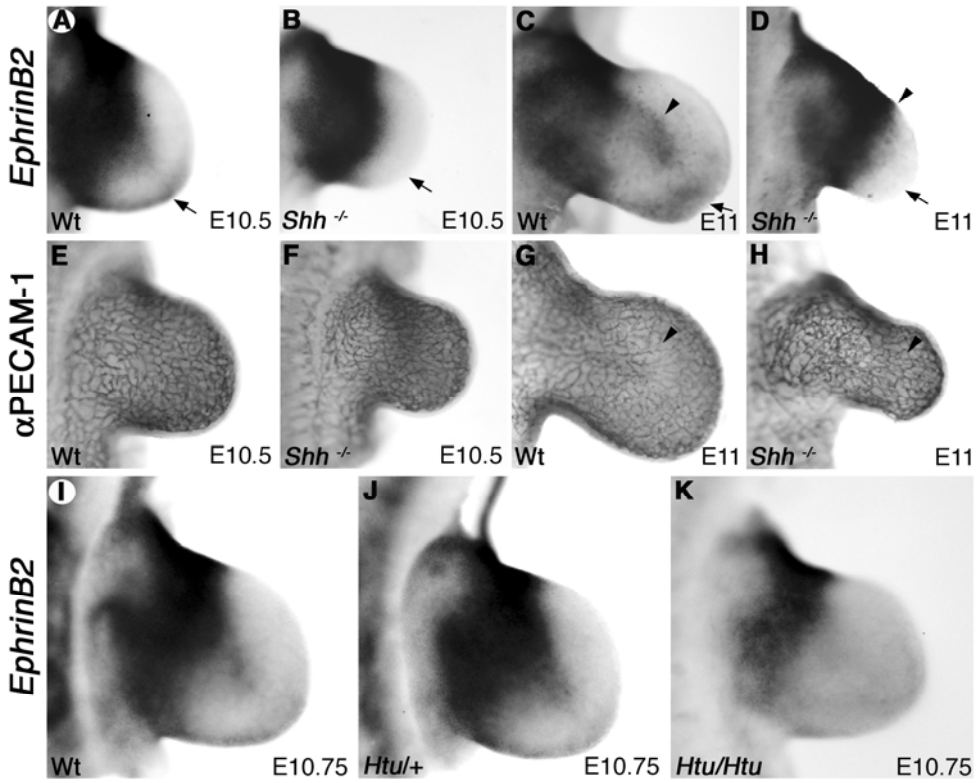

***Fig. 7**. SHH and Jagged-1 regulate development of the limb bud vascular system. (A-D) EphrinB2 expression in wild-type and Shh mutant forelimb buds. (A) EphrinB2 is expressed in proximal and distal-posterior mesenchyme in wild-type forelimb bud (E10.5; black arrow). (B) EphrinB2 expression is lost in distal-posterior limb bud mesenchyme of Shh deficient embryos (E10.5; black arrow). (C) At E11 EphrinB2 expression is observed in the core mesenchyme (black arrowhead) and in the posterior-distal mesenchyme (arrow) in wild-type limb buds. (D) EphrinB2 expression domain is expanded distally in Shh mutant limb buds (black arrowhead) and is lost in posterior-distal mesenchyme (arrow). (E-H) Endothelial lining of blood vessels is visualized by whole-mount immunohistochemistry with αPECAM-1 antibody. (E) Organization of blood vessels in wild-type limb buds (E10.5). (F) Organization of blood vessels in Shh deficient limb buds (E10.5). Note that at this stage no significant differences are observed between wildtype (E) and Shh (F) deficient limb buds. (G) Organization of blood vessels in wild-type limb buds (E11). (H) Organization of blood vessels in Shh deficient limb buds (E11). Note that at E11 the organisation of blood vessels in the core mesenchyme of Shh deficient limb buds differs from wild-type limb buds (arrows in G and H). (I-K) EphrinB2 expression in (I) wild-type, (J) Htu heterozygous and (K) Htu/Htu homozygous forelimb buds of E10.75. Note that mesenchymal expression of EphrinB2 is significantly reduced in Htu/Htu homozygous limb buds (K). Posterior is to the bottom, distal to the left.*

Discussion

In this study we provide evidence that mesenchymal responsiveness to SHH signalling is differential and activates secondary signals in a spatially and temporally restricted manner. In particular, we establish that SHH acts upstream of NOTCH signalling in the limb bud mesenchyme. Finally, we provide evidence that SHH signalling regulates patterning of the limb bud

vascular system through the NOTCH ligand Jagged-1, which may be essential to enable normal progression of limb bud morphogenesis.

Timing of induction and differential activation of *Shh* target genes

In wild-type mouse limb buds, anterior grafts of *Shh* expressing cells induce the direct transcriptional target *Gli1* (Lee et al., 1997) after 6 hrs. The other *Shh* targets examined in this study are induced by 9 hrs. It has been previously shown that response depends on the time cells are exposed to SHH signalling. Extended exposure to ectopic SHH signalling promotes the formation of more anterior digits in chicken limb buds and anterior expansion of gene expression domains (Francis et al., 1994; Yang et al., 1997; Drossopoulou et al., 2000). In general, expression of target genes is initiated in limb bud mesenchymal cells close to the source of SHH signalling and spreads in posterior-distal mesenchyme after prolonged exposure (this study, with exception of *Bmp2*). Grafts of *Shh* expressing cells restore gene expression in *Shh* deficient limb buds with kinetics similar to wild-type limb buds. Normally, *Shh* expression in posterior limb buds is first detected around E9.5. However, *Shh* cells grafted into *Shh* deficient limb buds around E10.5 are still able to induce or up-regulate all *Shh* target genes examined. By grafting *Shh* expressing cells into wild-type and mutant limb buds we also demonstrate that not all mesenchymal cells are competent to induce the same set of genes in response to SHH signalling. For instance, *Gli1* is induced in all the cells that receive SHH signal, while *Gremlin* is only induced in cells distal to the graft. Most strikingly, *Bmp2* is only activated by a very restricted subset of limb bud mesenchymal cells in response to SHH. Posterior grafts of *Shh* expressing cells into *Shh* $^{-/-}$ limb buds results in up-regulation of *Bmp2* expression specifically in proximal limb bud mesenchyme. In contrast *Bmp2* transcripts cannot be induced in anterior limb bud mesenchyme, while this is possible in chicken limb buds (Laufer et al., 1994; Yang et al., 1997; Drossopoulou et al., 2000). This discrepancy might be due to differences in experimental procedures, but more likely reflects a species difference. For example, in *Xt/Xt* homozygous mutant limb buds *Bmp2* remains expressed asymmetrically in mesenchyme, while its expression in AER is expanded anteriorly (Litingtung et al., 2002). In contrast to *Bmp2,* expression of all other *Shh* target genes like *5'HoxD* genes*, Gremlin, Jagged-1* and *Hey1* is expanded anteriorly in *Xt/Xt* mutant limb buds (Zuniga and Zeller, 1999; te Welscher et al., 2002a and b; this study)

Our study also shows that mesenchymal cells that have not received a SHH signal at the appropriate time do not lose their competence to respond and activate secondary signals in a differential fashion. This retention of differential responsiveness to SHH signalling indicates that the competence to activate target genes not only depends on SHH but also on independent other factors. Indeed, differential expression of *Gremlin, Bmp2* and *5'HoxD* genes is activated independent of SHH signalling in *Shh* deficient limb buds (Zuniga et al., 1999; Chiang et al., 2001; Lewis et al., 2001).

The mechanism by which SHH selectively regulates targets in the limb bud mesenchyme remains unknown. Interestingly, it was recently suggested that differential activation of *Hedgehog* target genes depends on apicobasel sorting of the Hedgehog protein (Gallet et al., 2003). In *Drososphila* larval ectoderm, Hedgehog protein sorted to the basolateral membrane activates

rho expression in posterior cells, while Hedgehog protein presented from the apical membrane activates *wg* expression in anterior cells (Gallet et al., 2003). As the Hedgehog signal transduction cascade is highly conserved, it is possible that differential responsiveness to SHH signalling could be regulated by a similar mechanism in the limb bud mesenchyme.

Mesenchymal responsiveness to SHH signalling in the absence of *Gremlin* mediated SHH/AER feedback signalling

The delay in up-regulation and anterior expansion of *Hoxd13* (Haramis et al., 1995), *Jagged-1* and *Hey1* expression in *ld* mutant limb buds lacking Gremlin function is likely caused by a disruption of mesenchymal-epithelial signalling. Posterior grafts of *Gremlin* and *Fgf4* expressing cells result in up-regulation of *Hoxd13* and *Jagged-1* expression in *ld* mutant limb buds. Up-regulation of these genes might be indirect through Gremlin/FGF mediated maintenance of SHH signalling. Indeed, posterior grafts of *Shh* expressing cells up-regulate these genes with similar kinetics (data not shown). However, posterior grafts of *Gremlin* expressing cells into *Shh* $^{-/-}$ mutant limb buds and anterior grafts in wild-type limb fail to induce *Hoxd13* and *Jagged-1* (data not shown). Furthermore it has been shown that ectopically applied FGF4 after AER removal only induces *Hoxd13* expression together with ectopic SHH signalling (Laufer et al., 1994). Taken together, these studies suggest that either activation or up-regulation of the expression of these genes depends critically on SHH signalling, while the subsequent modulation of their expression may depend on secondary signals, like Gremlin and FGF4 Indeed, Drossopoulou et al. (2000) proposed a model that SHH primes cells and renders them competent to respond to BMP2 signalling to specify digit identities (Drossopoulou et al., 2000).

Function of *Jagged-1* and *Hey1* during limb bud development

Analysis of *Jagged-1* and *Hey1* expression in mouse mutants with altered or no SHH signalling shows that these genes are targets of SHH signalling. Furthermore, mesenchymal-epithelial signalling interactions participate in modulating *Jagged-1* and *Hey1* expression in the limb bud mesenchyme. Analogous to the limb bud, expression of *Jagged-1* in dental mesenchyme during tooth development depends on epithelial-mesenchymal feedback signalling (Mitsiadis et al., 1997). The early lethality of *Jagged-1*$^{-/-}$ and *Htu/Htu* mutant mouse embryos (Xue et al., 1999; Kiernan et al., 2001) has so far precluded analysis of the phenotypic consequences of *Jagged-1* deficiency on limb development. Our analysis indicates that *Jagged-1* may only be critically required during progression of limb bud development and its expression in the limb bud mesenchyme is indeed only detected around E10.25, long after other genes like *Shh, Gremlin* and *5'HoxD* genes. Our gain- and loss-of-function analysis shows that *Jagged-1* positively modulates *Hey1* expression in the limb bud mesenchyme. Reduced *EphrinB2* expression in *Htu/Htu* mutant embryo reveals that *Jagged-1* might regulate the vascular system in the limb bud mesenchyme, like it has been shown for other embryonic structures (Xue et al. 1999). During vascular development, *EphrinB2* is expressed in arterial endothelium and is required for angiogenic vascular remodelling (Wang et al., 1998; Adams et al., 1999). Analysis of several NOTCH signalling pathway mutants has demonstrated that NOTCH

signalling pathway plays an important role during angiogenesis (reviewed by (Gridley, 2001). Furthermore ligands and receptors of the NOTCH signalling pathway are expressed in arterial vessels of mouse embryos (Villa et al., 2001). Interestingly, studies in the zebrafish have revealed that SHH signalling is required for arterial differentiation. SHH acts upstream of the NOTCH pathway in regulating artery specific *EphrinB2* expression (Lawson et al., 2002). Furthermore it has been shown that SHH induces angiogenic factors and thereby promotes angiogenesis (Pola et al., 2001). Analysis of *Shh* deficient limb buds indeed reveals changes in both *EphrinB2* and PECAM-1 expression, which points to a requirement of SHH in patterning of the vascular system in the vertebrate limb bud. These results suggest that SHH modulates development of the limb bud vascular system through regulation of the NOTCH ligand Jagged-1in the mesenchyme.

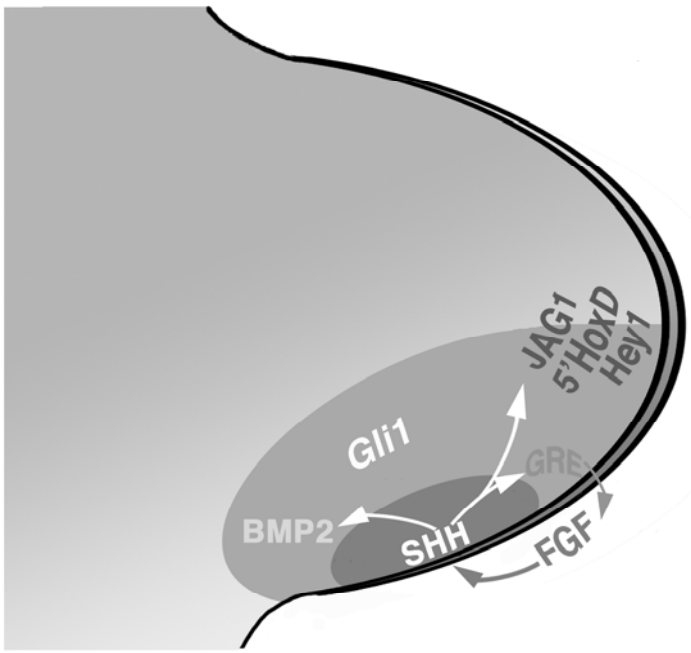

Fig. 8. *Limb bud mesenchymal cells respond differentially to SHH signalling. SHH signalling by cells of the polarizing region induces Gli1 expression in the posterior half of the limb bud, indicating direct response to SHH signalling. The SHH signal is relayed to the AER by activation of Gremlin in distal-posterior mesenchymal cells. In turn, FGF signalling from the AER maintains SHH signalling by the polarising region. SHH induces Bmp2 expression in proximal limb bud cells, while Jagged-1, Hey1 and HoxD13 are induced in the distal cells of the limb bud mesenchyme.*

In summary this study establishes the kinetics of differential mesenchymal responsiveness to SHH signalling in mouse limb buds (Fig. 8). SHH regulates *Bmp2* expression in the proximal limb bud mesenchyme, while it regulates other target genes like *Jagged-1, Hey1* and *5'HoxD* genes in distal limb bud mesenchyme. As a consequence limb bud cells will receive and activate different signals depending on their positions in the limb bud, which may trigger their differentiation into the appropriate cell-types according to their position. SHH achieves its long-range influence on limb patterning by induction of signal relays. For example the SHH signal is relayed to the AER by the BMP antagonist Gremlin and FGF signalling by the AER maintains *Shh* expression. The GRE/FGF mediated maintenance of SHH signalling is required for the proper initiation and propagation of *Jagged-1, Hey1* and *5'HoxD* gene expression in the distal limb bud mesenchyme. In addition, it has been proposed that SHH regulates specification of digit identities through induction of BMP2 signalling (Drossopoulou et al., 2000). And in this study we provide

evidence that SHH modulates the limb bud vascular system through induction of Jagged-1 signalling.

Materials and Methods

Mouse strains and embryos

To obtain *ld/ld* mutant embryos homozygous mice carrying the *ld* ^{ln2} allele were intercrossed. For *Xt* homozygous embryos, mice heterozygous for the *Xt*^{J} allele were intercrossed and genotyped as described by Buscher et al. (1997). *Shh* deficient embryos were obtained by intercrossing *Shh* heterozygous mice and genotyped as described by St-Jacques et al., (1998). *Htu/Htu* mutant embryos were obtained and genotyped as described by Kiernan et al. (2001). The day of vaginal plug detection was considered as day 0.5. Wild-type and mutant embryos were age-matched according to their somite number (variation of ± 2 somites).

Whole-mount *in situ* hybridization

Whole-mount *in situ* hybridization using digoxygenin-labeled antisense riboprobes was preformed as described by Haramis et al. (1995). For embryos hybridized with *EphrinB2* probe the protocol was modified as follows: embryos were stained with BM Purple containing levamisole (2 mM) overnight at 4ºC. Stained embryos were fixed with 2% PFA/0.1% gluteraldehyde in PBS overnight at 4ºC. Subsequently embryos were dehydrated and cleared with benzylbenzoate/benzylalcohol 2:1.

In situ hybridization on section

Embryos were fixed with 4% Paraformaldehyde (PFA), embedded in paraffin wax and sectioned. Dewaxed sections were counterstained with haematoxylin and eosin. *In situ* hybridization on sections was preformed as described by Dono et al. (1998).

Whole-mount immunohistochemistry

Embryos were fixed with 4% PFA and stained with primary monoclonal antibody against PECAM-1 (Pharmingen, clone MEC13.3, isotype rat, 1:100 dilution) and secondary antibody against rat IgG, and avidin conjugated peroxidase (Rat IgG VECTA-STAIN ABC kit, dilution 1:100). After staining embryos were fixed with 2% PFA, 0.1% gluteraldehyde in PBS overnight at 4ºC and afterwards cleared in glycerol.

In Vitro grafting and culturing of mouse limb buds (trunk cultures)

Mouse forelimb buds were cultured and grafted as described (Zuniga et al., 1999) with some modifications. Trunks with attached fore limb buds were isolated from wild-type, *ld/ld* mutant and *Shh* $^{-/-}$ mutant embryos of E10.5. After isolation non-proliferating, spherical cell aggregates (see below) were

grafted in the forelimb and trunks were subsequently cultured for either 6, 9,15, or 22 hrs. The fragments were cultured in serum free, 1× high glucose DMEM (Gibco) medium, supplemented with L-glutamine, penicillin/streptomycin, non-essential amino acids, sodium pyruvate, D-glucose, L-ascorbic acid, lactic acid, d-biotin, vitamin B12 and PABA in 6.5% CO2 at 37 °C. Cultured trunks were fixed in 4% PFA o/n at 4 °C. Each result could be reproduced at least 3 times in independent experiments.

Preparation of cell aggregates for grafting

QT6 cells expressing *Shh*, *Gremlin* (Zuniga et al., 1999), *Fgf4* (full-length coding sequence (Hebert et al., 1990) was cloned into pRc/CMV vector (Invitrogen)) and *Jagged1-Fc* (soluble form of Jagged-1; Hicks et al., 2000) under control of the CMV promoter were obtained by standard calcium phosphate transfection. One day after transfection, cell aggregates were prepared by plating the transfected cells at high density on bacterial plates. The day after cells were treated with mitomycin-C for one hour, blocking cell proliferation irreversibly. After washing the cells with PBS, the cells were grafted into the limb.

Acknowledgements

The authors are grateful to H. Goedemans, T. Drenth and O. Michos for technical assistance. We thank C. Mummery and F. Guillemot for providing probes for *in situ* hybridization and G. Weinmaster for providing the *Jagged-1* expression constructs. This research was supported by the Faculty of Biology at Utrecht University, grants from the Dutch KNAW (to A.Z.) and NWO (to R.Z.).

Chapter 4

Gremlin propagates the dynamic epithelial-mesenchymal signalling interactions regulating limb bud development

Odyssé Michos[1,2], Lia Panman[2], Rosanna Dono[2], Kristina Vintersten[3,5], Konstantin Beier[4], Rolf Zeller[1,2] and Aimée Zuniga[1,2]

[1]Developmental Genetics, Dept. of Clinical-Biological Sciences (DKBW), University of Basel Medical School, c/o Anatomy Institute, Pestalozzistrasse 20, CH-4056 Basel, Switzerland, [2]Dept. of Developmental Biology, Utrecht University, Padualaan 8, NL-3584CH Utrecht, The Netherlands, [3]Transgenic Service, EMBL, Meyerhofstrasse 1, D-69117 Heidelberg, Germany, [4]Dept. of Histology, Anatomy Institute, Pestalozzistrasse 20, CH-4056 Basel, Switzerland.
[5]Present address: Mount Sinai Hospital, Samuel Lunenfeld Research Institute, Stem Cell Mutagenesis Laboratory, 600 University Avenue, Toronto, Ontario M5G1X5, Canada.

(Submitted)

Abstract

Functions of the BMP antagonist *Gremlin* (also called *Drm* or *Cktsf1b1*) were analyzed by generating a loss-of-function mutation in the mouse. Such *Gremlin* deficiency results in neonatal lethality due to lack of kidneys and defects in lung organogenesis. During limb bud development, *Gremlin* is required early in the mesenchyme to induce maturation of the apical ectodermal ridge and feedback signalling that propagates the *Sonic hedgehog* morphogen. In the absence of *Gremlin* mesenchymal-epithelial signalling is not established and mesenchymal cells undergo massive apoptosis. Thus *Gremlin* mediated BMP antagonism controls the dynamic epithelial-mesenchymal signalling that regulates limb bud development and cell survival

Introduction

Vertebrate organogenesis is orchestrated by signalling centres with organizer properties that dynamically coordinate cell proliferation and survival with cell specification and differentiation. In particular, two main signalling centres control limb bud development, the *Sonic hedgehog* (*Shh*) expressing polarizing region which is located in the posterior limb bud mesenchyme, and the apical ectodermal ridge (AER), a differentiated columnar epithelium expressing different types of signalling peptides. SHH signalling by the polarizing region controls patterning of distal limb structures and its expression is regulated by fibroblast growth factor (FGF) signalling from the AER (SHH/FGF feedback loop) (Panman and Zeller, 2003). Genetic analysis in the mouse indicates that the AER expressed FGFs, such as FGF8 and FGF4, cooperate to activate and positively regulate *Shh* expression in the posterior limb bud mesenchyme (Lewandoski et al., 2000; Moon and Capecchi, 2000; Sun et al., 2002). The bone morphogenetic protein (BMP) antagonist *Gremlin* (Hsu et al., 1998) is a cystein knot protein belonging to the CAN family that antagonizes preferentially BMP2 and BMP4 (Avsian-Kretchmer and Hsueh, 2003). *Gremlin* is expressed by a subset of SHH responsive mesenchymal cells and has been implicated in transducing the SHH signal to the posterior AER. This results in activation of *Fgf4* expression and establishment of the SHH/FGF4 feedback loop (Capdevila et al., 1999; Zuniga et al., 1999).

To study function of the BMP antagonist *Gremlin* during limb development, we have deleted the *Gremlin* open reading frame (ORF) by homologous recombination in mouse ES-cells. *Gremlin* deficient mice die shortly after birth due to disruption of kidney and lung organogenesis. During limb bud development, *Gremlin* is required for survival of core mesenchymal cells, AER maturation and activation of different types of AER signals, which regulate *Shh* expression and progression of limb bud morphogenesis.

Results

Disruption of the *Gremlin* ORF results in a *limb deformity* (*ld*) phenotype.

The *Gremlin* gene was inactivated by homologous recombination in R1 ES-cells as shown in **Figure 1a**. The complete *Gremlin* ORF (exon 2) was deleted and replaced by a *LacZ* marker and a *Neomycin* resistance (*Neo*^{R}) gene flanked by two *lox*P sites. Correctly targeted ES-cell clones were identified by Southern blot screening (**Fig. 1b, c**) and two independent clones were used to generate *Gre* $^{\Delta ORF}$ mice (**Fig. 1d**). Heterozygous mice of both strains appear normal and the distribution of *Gremlin* and *Gre-LacZ* fusion transcripts (**Fig. 1a**) are identical (**Fig. 1e**). In contrast, *Gre* $^{\Delta ORF}$ homozygous newborn mice display an *ld* limb phenotype together with complete renal agenesis and lung defects (**Fig. 2** and data not shown) that cause lethality shortly after birth. Cre recombinase mediated removal of the *Neo*^{R} gene does not alter the phenotypes, confirming that they are caused by loss of *Gremlin* function (data not shown). Genetic analysis reveals that the *Gre* $^{\Delta ORF}$ mutation belongs to the same complementation group as several of the available *ld* alleles (Zuniga et al., submitted and data not shown). Indeed, *Gremlin* and *Formin* are regulated by a shared cis-regulatory element (Zuniga et al., submitted).

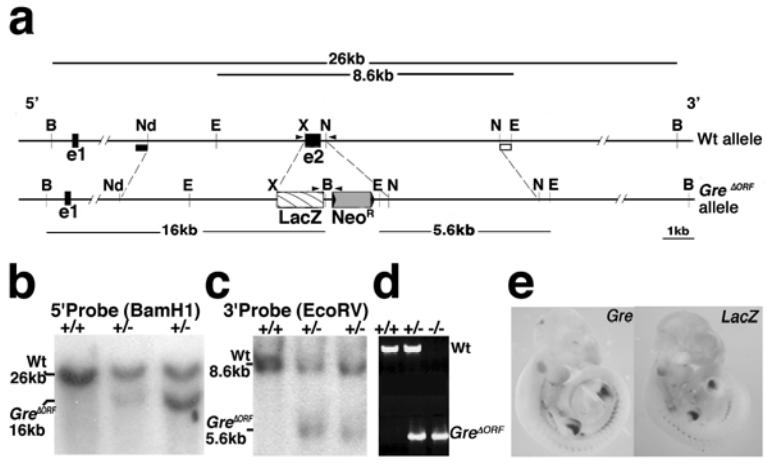

FFig. 1. *The Gremlin null allele disrupts the ORF encoded by exon 2. (**a**) Scheme: The Gre* $^{\Delta ORF}$ *loss-of-function allele was generated by homologous recombination in ES-cells. The entire ORF encoded by exon 2 (e2) was replaced with an IRES-LacZ gene and the Neo*^{R} *cassette (flanked by loxP sites indicated by black triangles). Exon 1 (e1) is non-coding and located 8.5 kb upstream of exon 2. The 5' and 3' genomic probes used to screen ES-cell clones by Southern blotting are indicated by black and white boxes respectively. Thin black lines indicate the sizes of the expected genomic bands detected by these probes. Arrowheads indicate the primers used to detect both wild-type (Wt) and mutant alleles (Gre* $^{\Delta ORF}$*). (**b, c**) Analysis of wild-type (+/+) and correctly targeted heterozygous (+/-) ES-cell clones by Southern blotting using 5' and 3' genomic probes. (**d**) PCR genotyping of embryos of F2 littermate embryos. (**e**) Whole mount in situ hybridization using Gre* $^{\Delta ORF/+}$ *embryos at embryonic day 11.0 reveals the identical distribution of Gremlin and LacZ transcripts.*

The limb phenotypes observed in *Gremlin* deficient mice correspond to the strongest and fully penetrant *ld* limb phenotypes (**Figs 2a-h**). The zeugopods are differentially affected as ulna and radius fuse during onset of ossification, while only one skeletal element forms in hind limbs (arrowheads, **Fig. 2b, d**). The autopods are severely truncated due to metacarpal fusions (arrowheads, **Fig. 2f, h**), reductions and fusions of digits with associated loss

of posterior identities and soft tissue webbing ((**Fig. 2f, h**) and data not shown).

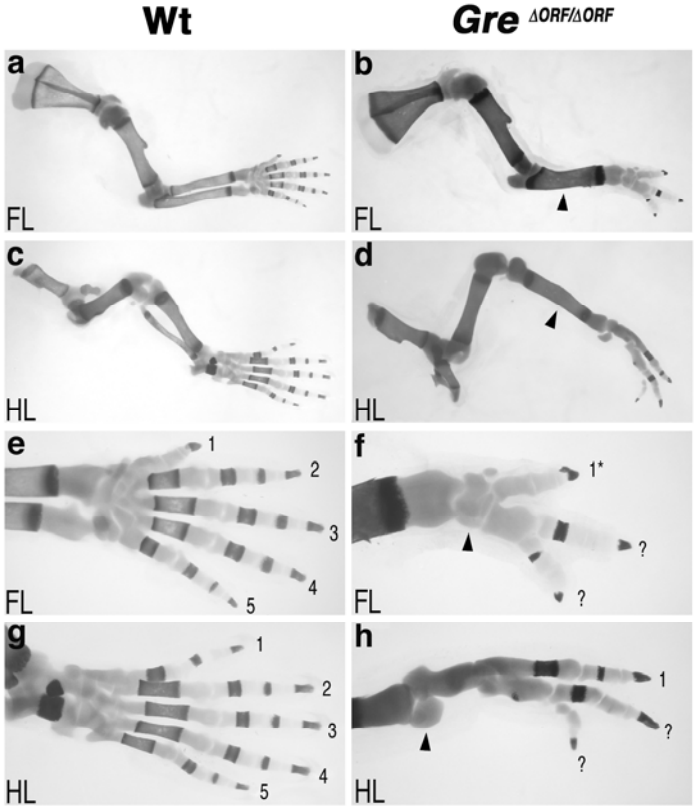

***Fig. 2**. The Gremlin deficiency causes a limb deformity phenotype. (**a-h**) Limb skeletal abnormalities in Gre $^{\Delta ORF}$ homozygous newborn mice. (**a, b, e, f**) fore limbs, (**c, d, g, h**) hind limbs. Arrowheads point to the fused ulna and radius in fore limbs (**b**) and the one zeugopodal bone formed in hind limbs (**d**). Arrowheads point to fused metacarpal bones (**f, h**). Digit numbers are reduced and identities lost in Gre $^{\Delta ORF/\Delta ORF}$ limbs. Asterisk indicates a fused digit 1 (**f**). Question marks indicate posterior digits with unclear identities (**f, h**).*

Gremlin controls AER maturation and epithelial-mesenchymal signalling in limb buds

During limb bud morphogenesis, reciprocal signalling between the polarizing region and the AER regulates the dynamic cell-cell interactions linking growth and patterning. During limb bud morphogenesis, the size of the *Shh* domain and transcript levels increase in wild-type embryos (Riddle et al., 1993) (**Fig. 3a**). In contrast, *Shh* transcription is not up-regulated and its expression domain remains small in limb buds of *Gre* $^{\Delta ORF}$ homozygous embryos (**Fig. 3a**). This failure to propagate SHH signalling has been attributed to disruption of the SHH/FGF4 feedback loop (Haramis et al., 1995; Zuniga et al., 1999; Khokha et al., 2003). However, analysis of *Gre* $^{\Delta ORF}$ homozygous embryos reveals a much earlier and general disruption of AER signalling (**Fig. 3b and Fig.4**). During the onset of limb bud development (**Fig. 3b**), the *Fgf8* expressing AER cells are more spread along the dorso-ventral ectoderm in *Gremlin* deficient limb buds, indicative of defects already during AER formation. However, around E10.25 *Fgf8* expressing cells become restricted to the apex, but the domain remains patchy (**Fig. 3b** and data not shown), owing to defects in AER morphology (**Fig. 4e**). FGF signalling by the differentiated posterior AER (Martin, 1998) is also disrupted as neither *Fgf4* (Chan et al., 1995; Haramis et al., 1995), nor *Fgf9* and *Fgf17* (**Fig. 3b** and data not shown) are expressed in *Gremlin* mutant limb buds.

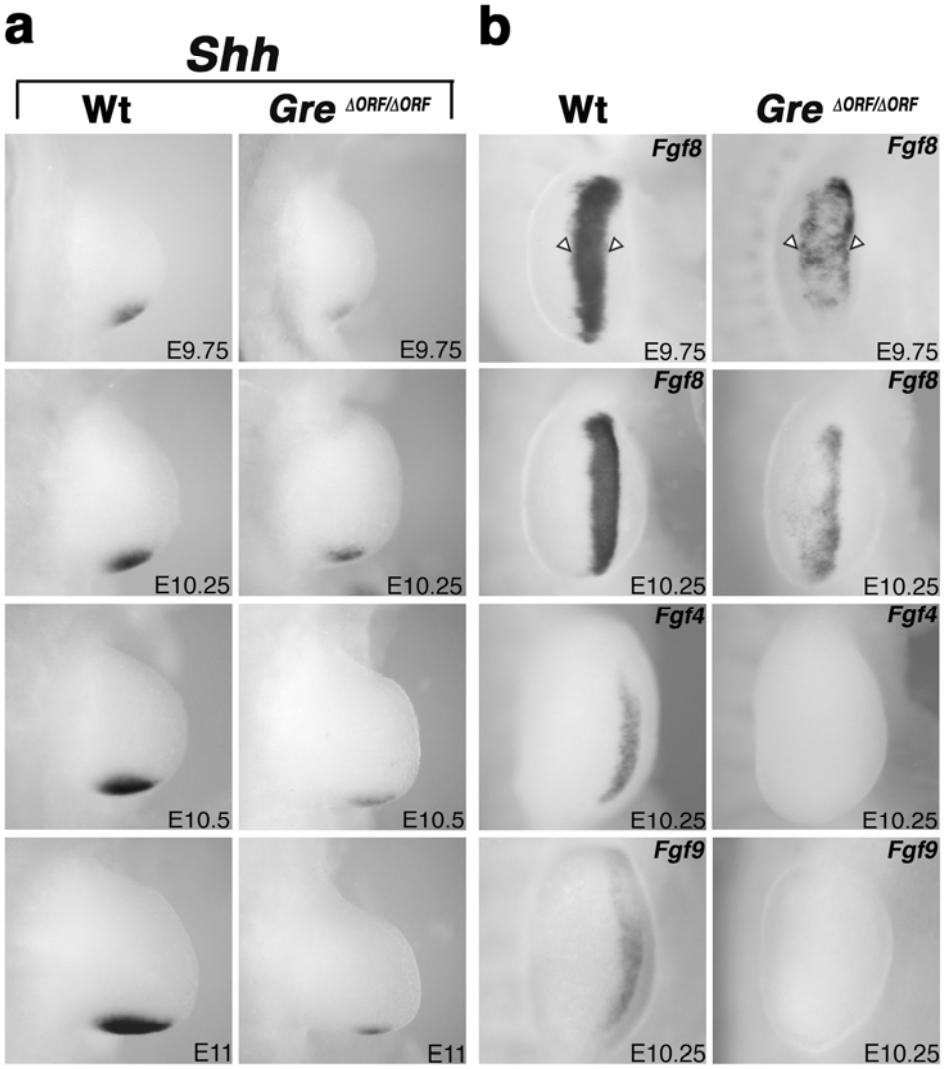

***Fig. 3**. Disruption of SHH/FGF feedback loop in Gremlin mutant limbs. (a) Shh expression in Wt and Gremlin deficient limb buds between E9.75 and E11.0. The Shh expression domain is activated but not propagated in mutant limb buds. In panel (a), posterior is to the bottom and distal to the right. (b) Expression of Fgf8 (E9.75 and E10.25), Fgf4 and Fgf9 (E10.25) in the AER of wild-type and mutant fore limb buds. Fgf8 expression in early limb buds (E9.75) is patchy and the domain broader in mutant limb buds (arrowheads). Later (E10.25) Fgf8 expressing cells become more restricted to the apex in mutant limb buds. No Fgf4 and Fgf9 transcripts are detected in mutant limb buds. Arrowheads indicate approximate positions of the presumptive AER. In panel (b), posterior is to the bottom and dorsal is to the left.*

It has been shown that BMPs inhibit AER maturation (Pizette and Niswander, 1999), therefore, these alterations could be a direct consequence of enhanced BMP signalling. However, *Bmp2* expression is reduced in the posterior mesenchyme at E10.75 (**Fig. 4a**), asterisks in panels *Bmp2* and data not shown), while *Bmp4* and *Bmp7* remain expressed normally in the mutant limb bud mesenchyme (data not shown). Expression of BMP targets such as *Msx1* and *Msx2* (Pizette and Niswander, 1999) is slightly increased

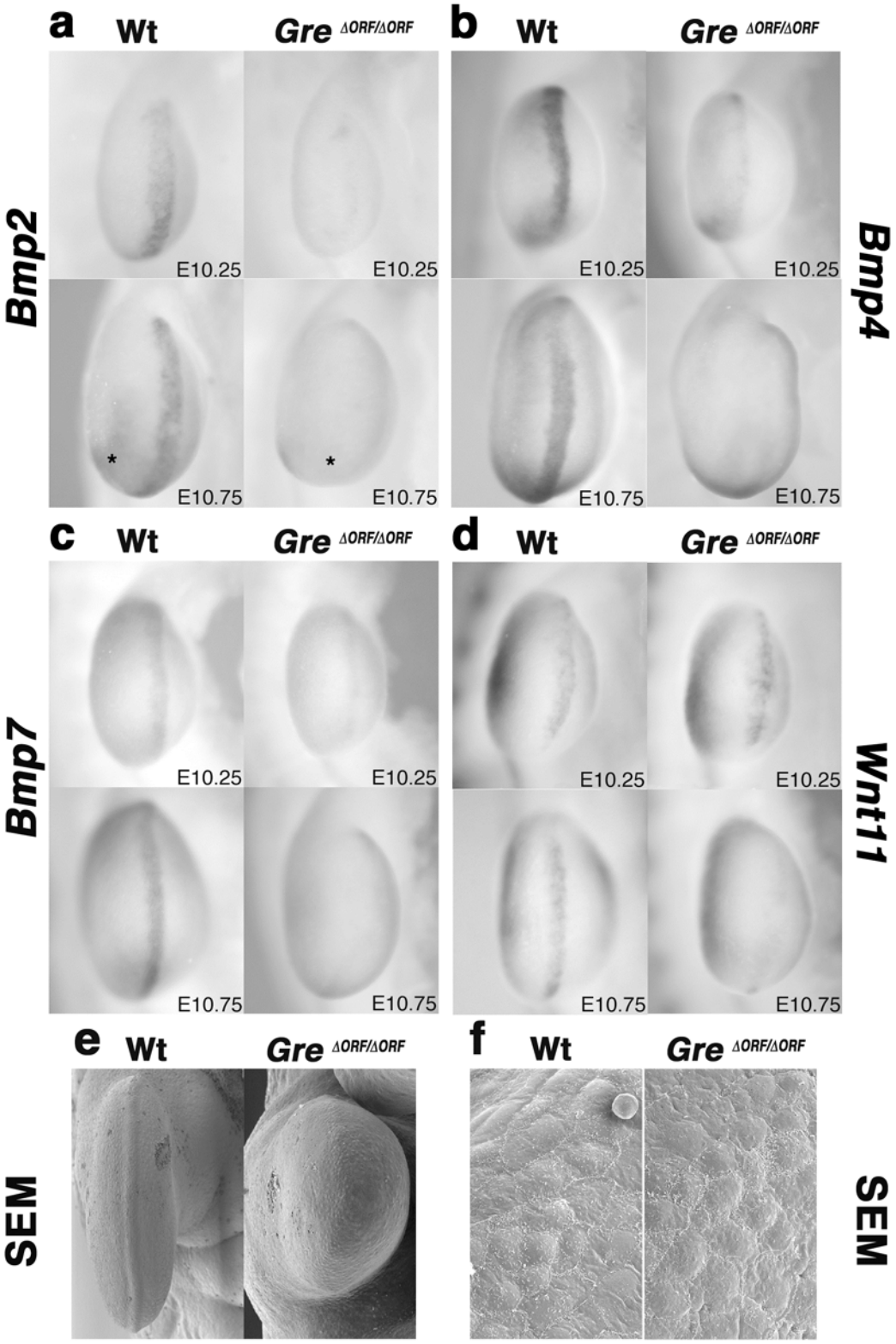
a
Wt
Gre ΔORF/ΔORF
b
Wt
Gre ΔORF/ΔORF
Bmp2
Bmp4
E10.25
E10.25
E10.25
E10.25
E10.75
E10.75
E10.75
E10.75
*
*
c
Wt
Gre ΔORF/ΔORF
d
Wt
Gre ΔORF/ΔORF
Bmp7
Wnt11
E10.25
E10.25
E10.25
E10.25
E10.75
E10.75
E10.75
E10.75
e
Wt
Gre ΔORF/ΔORF
f
Wt
Gre ΔORF/ΔORF
SEM
SEM

Fig.4. *Gremlin is required for AER maturation and regulation of additional AER signals. (**a, b, c**) Bmp2, Bmp4 and Bmp7 expression in the AER of wild-type and Gremlin mutant fore limb buds (E10.25 and E10.75). Expression of Bmp2, Bmp4 and Bmp7 is initiated (E10.25) but not maintained (E10.75) in the AER of mutant limb buds. Asterisks in panels Bmp2 point to expression in the mesenchyme. (**d**) Wnt11 expression in the AER of wild-type and Gremlin mutant fore limb buds (E10.25 and E10.75). Wnt11 expression is initiated in the AER of mutant limb buds (E10.25), but not maintained (E10.75). (**e**) Scanning electronic microscopy analysis of wild-type and Gremlin deficient fore limb buds (E11.5). Note that the AER of mutant limb buds is poorly differentiated and the anterior-posterior limb bud axis is shortened in comparison to the wild-type. In panel (**a**) to (**e**), posterior is to the bottom and dorsal is to the left. (**f**) High power SEM to reveal the morphology of AER ectodermal cells. Note the similarity of wild-type and mutant AER cells.*

(data not shown), which indicates that *Gremlin* indeed antagonizes BMP signalling in the mesenchyme (Khokha et al., 2003). In contrast to the mesenchyme, expression of all *Bmps* is disrupted in the ectoderm of *Gremlin* mutant limb buds (**Fig. 4a, b, c**). Expression of *Bmps* is initially induced in the AER of *Gremlin* mutant limb buds of E10.25, although the level of transcript is reduced in comparison to wild-type limb buds. However *Bmp* expression is not maintained in AER of mutant limb buds, because at E10.75 *Bmp* transcripts cannot be detected in mutant AER (**Fig. 4a, b, c**). In addition, *Wnt11* is activated in the AER of an early *Gremlin* mutant limb bud, but the expression has ceased by around E10.75 (**Fig. 4d)**. In contrast, the Notch ligand *Jag2* remains expressed (data not shown) in the AER of *Gremlin* deficient limb buds. In support of the molecular analysis, scanning electron microscopy reveals that the AER of *Gre* $^{\Delta ORF}$ homozygous limb buds fails to adopt the characteristic ridge-like morphology (**Fig. 4e**), although AER-type ectodermal cells are present (**Fig. 4f**). Taken together, these results show that *Fgf8* expressing AER cells are specified independently of *Gremlin*, while AER maturation and activation of additional AER signals depend critically on *Gremlin* mediated mesenchymal BMP antagonism.

Particularly, *Bmp2* is considered a direct transcriptional target of SHH signaling in the mesenchyme (Drossopoulou et al., 2000). Therefore, reduced *Bmp2* expression could be a consequence of reduced SHH signaling and thus secondary to the absence of *Gremlin*. However, posterior grafts of *Shh* expressing fibroblasts, capable of rescuing gene expression (Zuniga et al., 1999; L.P. and R.Z., unpublished), fail to up-regulate *Bmp2* expression in limb buds of *Gre* $^{\Delta ORF}$ homozygous embryos (**Fig. 5a, b**). In contrast, grafts of *Gremlin* expressing fibroblasts reproducibly enhance mesenchymal *Bmp2* transcription and restore *Bmp2* expression in the AER of mutant limb buds (**Fig. 5c, d**). Similarly, *Gremlin* (**Fig. 5g, h**) but not *Shh* grafts (**Fig. 5e, f**) restore *Fgf8*, *Fgf4* (Zuniga et al., 1999) and *Fgf9* (data not shown) expression in the AER of mutant limb buds. These results show that *Bmp2* and *Fgf8* up-regulation and activation of *Fgfs* in the posterior AER depend on mesenchymal *Gremlin* function.

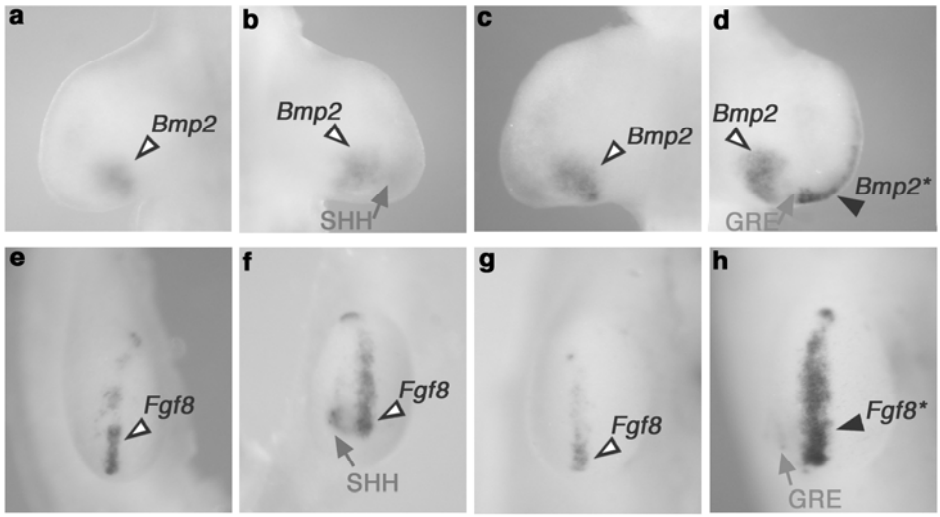

Fig. 5. *Gremlin, but not SHH, rescues Fgf8 and Bmp2 expression in the AER of Gre* $^{\Delta ORF/\Delta ORF}$ *limb buds. All grafted limb buds are fore limb buds (E10.5) of Gremlin mutant embryos. Limb buds either received Shh or Gremlin (arrows) expressing cell aggregates and were cultured for 15 hrs prior to analysis. Open arrowheads indicate the endogenous expression domains, filled arrowheads the induced expression. (**a**) Endogenous Bmp2 expression in a non-grafted control limb bud of a mutant embryo. (**b**) Posterior grafts of Shh expressing cell aggregates fail to rescue Bmp2 expression. (**c, d**) Posterior grafts of Gremlin expressing cells induce Bmp2 expression in the AER (**d**), while no Bmp2 transcripts are detected in the AER of non-grafted mutant limb buds (**c**). Note also the enhancement of mesenchymal Bmp2 expression (**d**). (**e, f**) Posterior grafts of Shh expressing cells do not rescue Fgf8 expression in the AER (**f**) in comparison to a non-grafted mutant limb buds (**e**). (**g, h**) Posterior grafts of Gremlin expressing cells induce up-regulation of Fgf8 expression in the AER (**h**) in comparison to endogenous Fgf8 expression in non-grafted mutant limb buds (**g**). Panels (**a**) to (**d**) are dorsal views with posterior to the bottom and distal to the right, in panels (**e**) to (**h**) posterior is to the bottom and dorsal to the left.*

Gremlin promotes survival of mesenchymal cells

To understand how the molecular alterations give rise to the distal limb patterning defects potential effects on programmed cell death were assayed (**Fig. 6a**). Massive cell death is observed in the core mesenchyme of *Gremlin* deficient limb buds by embryonic day 11.0 (**Fig. 6a**). However, the superficial dorsal and ventral limb bud mesenchymal cells normally expressing *Gremlin* (Merino et al., 1999) survive in limb buds of *Gre* $^{\Delta ORF}$ homozygous embryos as indicated by the continued presence of *LacZ* expressing cells (**Fig. 6b**).

.

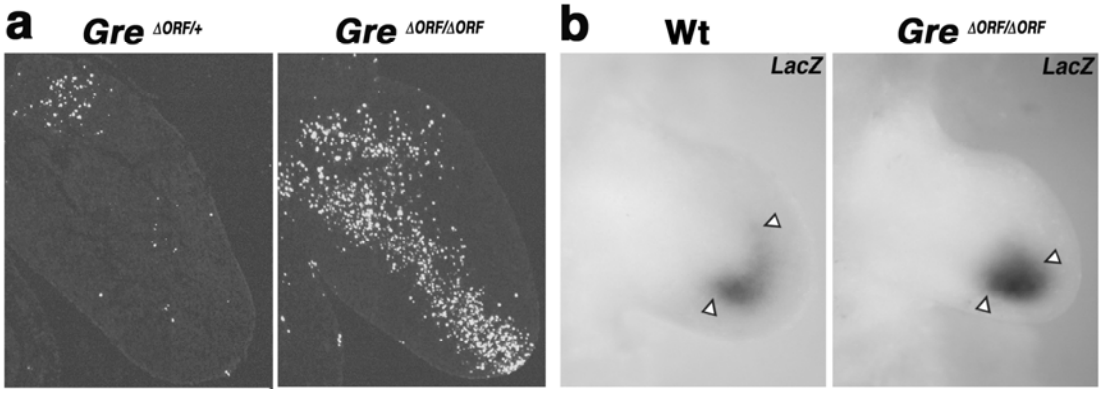

***Fig. 6**. Gremlin is required for cell survival during limb development. (a) TUNEL assay to reveal apoptotic cell death on histological sections. In the absence of Gremlin, cells in core limb bud mesenchyme undergo massive cell death by E11.0. (b) LacZ transcripts are detected in E11.0 fore limb buds (whole mount) to follow the fate of cells normally expressing Gremlin in both heterozygous and homozygous mutant limb buds. Note that LacZ expressing cells survive in Gre $^{\Delta ORF/\Delta ORF}$ limb buds. Open arrowheads indicate the anterior and posterior domain boundaries. Fore limb buds in (a, b) are shown with ventral to the bottom and distal to the right.*

Discussion

In this study we establish that disruption of the *Gremlin* ORF causes the *ld* limb phenotype. Our previous studies indicated that *Gremlin* participates in establishment of the SHH/FGF4 feedback loop (Zuniga et al., 1999). In the present study we show that lack of *Gremlin* causes a much earlier and more general disruption of AER signalling as apparent from patchy *Fgf8* expression already during AER formation. Others have shown (Lewandoski et al., 2000; Moon et al., 2000; Sun et al., 2002) that FGF8 signalling by the AER, in combination with FGF4, participates in *Shh* activation in the posterior limb bud mesenchyme. In particular, *Shh* is not activated in hind limb buds lacking *Fgf8* and *Fgf4* despite continued expression of *Gremlin* in the mesenchyme and *Fgf9*, *Fgf17* and *Bmps* in the mutant AER (Sun et al., 2002). These results together with our studies (Zuniga et al., 1999 and this study) show that *Gremlin* functions initially upstream and independent of SHH to induce AER maturation and *Fgfs* in the posterior AER. However, activation of *Fgf8* in the limb bud ectoderm and *Shh* in the posterior mesenchyme does not require *Gremlin* function.

During progression of limb bud morphogenesis, the number of *Shh* expressing cells is tightly regulated (Sanz-Ezquerro and Tickle, 2000). *Gremlin* induced AER-FGF signaling participates in dynamic SHH regulation as *Gremlin* rescues *Shh* expression with kinetics similar to FGF4 in *ld* mutant limb buds (see chapter 3). The general disruption of AER-FGF signaling underlies the failure to up-regulate *Shh* signaling in *Gremlin* deficient limb buds. In particular, the *Gremlin* mediated transition from initially “static” to “dynamically regulated” signaling centers is crucial for coordinating limb bud morphogenesis and cell survival (see below). For example, the distal-anterior progression of mesenchymal *Gremlin* expression during limb bud morphogenesis causes anterior expansion of FGF signaling in the AER, which

in turn regulates SHH signaling by the polarizing region (Zuniga et al., 1999; see chapter 3). Such changes will alter the ratios of different peptide signals received by AER cells and/or the underlying limb bud mesenchyme. Previous studies have already provided evidence that balanced BMP and FGF signaling by the mesenchyme and the AER are critical for AER maturation and limb bud development, respectively (Niswander and Martin, 1993; Pizette and Niswander, 1999). Therefore, the size and signaling strength of the SHH signaling domain in vertebrate limb buds is controlled by complex SHH-GRE/AER feedback signaling interactions rather than a mere SHH/FGF feedback loop.

In *Gremlin* deficient mouse limb buds, prominent apoptotic cell death is observed in the core mesenchyme from about embryonic day 11.0 onwards. This cell death pattern is rather distinct from the ones observed in *Shh* deficient (te Welscher et al., 2002b) and *Fgf4/8* double mutant (Sun et al., 2002) mouse embryos and following AER removal (Dudley et al., 2002). In addition, experiments in chicken embryos have provided evidence for a role of *Gremlin* mediated BMP antagonism in cell survival during digit formation and chondrogenesis (Merino et al., 1999). The anti-apoptotic effect of *Gremlin* is paracrine as the dorsal and ventral mesenchymal cells normally expressing *Gremlin* survive in limb buds of *Gremlin* deficient mouse embryos (this study). During the onset of chondrogenesis, *Gremlin* most likely acts on the adjacent (core-) mesenchyme to protect it from programmed cell death. This anti-apoptotic function of *Gremlin* provides a likely explanation for the reductions and fusions of distal limb skeletal elements observed in *ld* mutant and *Gremlin* deficient mouse embryos (Zuniga et al., submitted). In addition to the limb bud, *Gremlin* regulates epithelial-mesenchymal interactions during metanephric kidney and lung development (Michos et al., submitted). Therefore, *Gremlin* mediated BMP antagonism seems to regulate the dynamic propagation of epithelial and mesenchymal signaling centers and their interactions during morphogenesis of different vertebrate organs.

Materials and Methods

Generation of *Gre* $^{\Delta ORF}$ mutant mice We generated the targeting vector using a 4.8 kb NdeI-XbaI and a 5.6 kb NsiI-NsiI *Gre* genomic fragments isolated from a 129/SvJ Lambda FIXII library (Stratagene). We inserted an IRES-*LacZ* gene and a PGK-*Neo*^{R} cassette flanked by two *lox*P sites in the same transcriptional orientation as the *Gremlin* gene. R1 ES-cells were electroporated with the NotI linearised targeting vector and screened by genomic Southern with an NsiI-EcoRI probe mapping outside the 3' homology arm (Fig. 1a). Thirty-five homologous recombined ES-cell clones were obtained at a frequency of 9%. Correct recombination resulting in the deletion of the entire 552 base *Gremlin* ORF encoded by exon 2 and of 132 bases of the 3' UTR was confirmed by extensive Southern blot and PCR analysis. ES-cells carrying the *Gre* $^{\Delta ORF}$ null allele were injected into C57BL/6 blastocysts and following germ-line transmission, the mice were maintained in mixed B6; 129S and CD1 backgrounds. PCR genotyping was used for all subsequent studies to allow specific detection of both the wild-type and *Gre* $^{\Delta ORF}$ alleles. The floxed PGK-*neo*^{R} gene was removed by crossing *Gre* $^{\Delta ORF}$ heterozygous

mice with the *Cre* deleter strain. The sequence of the murine *Gremlin* locus was obtained from the UCSC Genome Bioinformatics Website(UCSC) and analyzed using the DNA Strider 1.3*TM* program.

Molecular and morphological analysis of embryos and newborn mice
Embryos and newborn mice were PCR genotyped and accurately staged by determining their somite numbers. Whole mount *in situ* hybridization was performed as described previously (Haramis et al., 1995) using digoxygenin–UTP labeled anti-sense riboprobes. Apoptotic cells were detected *in situ* by incorporating fluorescein-dUTP into fragmented DNA using terminal transferase (Roche Diagnostics). For scanning electron microscopy, embryos were fixed in 1% gluteraldehyde (Sigma) for one hour at 4°C and processed for SEM.

***In vitro* grafting and culturing of mouse limb buds (trunk cultures)**
Mouse fore limb buds were cultured and grafted as described (Zuniga et al., 1999) with the following modifications. Trunks with attached fore limb buds were isolated from either wild-type, heterozygous or *Gremlin* deficient embryos. Embryos were staged by counting somites and genotyped by PCR. Spherical cell aggregates were grafted into the fore limb buds and trunks and were cultured for 15 hrs in serum free medium in 6.5% CO_2 at 37°C. The culture medium was prepared by supplementing high glucose DMEM (GIBCO BRL) medium, with L-glutamine, penicillin/streptomycin, non-essential amino acids, sodium pyruvate, D-glucose, L-ascorbic acid, lactic acid, d-biotin, vitamin B12 and PABA. QT6 fibroblast cells expressing *Shh* and *Gremlin* under control of the CMV promoter were prepared using standard calcium phosphate transfection (Zuniga et al.,1999). One day after transfection, spherical cell aggregates were prepared by plating cells at high density on bacterial plates. The following day cells were treated with mitomycin-C for one hour to block proliferation. After washing the cell aggregates extensively, they were grafted into recipient limb buds (a detailed protocol for media preparation, limb bud grafting and culturing is available upon request).

Acknowledgements

The authors are grateful to I. Ginez, H. Goedemans, N. Lagarde, C. Lehmann and H. Schaller for technical assistance and mouse husbandry. We thank S. Kuc for performing the *lacZ in situ* analysis, the Zentrum für Mikroskopie der Universität Basel, M. Dürrenberger and M. Düggelin for assistance with SEM analysis and K. O'Leary for help in preparation of the manuscript. We are grateful to J. Deschamps, A. Galli, G. Holländer, F. Meijlink, I. Mattaj and C. Torres de los Reyes for helpful discussions and comments on the manuscript. This research was supported by the Faculty of Biology at Utrecht University, grants from the Dutch KNAW (to A.Z.) and NWO (to R.Z.), the Swiss National Science Foundation (to R.Z.) and both cantons of Basel (to R.Z. and K.B.).

Chapter 5

Summarising discussion

Summarising discussion

During embryonic development distinct groups of cells receive different combinations of signals that endow them to adapt a specific fate and differentiation program. It is assumed that cells located in a morphogenetic field "see" different concentrations of a signalling molecule according to their position and distance to the source. As a consequence, cells will activate different combinations of genes and secondary signals depending on their location in a developing tissue. However, not all genes expressed in a particular cell have essential and non-overlapping functions. In chapter 2 of my thesis, I show an example of genes that have partially overlapping functions. Two main mechanisms exist by which signalling molecules act long-range. A signalling molecule can act either directly by forming a morphogen gradient or exerts its long-range effect via induction of secondary signals (Lawrence and Struhl, 1996). In chapter 3 and 4 of my thesis I show that SHH achieves its long-range influence on limb bud patterning by activating secondary signals in a differential fashion. For example, the SHH signal is relayed to the AER by the BMP antagonist *Gremlin*. In addition, SHH regulates limb bud development through induction of BMP2 and Jagged-1 signalling. As a consequence of differential responsiveness of limb bud cells to SHH signal, mesenchymal cells will activate and receive different signals depending on their position in the limb bud.

A signalling molecule needs to fulfil several criteria to be considered as a morphogen. Morphogens are signalling molecules that are secreted by cells with organizer properties and form a concentration gradient across an embryonic field. Cells induce different target genes depending on the concentration of ligand they receive. Morphogens elicit high threshold responses in cells close to the source and progressively lower threshold responses in cells located farther away. Another important feature of a morphogen is that it patterns cells directly and not through signal relay (Gurdon and Bourillot, 2001). Here, I will discuss whether SHH acts as a morphogen during limb bud patterning. SHH is produced by polarizing region cells (Riddle et al., 1993) and is detected at a considerable distance from the source (Lewis et al., 2001). In addition, the *Shh* target genes *Gli1* and *Ptc1* are expressed in a graded fashion from posterior to anterior in the limb bud mesenchyme that correlates with SHH protein distribution (Marigo et al., 1996; Lee et al., 1997; Lewis et al., 2001). Furthermore, SHH instructs limb bud mesenchymal cells in a concentration dependent manner. Anterior ectopic SHH signalling induces formation of extra digits in a dose-dependent manner. Increasing concentration of SHH induces digits with progressively more posterior identities (Yang et al., 1997). In agreement, reduction of SHH signalling results in the loss of posterior digits and reduction in the expression of specific target genes (Lewis et al., 2001). However, Drossopoulou et al. (2000) already suggested that SHH does not directly specify digit identities, but indirectly through induction of the secondary signal BMP2. In addition to BMP2, SHH induces numerous other signals such as the BMP antagonist *Gremlin* (Zuniga et al., 1999) and *Jagged-1* in the mesenchyme (chapter 3) and *Fgfs* in the AER (Laufer et al., 1994). Although all these data are consistent with SHH forming a gradient through the limb bud mesenchyme,

they do not address whether SHH acts directly to instruct the fate of limb bud cells. Thus, it remains to be established whether SHH acts as a true morphogen during limb bud patterning.

In contrast to the limb bud, there is now clear evidence that SHH patterns the neural tube by forming a morphogen gradient. Patterning of the ventral neural tube is controlled by SHH signals secreted from notochord and floorplate cells (Chiang et al., 1996). Similar to the ZPA, the notochord and floorplate have organizing properties, which is mediated by SHH signalling (Yamada et al., 1991; Krauss et al., 1993; Roelink et al., 1994). The ventral neural tube is subdivided along its dorsoventral axis into five distinct progenitor domains, each of which generates a distinct class of postmitotic neurons (Briscoe and Ericson, 1999). There are several lines of evidence indicating that a gradient of SHH signalling activity patterns the ventral neural tube. Firstly, ventral neural tube cell types are lost in *Shh* $^{-/-}$ mutant embryos (Chiang et al., 1996). Secondly, homeodomain proteins that mark distinct ventral progenitor domains along the dorsoventral axis of the neural tube are regulated by specific thresholds of SHH signalling (Ericson et al., 1997; Briscoe et al., 2000). High concentrations of SHH signal are required for the induction of ventral progenitor cells that are located close to the floorplate, while lower concentrations of SHH signal induce cell types that are located far away from the source (Ericson et al., 1997; Briscoe et al., 2000). Finally, *Patched*, a direct transcriptional target of SHH, is expressed in a ventral to dorsal gradient in the neural tube (Goodrich et al., 1996; Marigo and Tabin, 1996). This SHH activity gradient may be modulated by opposing effects of BMP signalling on cellular responses to SHH signalling (Liem et al., 2000). In turn, the net level of BMP signalling cells receive may be regulated by secreted BMP antagonists like follistatin. Follistatin is not able to induce ventral progenitor cell types on its own, but it enhances the sensitivity of progenitor cells to SHH signalling (Liem et al., 2000). This shows that specification of ventral neural cell types depends on the integrated action of SHH, BMP and antagonists. In addition, Gli3 negatively regulates the patterning of the ventral neural tube (Litingtung and Chiang, 2000). In the absence of *Shh*, Gli3 repress the specification of ventral neural cell types. However, ventral neural cell types were rescued in embryos lacking both *Shh* and *Gli3,* revealing that SHH is required to antagonize Gli3-mediated repression of ventral neuronal fates (Litingtung and Chiang, 2000; Persson et al., 2002). Counteraction of Gli3 mediated repression by SHH signalling is also required during distal limb bud development (Litingtung et al., 2002; te Welscher et al., 2002).

To address whether SHH acts directly to specify neural tube cell fate chimeric embryos were generated composed of *Smoothened* (*Smo*) deficient and wild-type cells (Wijgerde et al., 2002). Smoothened is a seven-pass membrane protein required to mediate all Hedgehog (HH) signalling in vertebrate embryonic cells (Zhang et al., 2001). In the absence of *Smoothened,* cells are autonomously blocked in transduction of HH signals. Indeed, *Smo* $^{-/-}$ cells in the neural tube of chimeric embryos fail to adopt a ventral neuronal progenitor cell fate, showing a direct and cell autonomous requirement of HH signalling in specifying ventral cell fates (Wijgerde et al., 2002). These results exclude the possibility that SHH induces secondary signals to pattern the neural tube. To examine whether SHH acts directly to

pattern the vertebrate limb bud mesenchyme, a similar approach should be used.

Signalling molecules may pattern a tissue by a combination of morphogenetic and relay mechanisms. For example *Drosophila* Hedgehog (HH) controls patterning of the anterior-posterior wing axis by a combination of direct and relay signalling. Posterior compartment cells of *Drosophila* wing disc express the selector gene *Engrailed,* which subsequently induces *Hh* expression in these cells. HH signals short-range to induce *Decapentaplegic* (*Dpp*), which is homologues to *Bmp,* in a stripe of anterior compartment cells along the anteroposterior boundary. (Basler and Struhl, 1994; Zecca et al., 1995). Subsequently, DPP acts long-range to organize both the anterior and posterior compartment of the wing disc (Nellen et al., 1996; Entchev et al., 2000; Teleman and Cohen, 2000). Although most of the organizing activities of HH in the wing are indirect, there is evidence that HH patterns the central core of the wing directly and independently of DPP signalling (Strigini and Cohen, 1997).

Fine-tuning of BMP signalling in the limb bud mesenchyme

BMPs are implicated in distinct processes during vertebrate limb bud development. BMPs negatively influence limb bud outgrowth, but are also required for specification of digit identities. Therefore, BMP signalling needs to be tightly regulated during limb bud development. During initiation of limb bud outgrowth BMP signalling in ventral ectoderm is required for dorsal-ventral patterning of the limb bud and AER formation (Ahn et al., 2001; Pizette et al., 2001; Barrow et al., 2003; Soshnikova et al., 2003). However, once the AER is formed, BMPs negatively regulate the maintenance and function of the AER (Pizette and Niswander, 1999). To relay the SHH signal to the AER BMP signalling in distal limb is antagonized by *Gremlin* (Zuniga et al., 1999; chapter 4). In the absence of the BMP antagonist *Gremlin,* the AER fails to differentiate and expression of AER specific genes is affected (chapter 4). In addition, ectopic application of BMPs to limb buds results in inhibition of outgrowth and apoptosis (Niswander and Martin, 1993; Macias et al., 1997). This data are in sharp contrast with the proposed role for BMP2 signalling in specification of digit identities. Experiments in the chicken embryos suggest that BMPs act downstream of SHH to specify digit identities in a dose-dependent fashion, with higher levels required for specification of digits with a more posterior identity (Kawakami et al., 1996; Dahn and Fallon, 2000; Drossopoulou et al., 2000). However, BMP seems to promote digit identities only in limb bud mesenchymal cells that have been primed by SHH (Drossopoulou et al., 2000), providing one possible explanation of why application of BMP rather inhibits limb bud development (see before). Thus, SHH signalling seems to regulate digit formation and/or identities development through positive modulation of BMP signalling, while at the same time BMP signalling is locally antagonized to permit relay of the SHH signal to the AER.

Regulation of *Formin* and *Gremlin* in the limb bud mesenchyme

The *ld* mutations disrupt the establishment of mesenchymal-epithelial interactions in the limb bud mesenchyme (Haramis et al., 1995; Kuhlman and

Niswander, 1997). In addition, it was shown that *Gremlin* fails to be activated in *ld* mutant limb buds (Zuniga et al., 1999). Three *ld* alleles disrupt the *Formin* gene, therefore Formin was thought to function upstream of *Gremlin* in the limb bud mesenchyme. Indeed, inactivation of the *Gremlin* by gene targeting in the mouse causes the same limb bud phenotype as observed in *ld* mutant limb buds (Khokha et al., 2003). However, a recent study by our group (Zuniga et al., submitted) shows that the *ld* limb phenotype is not caused by disruption of the *Formin* gene, but by the disruption of a shared cis-regulatory element. This cis-regulatory element is required for both *Formin* and *Gremlin* expression in the limb bud mesenchyme (Zuniga et al., submitted). Most importantly, detailed genetic analysis shows that not *Formin*, but *Gremlin* is essential in the limb bud mesenchyme to establish SHH/AER signalling. This shared cis-regulatory element acts at a distance and activates the expression of unrelated genes, which are features reminiscent to the global control region, which regulates limb bud specific *5'HoxD* gene expression (Spitz et al., 2003).

The roles of NOTCH signalling during vertebrate limb development

NOTCH signalling is an evolutionary conserved signalling mechanism, which controls cell fate decisions through modulating local cell-cell interactions. Both ligand and receptors are transmembrane, allowing only short-range signalling interactions. In *Drosophila* wing imaginal discs, asymmetric activation of NOTCH signalling is required to establish a signalling centre at the dorsal-ventral boundary (Kim et al., 1995; Doherty et al., 1996; Panin et al., 1997). Furthermore, in the *Drosophila* leg disc NOTCH signalling is required for the establishment of joints that subdivides the appendage into segments (de Celis et al., 1998; Bishop et al., 1999). In vertebrates NOTCH signalling plays a crucial role in AER positioning and formation in limb buds. Genes like *Notch1, Jagged2* and *Radical Fringe* are expressed by the developing AER and have been implicated in its development (Myat et al., 1996; Laufer et al., 1997; Rodriguez-Esteban et al., 1997; Moran et al., 1999). The NOTCH ligand *Jagged-2* is required for the regulation of AER morphology and function. The digits of *Jagged-2* deficient limbs are fused, likely because of a hyperplastic AER (Jiang et al., 1998).

In contrast to the roles of NOTCH signalling in the limb bud ectoderm, much less is known about its roles in the limb bud mesenchyme. In chapter 3, I show that SHH regulates *Jagged-1* and *Hey1* expression in the distal limb bud mesenchyme. *Jagged-1* and *Hey1* are both components of the NOTCH signalling pathway (Lindsell et al., 1995; Maier and Gessler, 2000) and their expression implies functions of these genes in patterning of the distal limb bud mesenchyme. Using gain- and loss-of-function experiments, I show that *Jagged-1* modulates *Hey1* and *EphrinB2* expression in distal limb bud mesenchyme.

Besides the suggested role in regulating limb bud vasculature (see chapter 3), it is plausible that *Jagged-1* fulfils additional roles during limb bud development. For instance during digit formation, *Jagged-1* expression becomes restricted to the interdigital mesenchyme in a domain complementary to *Notch1* (Vargesson et al., 1998), suggesting a function for *Jagged-1* in cartilage formation. Indeed, NOTCH signalling has been implicated in skeletal development. Overexpression of *Delta-1* in chick limb

buds causes shortening of cartilage elements (Crowe et al., 1999). Similarly, overexpression of NOTCH target *c-Hairy-1* causes shortening of chicken limb bud skeletal elements (Vasiliauskas et al., 2003). In addition, the restriction of *Jagged-1* and *Hey1* expression to the distal limb bud mesenchyme during limb bud development suggest a role for *Jagged-1* signalling during limb pattering. Strikingly, *Jagged-1* expression is frequently detected at other sites where mesenchymal-epithelial interactions occur, like the dental mesenchyme, metanephric kidney and whisker follicles (Mitsiadis et al., 1997). Therefore, Jagged-1 could function in modulating mesenchymal-epithelial signalling interactions during limb bud development. Also remarkable is the similarity between *Jagged-1* and *5'HoxD* gene expression in wild-type and mutant limbs. However, *5'HoxD* genes remain expressed in *Htu* homozygous mutant limb buds and no changes in *Jagged-1* are detected in *Hoxd11-13* compound mutant limb buds (data not shown).

The methods I used to analyse Jagged-1 signalling in the limb bud may not be well suited to uncover such additional roles during limb bud development. First, grafts of *Jagged-1* expressing cells placed in anterior limb bud mesenchyme or into *Shh* $^{-/-}$ mutant limb buds did not induce *Hey1* expression. A reason for this may be that *Jagged-1* modulates target gene expression rather than inducing their expression "*de novo*". Alternatively, Jagged-1 may not be properly processed into an active protein in QT6 cells and/or components of NOTCH signalling pathway may not be expressed in anterior or *Shh* deficient cells and thereby result in failure to transduce the Jagged-1 signal. Second, the early lethality of *Htu* homozygous mutant embryos (Xue et al., 1999; Kiernan et al., 2001) severely constrained our analysis of the limb bud phenotype as *Htu* homozygous mutant embryos died shortly after activation of *Jagged-1* expression. Therefore, one approach to circumvent early lethality of *Jagged-1* $^{-/-}$ mutant embryos would be to generate a conditional knockout allele of *Jagged-1*. Alternatively Jagged-1 could be functionally redundant with another NOTCH ligand in the limb bud mesenchyme.

Future experiment to analyze NOTCH signalling in limb bud

To overcome the limitations of *Jagged-1* expressing cells to study NOTCH signalling in the limb bud, I have begun to introduce DNA into limb bud cells by electroporation. The DNA is injected into the tissue and subsequently an electric field is applied, resulting in uptake of DNA by cells in the tissue (Swartz et al., 2001). The advantage of electroporation is that DNA is incorporated into endogenous cells and expressed by them. This is especially advantageous for proteins that need to undergo cell specific modifications to regulate their activity. Initial electroporation experiments in limb buds using a GFP reporter construct are encouraging, however analysis of NOTCH signalling by electroporation is beyond the scope of my PhD thesis.

In addition to ligands, electroporation of dominant activating NOTCH constructs should also be used to study NOTCH signalling during limb bud development. Ligands binding to NOTCH trigger proteolytic cleavage of NOTCH resulting in the release of the NOTCH intracellular domain (NIC) from the membrane. This NOTCH intracellular domain forms a complex with Suppressor of Hairless [Su(H)], which is a downstream mediator of NOTCH

signalling during activation of gene expression (Artavanis-Tsakonas et al., 1999). The cleavage of NOTCH is essential for signal transduction (Huppert et al., 2000) and overexpression of NIC in cells results in constitutive activation of NOTCH signalling pathway (Kopan et al., 1994). For example ectopic expression of NIC rescues arterial *EphrinB2* expression in the absence of VEGF in the zebrafish (Lawson et al., 2002). Therefore electroporation of NIC into mesenchymal cells of the limb bud might be a potent way to ectopically activate NOTCH signalling. In addition dominant negative forms of Suppressor of Hairless [Su(H)], NOTCH receptor and ligand that efficiently block NOTCH signalling in several tissues (Sun and Artavanis-Tsakonas, 1996; Hukriede et al., 1997; Wettstein et al., 1997; Franklin et al., 1999; Lawson et al., 2001) could be electroporated into the limb bud to block NOTCH signalling.

References

Adams, R. H., Wilkinson, G. A., Weiss, C., Diella, F., Gale, N. W., Deutsch, U., Risau, W. and Klein, R. (1999). Roles of ephrinB ligands and EphB receptors in cardiovascular development: demarcation of arterial/venous domains, vascular morphogenesis, and sprouting angiogenesis. *Genes Dev* **13**, 295-306.

Ahn, K., Mishina, Y., Hanks, M. C., Behringer, R. R. and Crenshaw, E. B., 3rd. (2001). BMPR-IA signaling is required for the formation of the apical ectodermal ridge and dorsal-ventral patterning of the limb. *Development* **128**, 4449-61.

Aoto, K., Nishimura, T., Eto, K. and Motoyama, J. (2002). Mouse GLI3 regulates Fgf8 expression and apoptosis in the developing neural tube, face, and limb bud. *Dev Biol* **251**, 320-32.

Artavanis-Tsakonas, S., Rand, M. D. and Lake, R. J. (1999). Notch signaling: cell fate control and signal integration in development. *Science* **284**, 770-6.

Avsian-Kretchmer, O. and Hsueh, A. J. (2003). Comparative Genomic Analysis of the Eight-Membered-Ring Cystine-Knot-Containing Bone Morphogenetic Protein (BMP) Antagonists. *Mol Endocrinol*.

Aza-Blanc, P., Ramirez-Weber, F., Laget, M., Schwartz, C. and Kornberg, T. (1997). Proteolysis that is inhibited by hedgehog targets Cubitus interruptus protein to the nucleus and converts it to a repressor. *Cell* **89**, 1043-1053.

Barrow, J. R., Thomas, K. R., Boussadia-Zahui, O., Moore, R., Kemler, R., Capecchi, M. R. and McMahon, A. P. (2003). Ectodermal Wnt3/beta-catenin signaling is required for the establishment and maintenance of the apical ectodermal ridge. *Genes Dev* **17**, 394-409.

Basler, K. and Struhl, G. (1994). Compartment boundaries and the control of Drosophila limb pattern by hedgehog protein. *Nature* **368**, 208-214.

Beverdam, A., Brouwer, A., Reijnen, M., Korving, J. and Meijlink, F. (2001). Severe nasal clefting and abnormal embryonic apoptosis in Alx3/Alx4 double mutant mice. *Development* **128**, 3975-86.

Bishop, S. A., Klein, T., Arias, A. M. and Couso, J. P. (1999). Composite signalling from Serrate and Delta establishes leg segments in Drosophila through Notch. *Development* **126**, 2993-3003.

Briscoe, J. and Ericson, J. (1999). The specification of neuronal identity by graded Sonic Hedgehog signalling. *Semin Cell Dev Biol* **10**, 353-62.

Briscoe, J., Pierani, A., Jessell, T. M. and Ericson, J. (2000). A homeodomain protein code specifies progenitor cell identity and neuronal fate in the ventral neural tube. *Cell* **101**, 435-45.

Buescher, D., Bosse, B., Heymer, J. and Ruether, U. (1997). Evidence for genetic control of *Sonic hedgehog* by *Gli3* in mouse limb development. *Mech. Dev.* **1997**, 175-182.

Burke, R., Nellen, D., Bellotto, M., Hafen, E., Senti, K.-A., Dickson, B. J. and Basler, K. (1999). Dispatched, a novel sterol sensing domain protein dedicated to the release of cholesterol-modified hedgehog from signaling cells. *Cell* **99**, 803-815.

Buscher, D., Bosse, B., Heymer, J. and Ruther, U. (1997). Evidence for genetic control of Sonic hedgehog by Gli3 in mouse limb development. *Mech Dev* **62**, 175-82.

Capdevila, J. and Izpisua Belmonte, J. C. (2001). Patterning mechanisms controlling vertebrate limb development. *Annu Rev Cell Dev Biol* **17**, 87-132.

Capdevila, J., Tsukui, T., Rodriquez Esteban, C., Zappavigna, V. and Izpisua Belmonte, J. C. (1999). Control of vertebrate limb outgrowth by the proximal factor Meis2 and distal antagonism of BMPs by Gremlin. *Mol Cell* **4**, 839-49.

Caspary, T., Garcia-Garcia, M. J., Huangfu, D., Eggenschwiler, J. T., Wyler, M. R., Rakeman, A. S., Alcorn, H. L. and Anderson, K. V. (2002). Mouse Dispatched homolog1 is required for long-range, but not juxtacrine, Hh signaling. *Curr Biol* **12**, 1628-32.

Chan, D. C., A., W.-B. and Leder, P. (1995). Formin isoforms are differentially expressed in the mouse embryo and are required for normal expression of *fgf-4* and *shh* in the limb bud. *Development* **121**, 3151-3162.

Charité, J., de Graaff, W., Shen, S. and Deschamps, J. (1994). Ectopic expression of Hox-8 causes duplication of the ZPA in the forelimb and homeotic transformation of axial structures. *Cell* **78**, 589-601.

Charite, J., McFadden, D. G. and Olson, E. N. (2000). The bHLH transcription factor dHAND controls Sonic hedgehog expression and establishment of the zone of polarizing

activity during limb development. *Development* **127**, 2461-70.

Chiang, C., Litingtung, Y., Harris, M. P., Simandl, B. K., Li, Y., Beachy, P. A. and Fallon, J. F. (2001). Manifestation of the Limb Prepattern: Limb Development in the Absence of Sonic Hedgehog Function. *Developmental Biology* **236**, 421-435.

Chiang, C., Litingtung, Y., Lee, E., Young, K. E., Corden, J. L., Westphal, H. and Beachy, P. A. (1996). Cyclopia and defective axial patterning in mice lacking *Sonic hedgehog* gene function. *Nature* **383**, 407-413.

Chuang, P.-T. and McMahon, A. P. (1999). Vertebrate hedgehog signalling modulated by induction of a hedgehog-binding protein. *Nature* **987**, 617-621.

Cohn, M. J. (2000). Giving limbs a hand. *Nature* **406**, 953-954.

Cohn, M. J. and Tickle, C. (1999). Developmental basis of limblessness and axial patterning in snakes. *Nature* **399**, 474-9.

Cohn, M. J., Izpisúa-Belmonte, J.-C., Abud, H., Heath, J. K. and Tickle, C. (1995). Fibroblast growth factors induce additional limb development from the flank of chick embryos. *Cell* **80**, 739-746.

Colvin, J. S., Green, R. P., Schmahl, J., Capel, B. and Ornitz, D. M. (2001). Male-to-female sex reversal in mice lacking fibroblast growth factor 9. *Cell* **104**, 875-89.

Cooper, M. K., Wassif, C. A., Krakowiak, P. A., Taipale, J., Gong, R., Kelley, R. I., Porter, F. D. and Beachy, P. A. (2003). A defective response to Hedgehog signaling in disorders of cholesterol biosynthesis. *Nat Genet* **33**, 508-13.

Crowe, R., Zikherman, J. and Niswander, L. (1999). Delta-1 negatively regulates the transition from prehypertrophic to hypertrophic chondrocytes during cartilage formation. *Development* **126**, 987-98.

Dahn, R. D. and Fallon, J. F. (2000). Interdigital regulation of digit identity and homeotic transformation by modulated BMP signaling. *Science* **289**, 438-41.

Dai, P., Akimaru, H., Tanaka, Y., Maekawa, T., Nakafuku, M. and Ishii, S. (1999). Sonic Hedgehog-induced activation of the Gli1 promoter is mediated by GLI3. *J Biol Chem* **274**, 8143-52.

Dai, P., Shinagawa, T., Nomura, T., Harada, J., Kaul, S. C., Wadhwa, R., Khan, M. M., Akimaru, H., Sasaki, H., Colmenares, C. et al. (2002). Ski is involved in transcriptional regulation by the repressor and full-length forms of Gli3. *Genes Dev* **16**, 2843-8.

Davis, A. P., Witte, D. P., Hsieh-Li, H. M., Potter, S. and Capecchi, M. (1995). Absence of radius and ulna in mice lacking *hoxa-11* and *hoxd-11*. *Nature* **375**, 791-795.

de Celis, J. F., Tyler, D. M., de Celis, J. and Bray, S. J. (1998). Notch signalling mediates segmentation of the Drosophila leg. *Development* **125**, 4617-26.

Ding, Q., Motoyama, J., Gasca, S., Mo, R., Sasaki, H., Rossant, J. and Hui, C. C. (1998). Diminished Sonic hedgehog signaling and lack of floor plate differentiation in Gli2 mutant mice. *Development* **125**, 2533-43.

Doherty, D., Feger, G., Younger-Shepherd, S., Jan, L. Y. and Jan, Y. N. (1996). Delta is a ventral to dorsal signal complementary to Serrate, another Notch ligand, in Drosophila wing formation. *Genes Dev* **10**, 421-34.

Dolle, P., Izpisua-Belmonte, J. C., Brown, J., Tickle, C. and Duboule, D. (1993). Hox genes and the morphogenesis of the vertebrate limb. *Prog Clin Biol Res* **383A**, 11-20.

Dolle, P., Izpisua-Belmonte, J. C., Brown, J. M., Tickle, C. and Duboule, D. (1991). HOX-4 genes and the morphogenesis of mammalian genitalia. *Genes Dev* **5**, 1767-7.

Dolle, P., Izpisua-Belmonte, J. C., Falkenstein, H., Renucci, A. and Duboule, D. (1989). Coordinate expression of the murine Hox-5 complex homoeobox-containing genes during limb pattern formation. *Nature* **342**, 767-72.

Dono, R., Texido, G., Dussel, R., Ehmke, H. and Zeller, R. (1998). Impaired cerebral cortex development and blood pressure regulation in FGF-2-deficient mice. *EMBO J.* **17**, 4213-4225.

Drossopoulou, G., Lewis, K. E., Sanz-Ezquerro, J. J., Nikbakht, N., McMahon, A. P., Hofmann, C. and Tickle, C. (2000). A model for anteroposterior patterning of the vertebrate limb based on sequential long- and short-range Shh signalling and Bmp signalling. *Development* **127**, 1337-48.

Duboule, D. (1992). The vertebrate limb: a model system to study the HOX/HOM gene network during development and evolution. *Bioassays* **14**, 375-384.

Dudley, A. T., Ros, M. A. and Tabin, C. J. (2002). A re-examination of proximodistal patterning during vertebrate limb development. *Nature* **418**, 539-44.

Dunwoodie, S. L., Clements, M., Sparrow, D. B., Sa, X., Conlon, R. A. and Beddington, R. S. (2002). Axial skeletal defects caused by mutation in the spondylocostal dysplasia/pudgy gene Dll3 are associated with disruption of the segmentation clock within the presomitic mesoderm. *Development* **129**, 1795-806.
Duprez, D. M., Kostakopoulou, K., Francis-West, P. H., Tickle, C. and Brickell, P. M. (1996). Activation of *Fgf-4* and *HoxD* gene expression by BMP-2 expressing cells in the developing chick limb. *Development* **122**, 1821-1828.
Entchev, E. V., Schwabedissen, A. and Gonzalez-Gaitan, M. (2000). Gradient formation of the TGF-beta homolog Dpp. *Cell* **103**, 981-91.
Ericson, J., Rashbass, P., Schedl, A., Brenner-Morton, S., Kawakami, A., van Heyningen, V., Jessell, T. M. and Briscoe, J. (1997). Pax6 controls progenitor cell identity and neuronal fate in response to graded Shh signaling. *Cell* **90**, 169-80.
Fallon, J. F., Lopez, A., Ros, M. A., Savage, M. P., Olwin, B. B. and Simandl, B. K. (1994). FGF-2: apical ectodermal ridge growth factor for chick limb development. *Science* **264**, 104-107.
Fernandez-Teran, M., Piedra, M. E., Kathiriya, I. S., Srivastava, D., Rodriguez-Rey, J. C. and Ros, M. A. (2000). Role of dHAND in the anterior-posterior polarization of the limb bud: implications for the Sonic hedgehog pathway. *Development* **127**, 2133-2142.
Francis, P. H., Richardson, M. K., Brickell, P. M. and Tickle, C. (1994). Bone morphogenetic proteins and a signalling pathway that controls patterning in the developing chick limb. *Development* **120**, 209-218.
Franklin, J. L., Berechid, B. E., Cutting, F. B., Presente, A., Chambers, C. B., Foltz, D. R., Ferreira, A. and Nye, J. S. (1999). Autonomous and non-autonomous regulation of mammalian neurite development by Notch1 and Delta1. *Curr Biol* **9**, 1448-57.
Fromental-Ramain, C., Warot, X., Lakkaraju, S., Favier, B., Haack, H., Birling, C., Dierich, A., Dollé, P. and Chambon, P. (1996). Specific and redundant functions of the paralogous *Hoxa-9* and *Hoxd-9* genes in forelimb and axial skeleton patterning. *Development* **122**, 461-472.
Gallet, A., Rodriguez, R., Ruel, L. and Therond, P. P. (2003). Cholesterol modification of hedgehog is required for trafficking and movement, revealing an asymmetric cellular response to hedgehog. *Dev Cell* **4**, 191-204.
Goff, D. J. and Tabin, C. J. (1997). Analysis of *Hoxd-13* and *Hoxd-11* misexpression in chick limb buds reveals that *Hox* genes affect both bone condensation and growth. *Development* **124**, 627-636.
Goodrich, L. V., Johnson, R. L., Milenkovic, L., McMahon, J. A. and Scott, M. P. (1996). Conservation of the *hedgehog/patched* signaling pathway from flies to mice: induction of a mouse *patched* gene by Hedgehog. *Genes & Development* **10**, 301-312.
Goodrich, L. V., Milenkovic, L., Higgins, K. M. and Scott, M. P. (1997). Altered neural cell fates and medulloblastoma in mouse patched mutants. *Science* **277**, 1109-13.
Gridley, T. (2001). Notch signaling during vascular development. *Proc Natl Acad Sci U S A* **98**, 5377-8.
Gurdon, J. B. and Bourillot, P. Y. (2001). Morphogen gradient interpretation. *Nature* **413**, 797-803.
Haramis, A. G., Brown, J. M. and Zeller, R. (1995). The limb deformity mutation disrupts the SHH/FGF-4 feedback loop and regulation of 5'HoxD genes during limb pattern formation. *Development* **121**, 4237-4245.
Hebert, J. M., Basilico, C., Goldfarb, M., Haub, O. and Martin, G. R. (1990). Isolation of cDNAs encoding four mouse FGF family members and characterization of their expression pattern during embrogenesis. ***Dev. Biol.*** **138**, 454-463.
Herault, Y., Fraudeau, N., Zakany, J. and Duboule, D. (1997). Ulnaless (Ul), a regulatory mutation inducing both loss-of-function and gain-of-function of posterior Hoxd genes. *Development* **124**, 3493-500.
Hicks, C., Johnston, S. H., diSibio, G., Collazo, A., Vogt, T. F. and Weinmaster, G. (2000). Fringe differentially modulates Jagged1 and Delta1 signalling through Notch1 and Notch2. *Nat Cell Biol* **2**, 515-20.
Hornbruch, A. and Wolpert, L. (1991). The spatial and temporal distribution of polarizing activity in the flank of the pre-limb-bud stages in the chick embryo. *Development* **111**, 725-731.
Hsu, D., Economides, A., Wang, X., Eimon, P. and Harland, R. (1998). The Xenopus dorsalizing factor Gremlin identifies a novel family of secreted proteins that antagonize BMP

activities. *Mol Cell* **5**, 673-83.

Hui, C. and Joyner, A. (1993). A mouse model of greig cephalopolysyndactyly syndrome: the extra-toesJ mutation contains an intragenic deletion of the Gli3 gene. *Nat-Genet.* **3**, 241-246.
Hui, C., Slusarski, D., Platt, K., Holmgren, R. and Joyner, A. (1994). Expression of three mouse homologs of the Drosophila segment polarity gene cubitus interruptus, Gli, Gli-2, and Gli-3, in ectoderm- and mesoderm-derived tissues suggests multiple roles during postimplantation development. *Dev-Biol.* **162**, 402-413.
Hukriede, N. A., Gu, Y. and Fleming, R. J. (1997). A dominant-negative form of Serrate acts as a general antagonist of Notch activation. *Development* **124**, 3427-37.
Huppert, S. S., Le, A., Schroeter, E. H., Mumm, J. S., Saxena, M. T., Milner, L. A. and Kopan, R. (2000). Embryonic lethality in mice homozygous for a processing-deficient allele of Notch1. *Nature* **405**, 966-70.
Ianakiev, P., van Baren, M. J., Daly, M. J., Toledo, S. P., Cavalcanti, M. G., Neto, J. C., Silveira, E. L., Freire-Maia, A., Heutink, P., Kilpatrick, M. W. et al. (2001). Acheiropodia is caused by a genomic deletion in C7orf2, the human orthologue of the Lmbr1 gene. *Am J Hum Genet* **68**, 38-45.
Irvine, K. D. and Vogt, T. F. (1997). Dorsal-ventral signaling in limb development. *Curr Opin Cell Biol* **9**, 867-76.
Jiang, R., Lan, Y., Chapman, H. D., Shawber, C., Norton, C. R., Serreze, D. V., Weinmaster, G. and Gridley, T. (1998). Defects in limb, craniofacial, and thymic development in Jagged2 mutant mice. *Genes Dev* **12**, 1046-57.
Johnson, D. R. (1967). *Extra-toes*: a new mutant gene causing multiple abnormalities in the mouse. *J. Embryol. exp. Morph.* **17**, 543-581.
Johnson, R. L. and Tabin, C. J. (1997). Molecular Models for Vertebrate Limb Development. *Cell* **90**, 979-990.
Kawakami, T., Kawcak, T., Li, Y. J., Zhang, W., Hu, Y. and Chuang, P. T. (2002). Mouse dispatched mutants fail to distribute hedgehog proteins and are defective in hedgehog signaling. *Development* **129**, 5753-65.
Kawakami, Y., Ishikawa, T., Shimabara, M., Tanda, N., Enomoto-Iwamoto, M., Iwamoto, M., Kuwana, T., Ueki, A., Noji, S. and Nohno, T. (1996). BMP signaling during bone pattern determination in the developing limb. *Development* **122**, 3557-66.
Khokha, M. K., Hsu, D., Brunet, L. J., Dionne, M. S. and Harland, R. M. (2003). Gremlin is the BMP antagonist required for maintenance of Shh and Fgf signals during limb patterning. *Nat Genet* **34**, 303-7.
Kiernan, A. E., Ahituv, N., Fuchs, H., Balling, R., Avraham, K. B., Steel, K. P. and Hrabe de Angelis, M. (2001). The Notch ligand Jagged1 is required for inner ear sensory development. *Proc Natl Acad Sci U S A* **98**, 3873-8.
Kim, J., Irvine, K. D. and Carroll, S. B. (1995). Cell recognition, signal induction, and symmetrical gene activation at the dorso-ventral boundary of the developing Drosophila wing. *Cell* **82**, 795-802.
Kmita, M., Fraudeau, N., Herault, Y. and Duboule, D. (2002). Serial deletions and duplications suggest a mechanism for the collinearity of Hoxd genes in limbs. *Nature* **420**, 145-50.
Knezevic, V., De Santo, R., Schughart, K., Huffstadt, U., Chiang, C., Mahon, K. A. and Mackem, S. (1997). *Hoxd-12* differentially affects preaxial and postaxial chondrogenic branches in the limb and regulates *Sonic hedgehog* in a positive feedback loop. *Development* **124**, 4523-4536.
Kopan, R., Nye, J. S. and Weintraub, H. (1994). The intracellular domain of mouse Notch: a constitutively activated repressor of myogenesis directed at the basic helix-loop-helix region of MyoD. *Development* **120**, 2385-96.
Kraus, P., Fraidenraich, D. and Loomis, C. A. (2001). Some distal limb structures develop in mice lacking Sonic hedgehog signaling. *Mech Dev* **100**, 45-58.
Krauss, S., Concordet, J.-P. and Ingham, P. W. (1993). A functionally conserved homolog of the Drosophila segment polarity gene *hh* is expressed in tissues with polarizing activity in zebrafish embryos. *Cell* **75**, 1431-1444.
Kronenberg, H. M. (2003). Developmental regulation of the growth plate. *Nature* **423**, 332-6.
Krumlauf, R. (1994). Hox genes in vertebrate development. *Cell* **78**, 191-201.

Kuhlman, J. and Niswander, L. (1997). Limb deformity proteins: role in mesodermal induction of the apical ectodermal ridge. *Development* **124**, 133-139.

Laufer, E., Dahn, R., Orozco, O. E., Yeo, C. Y., Pisenti, J., Henrique, D., Abbott, U. K., Fallon, J. F. and C., T. (1997). Expression of *Radical fringe* in limb bud ectoderm regulates apical ectodermal ridge formation. *Nature*, 366.

Laufer, E., Nelson, C. E., Johnson, R. L., Morgan, B. A. and Tabin, C. (1994). Sonic hedgehog and Fgf-4 act through a signalling cascade and feedback loop to integrate growth and patterning of the development limb bud. *Cell* **79**, 993-1003.

Lawrence, P. A. and Struhl, G. (1996). Morphogens, compartments, and pattern: lessons from drosophila? *Cell* **85**, 951-61.

Lawson, N. D., Scheer, N., Pham, V. N., Kim, C. H., Chitnis, A. B., Campos-Ortega, J. A. and Weinstein, B. M. (2001). Notch signaling is required for arterial-venous differentiation during embryonic vascular development. *Development* **128**, 3675-83.

Lawson, N. D., Vogel, A. M. and Weinstein, B. M. (2002). sonic hedgehog and vascular endothelial growth factor act upstream of the Notch pathway during arterial endothelial differentiation. *Dev Cell* **3**, 127-36.

Lee, J., Platt, K. A., Censullo, P. and Ruiz i Altaba, A. (1997). Gli1 is a target of Sonic hedgehog that induces ventral neural tube development. *Development* **124**, 2537-2552.

Lee, J. J., Ekker, S. C., von Kessler, D. P., Porter, J. A., Sun, B. I. and Beachy, P. A. (1994). Autoproteolysis in hedgehog protein biogenesis. *Science* **266**, 1528-37.

Leimeister, C., Externbrink, A., Klamt, B. and Gessler, M. (1999). Hey genes: a novel subfamily of hairy- and Enhancer of split related genes specifically expressed during mouse embryogenesis. *Mech Dev* **85**, 173-7.

Lettice, L. A., Heaney, S. J., Purdie, L. A., Li, L., de Beer, P., Oostra, B. A., Goode, D., Elgar, G., Hill, R. E. and de Graaff, E. (2003). A long-range Shh enhancer regulates expression in the developing limb and fin and is associated with preaxial polydactyly. *Hum Mol Genet* **12**, 1725-35.

Lettice, L. A., Horikoshi, T., Heaney, S. J., Van Baren, M. J., Van Der Linde, H. C., Breedveld, G. J., Joosse, M., Akarsu, N., Oostra, B. A., Endo, N. et al. (2002). Disruption of a long-range cis-acting regulator for Shh causes preaxial polydactyly. *Proc Natl Acad Sci U S A* **99**, 7548-53.

Lewandoski, M., Sun, X. and Martin, G. R. (2000). Fgf8 signalling from the AER is essential for normal limb development. *Nat Genet* **26**, 460-3.

Lewis, P. M., Dunn, M. P., McMahon, J. A., Logan, M., Martin, J. F., St-Jacques, B. and McMahon, A. P. (2001). Cholesterol modification of sonic hedgehog is required for long-range signaling activity and effective modulation of signaling by Ptc1. *Cell* **105**, 599-612.

Li, L., Krantz, I. D., Deng, Y., Genin, A., Banta, A. B., Collins, C. C., Qi, M., Trask, B. J., Kuo, W. L., Cochran, J. et al. (1997). Alagille syndrome is caused by mutations in human Jagged1, which encodes a ligand for Notch1. *Nat Genet* **16**, 243-51.

Liem, K. F., Jr., Jessell, T. M. and Briscoe, J. (2000). Regulation of the neural patterning activity of sonic hedgehog by secreted BMP inhibitors expressed by notochord and somites. *Development* **127**, 4855-66.

Lindsell, C. E., Shawber, C. J., Boulter, J. and Weinmaster, G. (1995). Jagged: a mammalian ligand that activates Notch1. *Cell* **80**, 909-17.

Litingtung, Y. and Chiang, C. (2000). Specification of ventral neuron types is mediated by antagonistic interaction between Shh and Gli3. *Nat Neurosci* **3**, 979-985.

Litingtung, Y., Dahn, R. D., Li, Y., Fallon, J. F. and Chiang, C. (2002). Shh and Gli3 are dispensable for limb skeleton formation but regulate digit number and identity. *Nature* **418**, 979-83.

Ma, Y., Erkner, A., Gong, R., Yao, S., Taipale, J., Basler, K. and Beachy, P. A. (2002). Hedgehog-mediated patterning of the mammalian embryo requires transporter-like function of dispatched. *Cell* **111**, 63-75.

Macias, D., Ganan, Y., Rodriguez-Leon, J., Merino, R. and Hurle, J. M. (1999). Regulation by members of the transforming growth factor beta superfamily of the digital and interdigital fates of the autopodial limb mesoderm. *Cell Tissue Res* **296**, 95-102.

Macias, D., Ganan, Y., Sampath, T. K., Piedra, M. E., Ros, M. A. and Hurle, J. M. (1997). Role of BMP-2 and OP-1 (BMP-7) in programmed cell death and skeletogenesis during chick limb development. *Development* **124**, 1109-17.

Maier, M. M. and Gessler, M. (2000). Comparative analysis of the human and mouse Hey1 promoter: Hey genes are new Notch target genes. *Biochem Biophys Res Commun* **275**, 652-60.

Marcil, A., Dumontier, E., Chamberland, M., Camper, S. A. and Drouin, J. (2003). Pitx1 and Pitx2 are required for development of hindlimb buds. *Development* **130**, 45-55.
Marigo, V., Davey, R. A., Zuo, Y., Cunningham, J. M. and Tabin, C. J. (1996). Biochemical evidence that patched is the hedgehog receptor. *Nature* **384**, 176-179.
Marigo, V. and Tabin, C. J. (1996). Regulation of patched by sonic hedgehog in the developing neural tube. *Proc Natl Acad Sci U S A* **93**, 9346-51.
Martin, G. R. (1998). The roles of FGFs in the early development of vertebrate limbs. *Genes Dev* **12**, 1571-1586.
Masuya, H., Sagai, T., Moriwaki, K. and Shiroishi, T. (1997). Multigenic Control of the Localization of the Zone of Polarizing Activity in Limb Morphogenesis in the Mouse. *Dev. Biol.* **182**, 42-51.
Masuya, H., Sagai, T., Wakana, S., Moriwaki, K. and Shiroishi, T. (1995). A duplicated zone of polarizing activity in polydactylous mouse mutants. *Genes Dev* **9**, 1645-53.
Matise, M. P., Epstein, D. J., Park, H. L., Platt, K. A. and Joyner, A. L. (1998). Gli2 is required for induction of floor plate and adjacent cells, but not most ventral neurons in the mouse central nervous system. *Development* **125**, 2759-2770.
McFadden, D. G., McAnally, J., Richardson, J. A., Charite, J. and Olson, E. N. (2002). Misexpression of dHAND induces ectopic digits in the developing limb bud in the absence of direct DNA binding. *Development* **129**, 3077-88.
Merino, R., Rodriguez-Leon, J., Macias, D., Ganan, Y., Economides, A. N. and Hurle, J. M. (1999). The BMP antagonist Gremlin regulates outgrowth, chondrogenesis and programmed cell death in the developing limb. *Development* **126**, 5515-22.
Methot, N. and Basler, K. (1999). Hedgehog controls limb development by regulating the activities of distinct transcriptional activator and repressor forms of Cubitus interruptus. *Cell* **96**, 819-31.
Michos, O., Panman, L., Dono, R., Vintersten, K., Beier, K., Zeller, R. and Zuniga, A. Gremlin propagates dynamic epithelial-mesenchymal signaling interactions regulating limb and kidney organogenesis. *submitted*.
Milenkovic, L., Goodrich, L. V., Higgins, K. M. and Scott, M. P. (1999). Mouse patched1 controls body size determination and limb patterning. *Development* **126**, 4431-40.
Mitsiadis, T. A., Henrique, D., Thesleff, I. and Lendahl, U. (1997). Mouse Serrate-1 (Jagged-1): expression in the developing tooth is regulated by epithelial-mesenchymal interactions and fibroblast growth factor-4. *Development* **124**, 1473-83.
Monge, I., Kondo, T. and Duboule, D. (2003). An enhancer-titration effect induces digit-specific regulatory alleles of the HoxD cluster. *Dev Biol* **256**, 212-20.
Moon, A. M., Boulet, A. M. and Capecchi, M. R. (2000). Normal limb development in conditional mutants of Fgf4. *Development* **127**, 989-96.
Moon, A. M. and Capecchi, M. R. (2000). Fgf8 is required for outgrowth and patterning of the limbs. *Nat Genet* **26**, 455-9.
Moran, J. L., Levorse, J. M. and Vogt, T. F. (1999). Limbs move beyond the radical fringe. *Nature* **399**, 742-3.
Myat, A., Henrique, D., Ish-Horowicz, D. and Lewis, J. (1996). A chick homologue of Serrate and its relationship with Notch and Delta homologues during central neurogenesis. *Dev Biol* **174**, 233-47.
Nellen, D., Burke, R., Struhl, G. and Basler, K. (1996). Direct and long-range action of a DPP morphogen gradient. *Cell* **85**, 357-68.
Nelson, C. E., Morgan, B. A., Burke, A. C., Laufer, E., DiMambro, E., Murtaugh, L. C., Gonzales, E., Tessarollo, L., Parada, L. F. and Tabin, C. (1996). Analysis of *Hox* gene expression in the chick limb bud. *Development* **122**, 1449-1466.
Niederreither, K., Subbarayan, V., Dolle, P. and Chambon, P. (1999). Embryonic retinoic acid synthesis is essential for early mouse post- implantation development. *Nat Genet* **21**, 444-8.
Niederreither, K., Vermot, J., Schuhbaur, B., Chambon, P. and Dolle, P. (2002). Embryonic retinoic acid synthesis is required for forelimb growth and anteroposterior patterning in the mouse. *Development* **129**, 3563-3574.

Niswander, L. and Martin, G. R. (1993). FGF-4 and BMP-2 have opposite effects on limb growth. *Nature* **361**, 68-71.
Niswander, L., Tickle, C., Vogel, A., Booth, I. and Martin, G. R. (1993). FGF-4 replaces the apical ectodermal ridge and directs outgrowth and patterning of the limb. *Cell* **75**, 579-87.

Oda, T., Elkahloun, A. G., Pike, B. L., Okajima, K., Krantz, I. D., Genin, A., Piccoli, D. A., Meltzer, P. S., Spinner, N. B., Collins, F. S. et al. (1997). Mutations in the human Jagged1 gene are responsible for Alagille syndrome. *Nat Genet* **16**, 235-42.
Panin, V. M., Papayannopoulos, V., Wilson, R. and Irvine, K. D. (1997). Fringe modulates Notch-ligand interactions. *Nature* **387**, 908-12.
Panman, L. and Zeller, R. (2003). Patterning the limb before and after SHH signalling. *J Anat* **202**, 3-12.
Park, H. L., Bai, C., Platt, K. A., Matise, M. P., Beeghly, A., Hui, C. C., Nakashima, M. and Joyner, A. L. (2000). Mouse Gli1 mutants are viable but have defects in SHH signaling in combination with a Gli2 mutation. *Development* **127**, 1593-1605.
Peichel, C. L., Prabhakaran, B. and Vogt, T. F. (1997). The mouse *Ulnaless* mutation deregulates posterior HoxD gene expression and alters appendicular patterning. *Development* **124**, 3481-3492.
Persson, M., Stamataki, D., te Welscher, P., Andersson, E., Bose, J., Ruther, U., Ericson, J. and Briscoe, J. (2002). Dorsal-ventral patterning of the spinal cord requires Gli3 transcriptional repressor activity. *Genes Dev* **16**, 2865-78.
Pizette, S., Abate-Shen, C. and Niswander, L. (2001). BMP controls proximodistal outgrowth, via induction of the apical ectodermal ridge, and dorsoventral patterning in the vertebrate limb. *Development* **128**, 4463-74.
Pizette, S. and Niswander, L. (1999). BMPs negatively regulate structure and function of the limb apical ectodermal ridge. *Development* **126**, 883-94.
Pola, R., Ling, L. E., Silver, M., Corbley, M. J., Kearney, M., Blake Pepinsky, R., Shapiro, R., Taylor, F. R., Baker, D. P., Asahara, T. et al. (2001). The morphogen Sonic hedgehog is an indirect angiogenic agent upregulating two families of angiogenic growth factors. *Nat Med* **7**, 706-11.
Porter, J. A., von Kessler, D. P., Ekker, S. C., Young, K. E., Lee, J. J., Moses, K. and Beachy, P. A. (1995). The product of hedgehog autoproteolytic cleavage active in local and long-range signalling. *Nature* **374**, 363-366.
Porter, J. A., Young, K. E. and Beachy, P. A. (1996). Cholesterol modification of hedgehog signaling proteins in animal development. *Science* **274**, 255-259.
Qu, S., Niswender, K., Ji, Q., van der Meer, R., Keeny, D., Magnuson, M. A. and Wisdom, R. (1997). Polydactyly and ectopic ZPA formation in *Alx-4* mutant mice. *Development* **124**, 3999-4008.
Qu, S., Tucker, S. C., Ehrlich, J. S., Levorse, J. M., Flaherty, L. A., Wisdom, R. and Vogt, T. F. (1998). Mutations in mouse Aristaless-like4 cause Strong's luxoid polydactyly. *Development* **125**, 2711-21.
Qu, S., Tucker, S. C., Zhao, Q., deCrombrugghe, B. and Wisdom, R. (1999). Physical and genetic interactions between Alx4 and Cart1. *Development* **126**, 359-69.
Ramírez-Weber, F.-A. and Kornberg, T. B. (1999). Cytonemes: cellular processes that project to the principal signaling center in Drosohila imaginal discs. *Cell* **97**, 599-607.
Riddle, R. D., Johnson, R. L., Laufer, E. and Tabin, C. (1993). *Sonic hedgehog* mediates the polarizing activity of the ZPA. *Cell* **75**, 1401-1416.
Rodriguez-Esteban, C., Schwabe, J. W. R., DeLa Pena, J., Foys, B., Eshelman, B. and J.C., I.-B. (1997). Radical fringe positions the apical ectodermal ridge at the dorsoventral boundary of the vertebrate limb. *Nature* **386**, 360-366.
Roelink, H., Augsburger, A., Heemskerk, J., Korzh, V., Norlin, S., A., R. i. A., Tanabe, Y., Placzek, M., Edlund, T., Jessel, T. M. et al. (1994). Floor plate and motor neuron induction by *vhh-1*, a vertebrate homolog of *hedgehog* expressed by the notochord. *Cell* **76**, 761-775.
Ros, M. A., Dahn, R. D., Fernandez-Teran, M., Rashka, K., Caruccio, N. C., Hasso, S. M., Bitgood, J. J., Lancman, J. J. and Fallon, J. F. (2003). The chick oligozeugodactyly (ozd) mutant lacks sonic hedgehog function in the limb. *Development* **130**, 527-37.
Ruiz i Altaba, A. (1998). Combinatorial Gli gene function in floor plate and neuronal inductions by Sonic hedgehog. *Development* **125**, 2203-2212.

Sanz-Ezquerro, J. J. and Tickle, C. (2000). Autoregulation of Shh expression and Shh induction of cell death suggest a mechanism for modulating polarising activity during chick limb development. *Development* **127**, 4811-23.
Sasaki, H., Nishizaki, Y., Hui, C., Nakafuku, M. and Kondoh, H. (1999). Regulation of Gli2 and Gli3 activities by an amino-terminal repression domain: implication of Gli2 and Gli3 as primary mediators of Shh signaling. *Development* **126**, 3915-24.

Saunders, J. W. J. (1948). The proximo-distal sequence of origin of limb parts of the chick wing and the role of the ectoderm. *J. Exp. Zoology*, 363-404.
Saunders, J. W. J. and Gasseling, M. T. (1968). Ectodermal-mesenchymal interactions in the origin of limb symmetry. *Epithelial-Mesenchymal Interactions* **(eds. Fleischmajer R and Billingham, R.E), Williams and Wilkins, Baltimore**, 78-97.
Schimmang, T., Lemaistre, M., Vortkamp, A. and Rüther, U. (1992). Expression of the zinc finger gene Gli3 is affected in the morphogenetic mouse mutant extra-toes (Xt). *Development* **116**, 799-804.
Sestan, N., Artavanis-Tsakonas, S. and Rakic, P. (1999). Contact-dependent inhibition of cortical neurite growth mediated by notch signaling. *Science* **286**, 741-6.
Shimizu, K., Chiba, S., Kumano, K., Hosoya, N., Takahashi, T., Kanda, Y., Hamada, Y., Yazaki, Y. and Hirai, H. (1999). Mouse jagged1 physically interacts with notch2 and other notch receptors. Assessment by quantitative methods. *J Biol Chem* **274**, 32961-9.
Sordino, P. and Duboule, D. (1996). A molecular approach to the evolution of vertebrate paired appendages. *Trends in Ecology and Evolution* **11**, 114-119.
Soshnikova, N., Zechner, D., Huelsken, J., Mishina, Y., Behringer, R. R., Taketo, M. M., Crenshaw, E. B., 3rd and Birchmeier, W. (2003). Genetic interaction between Wnt/beta-catenin and BMP receptor signaling during formation of the AER and the dorsal-ventral axis in the limb. *Genes Dev* **17**, 1963-8.
Spemann, H. a. M. H. (2001, reprinted). Induction of Embryonic Primordia by Implantation of Organizers from a Different Species. *International Journal of Developmental Biology* **45**, 13-38.
Spitz, F., Gonzalez, F. and Duboule, D. (2003). A global control region defines a chromosomal regulatory landscape containing the HoxD cluster. *Cell* **113**, 405-17.
St-Jacques, B., Dassule, H., Karavanova, I., Botchkarev, V., Li, J., Danielian, P., McMahon, J., Lewis, P., Paus, R. and McMahon, A. (1998). Sonic hedgehog signaling is essential for hair development. *Curr Biol* **8**, 1058-68.
Strigini, M. and Cohen, S. M. (1997). A Hedgehog activity gradient contributes to AP axial patterning of the Drosophila wing. *Development* **124**, 4697-705.
Summerbell, D., Lewis, J. H. and Wolpert, L. (1973). Positional information in chick limb morphogenesis. *Nature* **244**, 492-6.
Sun, X. and Artavanis-Tsakonas, S. (1996). The intracellular deletions of Delta and Serrate define dominant negative forms of the Drosophila Notch ligands. *Development* **122**, 2465-74.
Sun, X., Lewandoski, M., Meyers, E. N., Liu, Y. H., Maxson, R. E., Jr. and Martin, G. R. (2000). Conditional inactivation of Fgf4 reveals complexity of signalling during limb bud development. *Nat Genet* **25**, 83-6.
Sun, X., Mariani, F. V. and Martin, G. R. (2002). Functions of FGF signalling from the apical ectodermal ridge in limb development. *Nature* **418**, 501-8.
Swartz, M., Eberhart, J., Mastick, G. S. and Krull, C. E. (2001). Sparking new frontiers: using in vivo electroporation for genetic manipulations. *Dev Biol* **233**, 13-21.
Takahashi, M., Tamura, K., Buescher, D., Masuya, H., Yonei-Tamura, S., Matsumoto, K., Naitoh-Matsuo, M., Takeuchi, J., Ogura, K., Shiroishi, T. et al. (1998). The role of *Alx-4* in the establishment of anteroposterior polarity during vertebrate limb development. *Development* **125**, 4417-4425.
Tanaka, M., Cohn, M. J., Ashby, P., Davey, M., Martin, P. and Tickle, C. (2000). Distribution of polarizing activity and potential for limb formation in mouse and chick embryos and possible relationships to polydactyly. *Development* **127**, 4011-4021.
te Welscher, P., Fernandez-Teran, M., Ros, M. A. and Zeller, R. (2002a). Mutual genetic antagonism involving GLI3 and dHAND prepatterns the vertebrate limb bud mesenchyme prior to SHH signaling. *Genes Dev* **16**, 421-6.
te Welscher, P., Zuniga, A., Kuijper, S., Drenth, T., Goedemans, H. J., Meijlink, F. and Zeller, R. (2002b). Progression of Vertebrate Limb Development through SHH-Mediated

Counteraction of GLI3. *Science* **298**, 827-30.

Teleman, A. A. and Cohen, S. M. (2000). Dpp gradient formation in the Drosophila wing imaginal disc. *Cell* **103**, 971-80.
Thaller, C. and Eichele, G. (1987). Identification and spatial distribution of retinoids in the developing chick limb bud. *Nature* **327**, 625-628.
Tickle, C. (2003). Patterning systems--from one end of the limb to the other. *Dev Cell* **4**, 449-58.

Tickle, C., Alberts, B. M., Wolpert, L. and Lee, J. (1982). Local application of retinoic acid in the limb bud mimics the action of the polarizing region. *Nature* **296**, 564-565.
UCSC. Mouse Genome Browser (http://genome.ucsc.edu/); Feb. 2003 Assembly, (ed.
van den Akker, E., Fromental-Ramain, C., de Graaff, W., Le Mouellic, H., Brulet, P., Chambon, P. and Deschamps, J. (2001). Axial skeletal patterning in mice lacking all paralogous group 8 Hox genes. *Development* **128**, 1911-21.
van der Hoeven, F., Zákány, J. and Duboule, D. (1996). Gene transpositions in the *HoxD* complex reveal a hierarchy of regulatory controls. *Cell* **85**, 1025-1035.
Vargesson, N., Patel, K., Lewis, J. and Tickle, C. (1998). Expression patterns of Notch1, Serrate1, Serrate2 and Delta1 in tissues of the developing chick limb. *Mech Dev* **77**, 197-9.
Varnum-Finney, B., Purton, L. E., Yu, M., Brashem-Stein, C., Flowers, D., Staats, S., Moore, K. A., Le Roux, I., Mann, R., Gray, G. et al. (1998). The Notch ligand, Jagged-1, influences the development of primitive hematopoietic precursor cells. *Blood* **91**, 4084-91.
Vasiliauskas, D., Laufer, E. and Stern, C. D. (2003). A role for hairy1 in regulating chick limb bud growth. *Dev Biol* **262**, 94-106.
Villa, N., Walker, L., Lindsell, C. E., Gasson, J., Iruela-Arispe, M. L. and Weinmaster, G. (2001). Vascular expression of Notch pathway receptors and ligands is restricted to arterial vessels. *Mech Dev* **108**, 161-4.
Vogel, A., Rodriguez, C. and Izpisua-Belmonte, J. C. (1996). Involvement of FGF-8 in initiation, outgrowth and patterning of the vertebrate limb. *Development* **122**, 1737-50.
Wang, B., Fallon, J. F. and Beachy, P. A. (2000). Hedgehog-Regulated Processing of Gli3 Produces an Anterior/Posterior Repressor gradient in the Developing Vertebrate Limb. *Cell* **100**, 423-434.
Wang, H. U., Chen, Z. F. and Anderson, D. J. (1998). Molecular distinction and angiogenic interaction between embryonic arteries and veins revealed by ephrin-B2 and its receptor Eph-B4. *Cell* **93**, 741-53.
Wellik, D. M. and Capecchi, M. R. (2003). Hox10 and Hox11 genes are required to globally pattern the mammalian skeleton. *Science* **301**, 363-7.
Wettstein, D. A., Turner, D. L. and Kintner, C. (1997). The Xenopus homolog of Drosophila Suppressor of Hairless mediates Notch signaling during primary neurogenesis. *Development* **124**, 693-702.
Wijgerde, M., McMahon, J. A., Rule, M. and McMahon, A. P. (2002). A direct requirement for Hedgehog signaling for normal specification of all ventral progenitor domains in the presumptive mammalian spinal cord. *Genes Dev* **16**, 2849-64.
Wolpert, L. (1969). Positional information and the spatial pattern of cellular differentiation. *J. Theor. Biol.* **25**, 1-47.
Wright, E., Hargrave, M. R., Christiansen, J., Cooper, L., Kun, J., Evans, T., Gangadharan, U., Greenfield, A. and Koopman, P. (1995). The Sry-related gene Sox9 is expressed during chondrogenesis in mouse embryos. *Nat Genet* **9**, 15-20.
Xu, J., Liu, Z. and Ornitz, D. M. (2000). Temporal and spatial gradients of Fgf8 and Fgf17 regulate proliferation and differentiation of midline cerebellar structures. *Development* **127**, 1833-43.
Xue, Y., Gao, X., Lindsell, C. E., Norton, C. R., Chang, B., Hicks, C., Gendron-Maguire, M., Rand, E. B., Weinmaster, G. and Gridley, T. (1999). Embryonic lethality and vascular defects in mice lacking the Notch ligand Jagged1. *Hum Mol Genet* **8**, 723-30.
Yamada, T., Placzek, M., Tanaka, H., Dodd, J. and Jessel, T. M. (1991). Control of cell pattern in the developing nervous system : polarizing activity of the floor plate and notochord. *Cell* **64**, 635-647.
Yang, Y., Drossopoulou, G., Chuang, P. T., Duprez, D., Marti, E., Bumcrot, D., Vargesson, N., Clarke, J., Niswander, L., McMahon, A. et al. (1997). Relationship between does, distance and time in *Sonic Hedgehog*-mediated regulation of anteroposterior polarity in

the chick limb. *Development* **124**, 4393-4404.

Yelon, D., Baruch, T., Halpern, M. E., Ruvinsky, I., Ho, R. K., Silver, L. M. and Stainier, D. Y. R. (2000). The bHLH transcription factor Hand2 plays parallel roles in zebrafish heart and pectoral fin development. *Development* **127**, 2573-2582.

Zakany, J. and Duboule, D. (1999). Hox genes in digit development and evolution. *Cell Tissue Res* **296**, 19-25.

Zakany, J., Fromental-Ramain, C., Warot, X. and Duboule, D. (1997). Regulation of number and size of digits by posterior *Hox* genes: A dose-dependant mechanism with potential evolutionary implications. *Proc. Natl. Acad. Sci. USA* **94**, 13695-13700.

Zecca, M., Basler, K. and Struhl, G. (1995). Sequential organizing activities of engrailed, hedgehog and decapentaplegic in the Drosophila wing. *Development* **121**, 2265-78.

Zeller, R., Haramis, A., Zuniga, A., McGuigan, C., Dono, R., Davidson, G., Chabanis, S. and Gibson, T. (1999). *Formin* defines a large family of morphoregulatory genes and functions in establishment of the polarising region. *Cell Tissue Res* **296**, 85-93.

Zeng, X., Goetz, J. A., Suber, L. M., Scott, W. J., Jr., Schreiner, C. M. and Robbins, D. J. (2001). A freely diffusible form of Sonic hedgehog mediates long-range signalling. *Nature* **411**, 716-20.

Zhang, X. M., Ramalho-Santos, M. and McMahon, A. P. (2001). Smoothened mutants reveal redundant roles for Shh and Ihh signaling including regulation of L/R symmetry by the mouse node. *Cell* **106**, 781-92.

Zuniga, A., Haramis, A. P., McMahon, A. P. and Zeller, R. (1999). Signal relay by BMP antagonism controls the SHH/FGF4 feedback loop in vertebrate limb buds. *Nature* **401**, 598-602.

Zuniga, A., Michos, O., Spitz, F., Haramis, A.-P. G., Panman, L., Vintersten, K., Klasen, C., Mansfield, W., Kuc, S., Dono, R. et al. A global control region shared by Formin and Gremlin is essential for mouse limb bud development. *submitted*.

Zuniga, A. and Zeller, R. (1999). Gli3 (Xt) and formin (ld) participate in the positioning of the polarising region and control of posterior limb-bud identity. *Development* **126**, 13-21.

Summary

Communication between cells is essential during embryonic development. The vertebrate limb bud provides us with a model in which to study signalling interactions between cells during patterning of embryonic tissues and organogenesis. In chapter 1, I give an introduction about limb bud development that is focused on the patterning of the anterior-posterior axis of the limb bud during outgrowth. Here I also introduce *Sonic Hedgehog* (SHH), which is a signalling molecule that is expressed by the cells of the polarising region. *Shh* mediates the organizing function of the polarising region and is required for patterning of the anterior-posterior axis of the distal limb. Mutual genetic antagonism between *Gli3* and *dHand* prepatterns the limb prior to SHH signalling, resulting in the establishment of the polarizing region in posterior limb bud mesenchyme.

In chapter 2, I show that *Gli3* and *Alx4* genetically interact during limb and craniofacial development. *Gli3* and *Alx4* are both expressed in anterior limb bud mesenchyme and are required to keep the *Shh* expression domain posteriorly restricted. Disruption of either *Gli3* or *Alx4* results in the establishment of an ectopic *Shh* domain and preaxial polydactyly. However, analysis of limbs lacking both *Gli3* and *Alx4* reveal that these genes synergistically interact during patterning of all three groups of limb skeletal elements. In addition, skulls of embryos lacking both *Gli3* and *Alx4* exhibit craniofacial defects.

In Chapter 3, I have established that limb bud mesenchymal cells response differentially to SHH signalling. During limb bud patterning SHH differentially activates secondary signalling molecules, like BMP2 and Gremlin. Here I show that SHH also acts upstream of NOTCH signalling during limb bud development. SHH regulates the expression of *Jagged-1* and *Hey,* which are involved in NOTCH signal transduction, in the limb bud mesenchyme. Furthermore, I provide evidence that SHH acts upstream of *Jagged-1* during patterning of the limb bud vascular system.

The SHH signal is relayed to the AER by BMP antagonist *Gremlin.* In chapter 4, I describe the *Gremlin* mutant limb phenotype, which corresponds to the *limb deformity* limb phenotype. *Gremlin* mutant limbs exhibit fusions of zeugopodal elements and digit syndactyly, indicating that anterior-posterior patterning is affected. I show that the absence of *Gremlin* mediated BMP antagonism disrupts the feedback loop between SHH and the AER. In *Gremlin* deficient limb buds, activation of *Fgfs* and *Bmps* in the AER is disrupted and *Shh* expression is not propagated. Furthermore, mesenchymal limb buds cells undergo massive apoptosis in the absence of *Gremlin.*

In the final chapter, I discuss whether SHH acts as a morphogen during limb bud patterning. It has been proven that SHH patterns the neural tube directly and not through induction of secondary signals. However, it is still unclear whether SHH acts as a “true” morphogen during limb bud patterning. Furthermore, I discuss the role of NOTCH signalling during limb bud development. I propose future experiments that will allow us finding additional roles for NOTCH signalling during limb bud development.

Samenvatting

Intercellulaire communicatie is essentieel tijdens de embryonale ontwikkeling. Om de intercellulaire communicatie tijdens de patroonvorming van embryonale weefsels en van organen te kunnen bestuderen, hebben we de ontwikkeling van ledematen bij vertebraten als model gebruikt. In hoofdstuk 1 geef ik een introductie over de ontwikkeling van ledematen, waarbij ik de nadruk leg op het vastleggen van de anterior-posterior polariteit van de ledematen tijdens de uitgroei. Ik introduceer hier ook het signaalmolecuul *Sonic Hedgehog* (SHH), dat tot expressie komt in cellen die zich in het posteriore gedeelte van de ledematen bevinden. Deze SHH uitscheidende cellen vormen een signaal centrum, de zogenoemde "zone of polarizing activity" (ZPA). SHH kan de functie van de ZPA bij het vastleggen van de anterior-posterior polariteit van ledematen volledig simuleren. *Gli3* en *dHand* komen eerder dan *Shh* in de ledematen tot expressie. De genetische interactie tussen *Gli3* en *dHand* resulteert in het vastleggen van de ZPA in het posteriore gedeelte van de ledematen.

In hoofdstuk 2 toon ik aan dat *Gli3* en *Alx4* een overlappende functie hebben tijdens de ledematen en craniofaciale ontwikkeling. *Gli3* en *Alx4* komen beide in het anteriore gedeelte van de ledematen tot expressie en zorgen er beide voor dat het gebied waar *Shh* tot expressie komt beperkt blijft tot het posteriore gedeelte van de ledematen. In zowel *Gli3* als in *Alx4* mutanten komt *Shh* ook in het anteriore gedeelte van de ledematen tot expressie, wat resulteert in preaxial polydactyly. Analyse van ledematen van embryo's die een mutatie hebben in zowel *Gli3* als in *Alx4* laat echter zien dat *Gli3* en *Alx4* ook een overlappende functie hebben tijdens de ontwikkeling van de ledematen. Verder hebben embryo's die mutant zijn voor zowel *Gli3* als *Alx4* craniofaciale afwijkingen.

In hoofdstuk 3 laat ik zien dat mesenchymale cellen van de zich ontwikkelende ledematen verschillend reageren op SHH signalen. Tijdens de patroonvorming van ledematen activeert SHH verschillende secundaire signalerings moleculen, zoals BMP2 en Gremlin. Ik laat hier zien dat SHH ook NOTCH signalering activeert tijdens de ontwikkeling van ledematen. SHH reguleert de expressie van *Jagged-1* en *Hey1*, die beide betrokken zijn bij het overbrengen van NOTCH signalering. Verder bewijs ik dat de activatie van *Jagged-1* door SHH van belang is voor de ontwikkeling van het bloedvaten stelsel in ledematen.

Het SHH signaal wordt door Gremlin overgebracht naar de zogenaamde "apical ectodermal ridge" (AER), wat het tweede signaal centrum van de ledematen is. Gremlin is een BMP antagonist. In hoofdstuk 4 beschrijf ik het fenotype van de ledematen van *Gremlin* mutante embryo's. De beenstukken van het zeugopodium en de vingers zijn gefuseerd in deze mutanten, wat aantoont dat er zich problemen voordoen bij het vastleggen van de anterior-posterior polariteit van de ledematen. In de afwezigheid van *Gremlin* kan de feedback loop tussen SHH en de AER niet tot stand worden gebracht. In de afwezigheid van *Gremlin* wordt de expressie van *Fgfs* en *Bmps* in de AER niet geactiveerd. Verder neemt *Shh* expressie niet toe in de zich ontwikkelende mutante ledematen. Ook treedt er cel dood op in het mesenchyme van de zich ontwikkelende mutante ledematen.

In het laatste hoofdstuk bediscussieer ik of SHH te werk gaat als morphogen tijdens de ontwikkeling van ledematen. Het is bewezen dat SHH tijdens de ontwikkeling van de neurale buis directe instructies geeft aan cellen en de ontwikkeling niet reguleert via het induceren van secundaire signalering moleculen. Het is echter nog steeds onduidelijk of SHH ook de ontwikkeling van de ledematen reguleert volgens de principes van een morphogen. Verder bediscussieer ik wat de functie van NOTCH signalering is tijdens de ontwikkeling van ledematen. Tenslotte doe ik een voorstel voor verdere experimenten om de rol van NOTCH signalering te kunnen onderzoeken.

Dankwoord

Eindelijk, het is af! Mijn proefschrift is geschreven! En ik ben blij en trots met wat ik bereikt heb. Ik kan nu terugkijken op vijf plezierige, leerzame en productieve jaren als aio. En ik ben hiervoor natuurlijk veel mensen dankbaar.
At the first place I would like to thank Rolf for giving me the opportunity to do research in his group. Thanks for all your support, stimulating discussions and for teaching me so many things. Doing grafting experiments together with you was great fun. Aimée, thanks for all your help and support. It was always nice chatting with you about food. I wish you and Rolf all the best in Basel!
Rosanna, thanks a lot for your support and your interest in my work. I enjoyed the stimulating discussions with you. I wish you all the best in the future with hopefully your own group. Odyssé, thanks for the nice and productive time I had when I was working together with you on the analysis of the Gremlin KO. I have enjoyed it a lot. Also thanks for all the fun and the discussions I had with you about the situation in the world. Only the time you threw me into the water… Antonella, Italian girl, it was fantastic to share the office and lab with you. I had a great time. Thanks for not getting annoyed when I was singing in the lab. And because of you and Odyssé I was never alone in the building during the evening hours and the weekends. Pascal, bedankt voor de vele discussies. Agnes, thanks for everything and for the fun during lunch time. Thijs, ik vond het leuk om jou als student te begeleiden en bedankt voor je bijdrage aan hoofdstuk 2. Sylwia, het was altijd erg gezellig om met jou te praten over ditjes en datjes. Hans, bedankt voor de vele bestelling van enzymen, buffers en van andere dingen die je hebt gedaan en voor het genotyperen van een ontelbare hoeveelheid muizen en embryo's. Verder wil ik ook Vincent bedanken voor het helpen met genotyperen. En Nebal, bedankt voor al je hulp. Jouw lach 's ochtends zorgde er altijd voor dat de dag goed begon. Rene, Bert, Adri en Miriam, bedankt voor alles.
Frits, Jacqueline, Kirstie en alle (ex-)groepsleden, bedankt voor de gezamenlijke werkbesprekingen en de borrels. Vele andere Hubrechters wil ik bedanken voor alle gezelligheid buiten de werkuren en -muren.
Jelly, bedankt voor je vriendschap en de vele diepzinnige en minder diepzinnige gesprekken. Ik ben blij dat je mijn paranimf wilt zijn. En nu op naar jouw promotie! Michiel, onder jouw supervisie heb ik als student mijn intrede op het lab gedaan. Ik vind het erg leuk dat je nu tijdens mijn promotie mijn paranimf wilt zijn. Pim, Martha, Jellie, Lotte, studiegenoten uit Groningen en de jongens uit Gieten bedankt voor de vele gezellige avonden, feesten en nieuwjaarsvieringen. Hopelijk volgen er nog veel meer.
Lieve pappa en mamma, bedankt voor al jullie steun en voor de mogelijkheden die jullie me hebben gegeven. Ook al stapte ik de afgelopen jaren niet vaak in trein richting het noorden, ik vond het altijd erg gezellig om bij jullie te zijn. Frank, broertje van me, ook bedankt voor al je belangstelling.
Lieve Tony, bedankt voor al je liefde, steun en je vrolijkheid. Waar we straks ook gaan wonen en werken, met jou wordt het vast een feest!

Curriculum Vitae

Lia Panman werd op 26 oktober 1974 geboren in Veendam. Na het behalen van het VWO diploma aan de O.S.G Winkler Prins in Veendam in 1993 begon zij in hetzelfde jaar de studie Biologie aan de Rijksuniversiteit Groningen. De eerste afstudeerstage werd gedaan bij de vakgroep ontwikkelingsgenetica (Prof. W. Kruijer) van de Rijksuniversiteit Groningen. Haar tweede afstudeerstage deed ze in de groep van Dr. M.G. Parker aan de ICRF in Londen onder begeleiding van Dr. E. Kalkhoven. Het doctoraal diploma Biologie, specialisatie Moleculaire biologie werd behaald in 1998. In 1999 begon ze haar promotie onderzoek bij de vakgroep ontwikkelingsbiologie aan de Universiteit Utrecht onder begeleiding van Prof. R. Zeller en Dr. A. Zuniga. De resultaten van dit onderzoek staan in dit proefschrift beschreven.